Aus der

Medizinischen Universitätsklinik und Poliklinik Tübingen

Abteilung VIII, Medizinische Onkologie und Pneumologie

The DNA Damage Response as a target for Senolytic Therapies

Inaugural-Dissertation
zur Erlangung des Doktorgrades
der Medizin

der Medizinischen Fakultät
der Eberhard Karls Universität
zu Tübingen

vorgelegt von

Stas, Ingrid Marie-Madeleine

2023

Dekan:	Professor Dr. B. Pichler
1. Berichterstatter:	Professor Dr. L. Zender
2. Berichterstatter:	Privatdozentin Dr. Dr. M. André
Tag der Disputation:	17.08.2023

Table of contents

List of Tables

List of Figures

List of Abbreviations

53BP1 .... p53 binding protein 1
ADP .... adenosine diphosphate
ALL .... acute lymphoblastic leukemia
APS .... ammonium persulfate
ATM .... ataxia telangiectasia mutated kinase
ATR .... ataxia telangiectasia and Rad3 related kinase
ATRIP .... ATR-interacting protein
Bcl-2 .... B-cell lymphoma 2
BRCA1 .... breast cancer type 1 susceptibility protein
BRCA2 .... breast cancer type 2 susceptibility protein
BSA .... bovine serum albumin
CDC25 .... cell division cycle 25
CDK .... cyclin dependent kinase
CHK1 .... checkpoint kinase 1
CHK2 .... checkpoint kinase 2
DAPI .... 4’,6-diamidin-2-phenylindol
DDR .... DNA damage response
D-loop .... displacement-loop
DMEM .... Dulbecco’s Modified Eagle Medium
DMF .... N-N-dimethylformamide
DMSO .... dimethylsulfoxide
DNA .... deoxyribonucleic acid
DNA-PK .... DNA-dependent protein kinase
DNA-PKcs .... DNA-PK catalytic subunit
DSB .... double strand break
EDTA .... ethylenediaminetetraacetic acid
EGTA .... ethylene glycol tetraacetic acid
ERK .... extracellular-signal-regulated kinase
FA .... Fanconi Anemia
FANC .... FA complementation group protein

FBS .... fetal bovine serum
GAA .... glacial acetic acid
H2AX .... H2A histone family member X
HBSS .... Hanks' Balanced Salt Solution
HCC .... hepatocellular carcinoma
HMGA .... high-mobility group A
HR .... homologous recombination
-i .... inhibitor
IC_{50} .... half-maximal inhibitory concentration
ICL .... interstrand crosslink
IF .... immunofluorescence
JAK2 .... janus kinase 2
KAP1 .... KRAB-interacting protein 1
KRAB .... Krüppel associated box
Ku .... Ku70/Ku80 heterodimer
MEM-NEAA .... minimum essential medium non-essential amino acids
MRN MRE11-RAD50-NBS1-complex
MW .... molecular weight
NGS .... normal goat serum
NHEJ .... non-homologous DNA end-joining
OIS .... oxidative stress induced senescence
p- .... phosphorylated
PARP .... poly-ADP-ribose polymerase
PBS .... phosphate-buffered saline
PenStrep .... penicillin-streptomycin
PFA .... paraformaldehyde
PI .... propidium iodide
PI3K .... phosphoinositide 3-kinase
PMS .... phenazine methosulfate
RCIS .... ribosomal checkpoint induced senescence
rDNA .... ribosomal DNA
RNA .... ribonucleic acid

RNAP .... RNA polymerase
ROS .... reactive oxygen species
RPA .... replication protein A
rpm .... revolutions per minute
rRNA .... ribosomal RNA
RS .... replicative senescence
SAHF .... senescence-associated heterochromatin foci
SASP .... senescence-associated secretory phenotype
SA-β-Gal .... senescence-associated β-galactosidase
SDS .... sodium dodecyl sulfate
SL1 .... selective factor 1
SSB .... single strand break
ssDNA .... single stranded DNA
TAF .... TBP associated factor
TBP .... TATA binding protein
TEMED .... tetramethylethylenediamine
TIS .... therapy induced senescence
TRC .... transcription-replication collision
Tris .... tris(hydroxymethyl)aminomethane
XRCC1 .... X-ray repair cross-complementing protein 1
γH2AX .... phosphorylated H2AX

1 Introduction

1.1 Definition and hallmarks of cellular senescence

Cells perpetually have to select between responding with recovery or cell death to stress and damage from diverse exogenous and endogenous sources (Fulda et al., 2009). However, proliferating cells harbour a further option how to react towards stress, named cellular senescence. Cellular senescence is a phenomenon by which normal cells cease to divide but stay transcriptionally and metabolically active while their cell cycle is durably arrested (Campisi and Fagagna, 2007; Hernandez-Segura et al., 2018). Establishing the senescent state goes along with a multifarious set of cellular changes. One of the most characterising features of senescent cells is missing proliferative activity (Hayflick and Moorhead, 1961). For this purpose, the tumour suppressor protein p53 (El-Deiry et al., 1993) and the cyclin dependent kinase (CDK) inhibitors p16 and p21 (Alcorta et al., 1996) trigger cell cycle arrest, mainly in G1 or G2 cell cycle phases (Mao et al., 2013). Further, high-mobility group A (HMGA) protein dependent (Narita et al., 2006) formation of senescence-associated heterochromatin foci (SAHFs) prevents transcription of E2F target genes needed for cell cycle progression (Narita et al., 2003). Together with a lack of key enzyme activities like caspase-3 (Marcotte et al., 2004), enhanced expression of pro-apoptotic genes like Bax and failing to undergo stress-induced downregulation of anti-apoptotic genes like B-cell lymphoma 2 (Bcl-2) (Ryu et al., 2007; Sanders et al., 2013) permit apoptosis resistance in senescent cells. Another main characteristic of senescent cells is their altered cellular appearance: The cell body enlarges and becomes irregular due to rearrangements of the cytoskeleton (Nishio et al., 2001). Further, nuclear envelope integrity is disturbed, probably due to down-regulation of lamin B1 (Freund et al., 2012). Impaired degradation of lysosomes results in an accumulation of old and dysfunctional lysosomes (Lee et al., 2006) that are characterised by residual bodies, named lipofuscins (Georgakopoulou et al., 2013), and enhanced activity of the lysosomal enzyme β-galactosidase. The latter is utilised to detect senescent cells with the widely-used senescence-associated β-galactosidase (SA-β-Gal) staining (Dimri et al., 1995). Analogous to lysosomes, reduced mitophagy causes abundant old and dysfunctional mitochondria (Passos et al., 2007) that enhance cellular levels of reactive oxygen species (ROS) (Passos et al., 2007). Last but not least, senescent cells acquire a typical secretory phenotype with mainly proinflammatory activity, called senescence-associated secretory phenotype (SASP) (Kuilman and Peeper, 2009; Coppé et al., 2010). Depending on the provoking mechanism and microenvironment, the SASP is a double-edged sword as it mediates positive effects on the cell and the neighbouring tissue like wound healing (Demaria et al., 2014) but also negative effects like tumour progression (Coppé et al., 2010). In this context, senescence poses a tremendous risk for human health (Coppé et al., 2010).

1.2 Inducers of cellular senescence

The senescent state was first described more than five decades ago by Leonard Hayflick and Paul Moorhead, who had observed that proliferative potential and cell division are limited in normal human foetal fibroblasts upon continuous subculture (Hayflick and Moorhead, 1961). Almost 30 years later, shortening of telomeres, repetitive deoxyribonucleic acid (DNA) sequences at chromosome endings, was recognised as origin of replicative senescence (RS) (Harley et al., 1990). Thus, telomere shortening is a molecular clock triggering not only the ageing process, but also cellular senescence (Baerlocher et al., 2003). Nowadays, various other stress factors are known to induce premature senescence, such as aberrant oncogene activation (Serrano et al., 1997), inactivation of tumour suppressor proteins (Chen et al., 2005), epigenetic changes (Young and Smith, 2001; Lagger et al., 2002), oxidative agents (Chen and Ames, 1994), autophagy (Young et al., 2009; White and Lowe, 2009), and mitochondrial dysfunction (Wiley et al., 2016). However, senescence was also observed in connection with therapeutic procedures, like cytotoxic drug treatment (Robles and Adami, 1998; Chang et al., 1999) or ionizing radiation (Poele et al., 2002; Ye et al., 2013). Next to these published types of therapy induced senescence (TIS) (Ewald, 2010), unpublished work by the Zender laboratory (K. Wolter) has identified a new subtype of TIS, designated ribosomal checkpoint induced senescence (RCIS). Among other things, RCIS can be induced pharmacologically by the ribonucleic acid (RNA) polymerase (RNAP) I inhibitor CX-5461 (K. Wolter, unpublished).

1.3 RNA polymerase I inhibitor CX-5461

1.3.1 RNA polymerase I

RNA polymerase I (RNAP I) is a 590 kDa multi-enzyme complex consisting of 14 protein subunits (Engel et al., 2013; Fernández-Tornero et al., 2013) which is located in the nucleolus (Roeder and Rutter, 1969). Its main function is to transcribe a 45 S precursor ribosomal RNA (rRNA) molecule that is subsequently processed to 5.8 S, 18 S and 28 S rRNA subunits that – together with 5 S rRNA synthesised by RNAP III – are needed for ribosomal biogenesis (Russell and Zomerdijk, 2006). To start transcription, selective factor 1 (SL1) (Learned et al., 1985) (an assembly of TATA binding protein (TBP) and RNAP I-specific TBP associated factors (TAFs) (TAF_I48, TAF_I63, TAF_I110) (Di Pietro et al., 2000)) binds RNAP I and the core promotor of ribosomal DNA (rDNA). Since multiple RNAP I molecules can transcribe the same gene simultaneously (Dundr et al., 2002) with a transcription rate of 95 nucleotides per second (Dundr et al., 2002), RNAP I is a very fast-acting polymerase making up to 60% of cellular transcription in growing cells (Moss and Stefanovsky, 2002). Crucially, excessive cancer growth requires accelerated ribosomal biosynthesis, thus making augmented RNAP I activity an important feature of tumourigenesis (White, 2005). Therefore, nucleoli enlargement and rRNA synthesis acceleration are both commonly used markers for aggressive tumour cells (Derenzini et al., 2000; Maggi and Weber, 2005). As boosted rRNA synthesis in tumours is correlated with an adverse prognosis (Williamson et al., 2006), RNAP I inhibition is a promising approach in current cancer research (White, 2005).

1.3.2 Mechanism of action of CX-5461

CX-5461 (2-(4-methyl[1,4]diazepan-1-yl)-5-oxo-5H-7-thia-1,11b-diazabenzo[c]-fluorene-6-carboxylic acid (5-methyl-pyrazin-2-ylmethyl)-amide (Haddach et al., 2012)) is a potent selective small molecule inhibitor of RNAP I (Drygin et al., 2011). Mechanistically, CX-5461 disrupts the SL1/rDNA complex with the TBP and TAF_I110 subunits being most affected, thus inhibiting rRNA synthesis at the initiation stage (Drygin et al., 2011). 2 µM of CX-5461 were shown to reduce the association between RNAP I and the rDNA promotor by approximately 40 to 60% in human colorectal carcinoma HCT116, melanoma A375, and pancreatic carcinoma MIA PaCa-2 cell lines (Drygin et al., 2011). Although TBP is involved not only in RNAP I, but also RNAP II machinery, CX-5461 inhibits RNAP I with 200-fold selectivity in HCT116 cells (Drygin et al., 2011), probably due to its specific interaction with SL1 (Russell and Zomerdijk, 2006). Further, CX-5461 has 250- to 300-fold selectivity for rRNA transcription inhibition versus DNA replication and protein translation (Drygin et al., 2011).

Although CX-5461 inhibits RNAP I in both normal and cancer cells, the accelerated rRNA synthesis rate makes cancer cells more sensitive to CX-5461 (White, 2005). Initially, CX-5461 was shown to trigger a stress response resulting in cell death in cell lines derived from hematopoietic malignancies (Drygin et al., 2011). Thereby, CX-5461 significantly inhibits tumour growth not only *in vitro*, but also *in vivo* without changes in body weight or overt toxicity (Drygin et al., 2011). More recently, the Zender laboratory has shown that CX-5461 induces a robust senescence response in a broad range of murine and human solid tumour entities and significantly prolongs survival in otherwise highly aggressive and therapy resistant liver cancer mouse models (K. Wolter, unpublished).

Given that effectiveness of CX-5461 was initially demonstrated in lymphoma and leukaemia cells (Bywater et al., 2012; Negi and Brown, 2015), CX-5461 is now in advanced phase I clinical trial for haematologic malignancies (Australian trial, ACTRN12613001061729). However, a further trial includes solid tumours as well (Canadian trial, NCT02719977) since some data have indicated broad effectiveness also in solid tumours (Drygin et al., 2011; Li et al., 2016; Yan et al., 2016; Xu et al., 2017).

1.4 Senescence in physiological and pathological contexts

Senescent cells are common in living organisms and have beneficial but also detrimental properties in a variety of physiological and pathological contexts. For instance, senescence is involved in embryonic development (Muñoz-Espín et al., 2013; Storer et al., 2013), vascular remodelling (Rajagopalan and Long, 2012), wound healing (Jun and Lau, 2010), tissue regeneration (Ritschka et al., 2017), fibrosis prevention (Krizhanovsky et al., 2008) and ageing (Zindy et al., 1997; Krishnamurthy et al., 2004; Jeyapalan et al., 2007; Wang et al., 2009). As ageing and therefore senescence is one of the greatest risk factors for many chronic diseases, such as cardiovascular disease, diabetes, neurodegeneration and cancer (Niccoli and Partridge, 2012; McHugh and Gil, 2018), senescence has been extensively studied within the last decades. Nevertheless, the interplay between senescence and cancer remains controversial (Campisi, 2005). Senescence was first described as tumour protective mechanism that triggers proliferation arrest in cells with dysfunctional telomeres and other cellular damages to prevent malignant transformation (Chen et al., 2005; Collado et al., 2005; Braig et al., 2005). Moreover, tumourigenesis is prevented by extrinsic SASP-dependent immunosurveillance mechanisms (Kang et al., 2011). Yet, some SASP-associated cytokines and chemokines fuel tumorigenic properties like survival, proliferation, and angiogenesis (Krtolica et al., 2001; Coppé et al., 2008; Cahu et al., 2012). These SASP factors promote growth of neighbouring premalignant and malignant, but not normal, epithelial cells to form tumours in mice (Krtolica et al., 2001). Thus, the current working model suggests that senescence acts as a barrier for early tumourigenesis but poses a risk for tumour progression in pre-existing tumour cells (Krtolica et al., 2001;

Eggert et al., 2016). In line with this model, malignant pleural mesothelioma patients whose tumours had responded predominantly with senescence instead of apoptosis upon platinum-based chemotherapy had shorter time to progression and worse overall survival (Sidi et al., 2011). Among others, this data indicates senescence as a significantly inferior chemotherapy response with worse clinical outcome than apoptosis (Sidi et al., 2011; Jackson et al., 2012).

1.5 Senolytic therapy

Suppressing the adverse effects of senescent cells is on focus of many medical research projects since Baker et al. have provided proof-of-principle that abolishing senescent cells prevents or delays tissue dysfunction and increases both lifespan and healthspan (Baker et al., 2011). Currently, two promising approaches are investigated to suppress the shady side of senescent cells: SASP-modulating therapy, and specific eradication of senescent cells, called senolysis. The effectiveness of a SASP-modulating therapy concept was evidenced for instance by janus kinase 2 (JAK2) inhibitor dependent reprogramming of the SASP that triggered strong antitumour immune response and improved efficacy of docetaxel-induced senescence in a prostate cancer mouse model (Toso et al., 2014). The other approach, senolysis, is based on attacking selective vulnerabilities of senescent cells that are less or even not at all present in non-senescent cells (Zhu et al., 2015). Although the probably most common senolytic drug is navitoclax (ABT-263), an inhibitor of the anti-apoptotic protein Bcl-2 (Zhu et al., 2016), effectiveness of the senolytic therapy concept was first demonstrated for quercetin (phosphoinositide 3-kinase (PI3K) inhibitor) and dasatinib (multiple tyrosine kinase inhibitor) (Zhu et al., 2015). Both delayed age-related diseases like osteoporosis, as well as physical declines of cardiac function, carotid vascular reactivity, and intervertebral discs' structure *in vivo* (Zhu et al., 2015). Such widespread beneficial effects on human health are the reason why search for senolytic drugs is on focus of both cancer and ageing research. More recently, senolytic properties were even shown for the Na^+/K^+-

ATPase inhibitors ouabain, digoxin and digitoxin that are known as cardiac glycosides in heart failure and atrial fibrillation treatment (Guerrero et al., 2019; Triana-Martínez et al., 2019).

1.6 DNA damage response as a hallmark of senescence

Attacking the hallmarks of senescent cells presents a promising strategy to uncover new senolytic drugs (Zhu et al., 2015). One of these hallmarks is an activated DNA damage response (DDR) (Fagagna, 2008). The first link between senescence and DDR activation was shown in the context of telomere-initiated senescence (Fagagna et al., 2003). Telomeres are defined as chromosome endings and therefore resemble DNA double strand breaks (DSBs). Thus, telomere capping proteins are required to avoid DDR activation at telomeres (Karlseder et al., 2004; Denchi and Lange, 2007). However, it is believed that the probability of telomere uncapping increases at critically shortened telomeres due to destabilised telomeric loops, thus allowing DDR activation (Griffith et al., 1999). This hypothesis is assisted by the finding that DNA damage foci (γH2AX/53BP1) co-localise with the shortest telomeres in replicative senescent BJ foreskin fibroblasts (Zou et al., 2004). Based on these observations, a causal connection between senescence and DDR activation has been suggested and some authors proposed senescence as an outcome of a protracted DDR (Fagagna et al., 2003; Herbig et al., 2004; Jeyapalan et al., 2007). The concept of DDR associated senescence was confirmed by following studies that demonstrated that not only RS (Fagagna et al., 2003) but also oncogene-induced senescence is accompanied by DDR activation based on replication fork stalling and DSB formation (Bartkova et al., 2006; Di Micco et al., 2006). Moreover, the DNA damage marker γH2AX and the senescence marker heterochromatin protein 1γ (HP1γ) – but not p16 – co-segregate closely in human colon adenomas, thus indicating DDR associated senescence in the early phase of tumourigenesis (Bartkova et al., 2006).

1.7 Overview of the DNA damage response (DDR)

1.7.1 DNA damage

DNA damage poses a tremendous danger for cellular stability and functionality as it affects the basic cellular mechanisms of transcription and replication intensively (Jackson and Bartek, 2009). While normal cells undergo apoptosis or cellular senescence in response to unrepairable DNA lesions (Robles and Adami, 1998), tumour cells continue proliferation due to activated oncogenes or reduced levels of tumour suppressor proteins thus making DNA damage one of the most important risk factors for initiation and propagation of cancer (Hanahan and Weinberg, 2011). DNA damage can be caused by various triggers, for instance spontaneous hydrolysis of nucleotide residues (Gates, 2009), endogenous mediators like ROS (Srinivas et al., 2019), or exogenous factors such as chemotoxic drugs and ultraviolet radiation (Boyce and Howard-Flanders, 1964; Rasmussen and Painter, 1964). Since each cell of the human body is confronted with approximately 10^4-10^5 DNA lesions per day (Lindahl and Barnes, 2000; Tubbs and Nussenzweig, 2017), systematic repair of genomic injuries is indispensable for human life. This system, named the DNA damage response (DDR), consists of various DNA repair mechanisms (Jackson and Bartek, 2009), but also cell cycle checkpoint pathways (Barnum and O’Connell, 2014), and chromatin modification processes (Luijsterburg and Attikum, 2011). Inherited defects in DDR factors are responsible for severe diseases, like the bone marrow failure syndrome Fanconi Anemia (FA) (Ceccaldi et al., 2012), the cancer susceptibility syndromes Lynch syndrome (Fishel et al., 1993; Bronner et al., 1994) and Xeroderma pigmentosum (Cleaver, 1968), the neurodegenerative disease Ataxia-oculomotor apraxia (Moreira et al., 2001), and the immune deficiency syndrome Ataxia telangiectasia (Savitsky et al., 1995). Together, these examples underline the inevitable role of a functional DDR for human health.

1.7.2 DNA repair mechanisms

Relating to the multiplicity of different kinds of DNA damages, a large set of diverse DNA repair mechanisms exists with each of them having its own damage specificity (Jackson and Bartek, 2009). In the following, four different types of DNA damage are distinguished: 1) damage of a single base, 2) DNA single strand breaks (SSB), 3) DNA double strand breaks (DSB), and 4) interstrand crosslinks (ICL). Base defects are repaired by three different mechanisms: Mismatch repair removes biosynthetic errors like base-base mismatches (Jiricny, 2006), while base excision repair fixes DNA damages from oxidation, deamination or alkylation (Krokan and Bjørås, 2013), and nucleotide excision repair corrects bulky DNA adducts and intrastrand crosslinks (Marteijn et al., 2014). In single strand break (SSB) repair, poly-adenosine-diphosphate-ribose-polymerase 1 (PARP1) recognises free DNA endings (Chaudhuri and Nussenzweig, 2017) and – together with X-ray repair cross-complementing protein 1 (XRCC1) – facilitates the assembly of SSB repair proteins like DNA polymerase β and DNA ligase III that finally fix the break (Chaudhuri and Nussenzweig, 2017).

However, double strand break (DSB) repair is much more complex and four different DSB repair pathways are discriminated (Scully et al., 2019). The predominant DSB repair pathway in all mammalian cells is non-homologous DNA end-joining (NHEJ) (Chang et al., 2017). Since NHEJ is based on simple DNA ending recognition and ligation independent of DNA sequences and cell cycle phases, it is very fast but error-prone (Chang et al., 2017). NHEJ starts with DNA ending recognition by Ku70/Ku80 heterodimer (Ku) (Mimori and Hardin, 1986) that prevents free DNA endings from extensive end resection (Mimitou and Symington, 2010). Ku forms a complex with the catalytic subunit of DNA-PK (DNA-PKcs), thus generating the full DNA-dependent protein kinase (DNA-PK) (Gottlieb and Jackson, 1993). Pairing of two DNA-PK complexes results in autophosphorylation and triggers the activation of exo- and endonucleases that edit incompatible DNA endings (Goodarzi et al., 2006). Further, Ku facilitates the binding of repair proteins like DNA polymerases and DNA ligase IV that fix the damage (Grawunder et al., 1997; Mahajan et al., 2002). While NHEJ is very fallible, homologous recombination (HR) is the most accurate DSB repair pathway (Scully et al., 2019). In HR, accuracy is reached by previous DNA end resection (Bonetti et al., 2018) and the use of homologous DNA sequences as templates for DNA refilling (Resnick, 1976). Due to its need for a sister chromatid serving as template, HR is limited on S and G2 cell cycle phases (Escribano-Díaz et al., 2013). In HR, DNA endings are bound by MRE11-RAD50-NBS1-complex (MRN) (Lavin, 2007) that conducts DNA end resection via its exo- and endonuclease activity. The resected single stranded DNA (ssDNA) endings are rapidly bound by the heterotrimeric replication protein A (RPA) complex to protect them from forming secondary structures (Raderschall et al., 1999). However, RPA competes with the strand-exchange protein RAD51 (Shinohara et al., 1992), and breast cancer type 2 susceptibility protein (BRCA2) facilitates the displacement of RPA by RAD51 (Jensen et al., 2010). Subsequently, RAD51 catalyses the invasion of the ssDNA strand into a homologous sister chromatid to form a displacement-loop (D-loop) (Sung, 1994). The invaded strand is extended by DNA-polymerases (McIlwraith et al., 2005), dissociates, and anneals with the other DNA ending of the broken molecule to serve as template for its complementary strand to regenerate (Nassif et al., 1994). Alternatively, the complementary strand forms a second D-loop, thus building a double Holliday junction, that is resolved at its crossing points either in non-crossover or crossover mode (Bzymek et al., 2010). The two further DSB repair pathways, alternative end joining (a-EJ) and single-strand annealing (SSA), simply anneal homologous sequences flanking the DSB (Chang et al., 2017). Hence, DNA sequences between these repeats are always lost by MRN-dependent end resection, making these two pathways very mutagenic (Chang et al., 2017). However, a-EJ is promoted by PARP1 (Robert et al., 2009) and needs only short sequence homology of at least five nucleotides (Sharma et al., 2015). In contrast, SSA requires homology of at least 30 base pairs, and RPA is needed to protect these long ssDNA molecules (Shinohara et al., 1998).

False covalent joints between nucleotide residues of complementary DNA strands, called interstrand crosslinks (ICLs), are another highly toxic type of

DNA damage since they prevent DNA unwinding needed for DNA replication and transcription (Deans and West, 2011). Their repair is conducted by the FA pathway (Rodríguez and A., 2017). To this end, ICLs are recognised by a heterodimeric complex consisting of FA complementation group protein M (FANCM) and FAAP24 (Ciccia et al., 2007). Subsequently, the FA core complex and the FANCD2-FANCI complex are recruited to the damaged site (Liang et al., 2016). The FANCD2-FANCI complex is activated by mono-ubiquitinylation at K561 (FANCD2) (Meetei et al., 2004) and K523 (FANCI) (Smogorzewska et al., 2007) by the E3 ubiquitin-ligase FANCL (Meetei et al., 2003) which is one of the eight subunits of the FA core complex (Shakeel et al., 2019). Ultimately, the activated FANCD2-FANCI complex recruits FA-associated nuclease 1 (FAN1) to incise one DNA strand (Liu et al., 2010; Pizzolato et al., 2015). The resulting DSB is finally repaired by HR (De Silva et al., 2000).

1.7.3 Coordination of the DDR

The DDR system is not limited on DNA repair mechanisms (Jackson and Bartek, 2009) but further includes complex cellular processes like cell cycle checkpoint activation (Barnum and O'Connell, 2014) and chromatin modifications (Luijsterburg and Attikum, 2011). The coordination of these different cascades is realised by two PI3K-related kinase family members: ataxia telangiectasia and Rad3 related kinase (ATR) and ataxia telangiectasia mutated kinase (ATM). ATR activation is mainly triggered by ssDNA (Zou and Elledge, 2003) that arises for instance at stalled replication forks upon replicative stress. ssDNA is stabilised by RPA (Wold and Kelly, 1988) that interacts with ATR-interacting protein (ATRIP) to stimulate the binding of ATR-ATRIP to ssDNA (Zou and Elledge, 2003). Subsequently, ATR is activated by autophosphorylation at T1989 (Liu et al., 2011; Nam et al., 2011). Activated ATR phosphorylates numerous downstream targets, for instance checkpoint kinase 1 (CHK1) that supports cell cycle checkpoint arrest (Liu et al., 2000). ATM, the other important DDR regulative kinase, is activated as part of cellular DSB response (Lee and Paull, 2004; Lee and Paull, 2005; Jazayeri et al., 2008) by MRN via monomerisation and autophosphorylation at S1981 (Bakkenist and

Kastan, 2003). Amongst the downstream targets getting phosphorylated and therefore activated by ATM are the cell cycle protein checkpoint kinase 2 (CHK2) (Matsuoka et al., 1998), the chromatin regulating protein Krüppel associated box (KRAB)-interacting protein 1 (KAP1) (Ziv et al., 2006), and the H2A histone family member X (H2AX) (Burma et al., 2001). Phosphorylated H2AX (γH2AX) accumulates rapidly in nucleosomes adjacent to DSBs (Rogakou et al., 1998) and promotes chromatin decondensation to facilitate the recruitment of further DDR proteins, like MRN (Kobayashi et al., 2002), RAD51 (Paull et al., 2000), p53 binding protein 1 (53BP1) (Ward et al., 2003) and breast cancer type 1 susceptibility protein (BRCA1) (Paull et al., 2000). The balance between BRCA1 and 53BP1 is suggested to determine DSB repair pathway choice (Escribano-Díaz et al., 2013) since BRCA1 supports HR (Moynahan et al., 1999) while 53BP1 stimulates NHEJ (Nakamura et al., 2006).

1.7.4 Cell cycle checkpoints

Prohibiting cell cycle progression and cell division in the presence of DNA damage is crucial for guarding genomic stability (Barnum and O’Connell, 2014). Thus, cell cycle checkpoint activation is a relevant part of the DDR system (Barnum and O’Connell, 2014). The cell cycle is a strictly regulated cellular process that is classified in four main phases: first gap phase (G1), DNA synthesis phase (S), second gap phase (G2), and mitosis (M) (Barnum and O’Connell, 2014). Cell cycle progression through these phases is stimulated by a group of serine/threonine kinases, called CDKs, that promote DNA synthesis and mitotic progression by phosphorylating key substrates (Malumbres and Barbacid, 2001; 2009). The activation of these CDKs is regulated by periodic synthesis and ubiquitin-dependent proteolysis of their regulatory subunits, called cyclins (Glotzer et al., 1991). If a cyclin binds to its CDK, the CDK forms an active heterodimeric complex (Malumbres and Barbacid, 2001; 2009). Moreover, CDK activity is regulated by the two families of cyclin-dependent kinase inhibitors INK4 (including $p16^{INK4a}$ (McConnell et al., 1981)) and CIP/KIP (including $p21^{cip1/waf1}$ (Xiong et al., 1993)). Last but not least, CDKs are influenced by phosphorylation events. Most importantly, inhibitory phosphorylations at CDK residues within their ATP binding loop are carried out by the protein kinase WEE1 (Parker and Piwnica-Worms, 1992) and removed by the phosphatase cell division cycle 25 (CDC25) (Strausfeld et al., 1991; Hoffmann et al., 1994). Thereby, CDC25 promotes transition from G1 to S (mainly CDC25A (Hoffmann et al., 1994)) and G2 to M (mainly CDC25B and CDC25C (Strausfeld et al., 1991)) phase. In response to DNA damage, the serine-threonine kinases CHK1 and CHK2 trigger cell cycle arrest at diverse stages by phosphorylating CDC25, thus targeting it for proteasomal degradation (Peng et al., 1997; Sanchez et al., 1997; Matsuoka et al., 1998).

CHK1 and CHK2 are part of a complex internal supervision system containing four main cell cycle checkpoints (G1 checkpoint, intra-S-phase checkpoint, G2 checkpoint, spindle assembly checkpoint) that trigger cell cycle arrest after error detection (Hartwell and Weinert, 1989). If cellular reserves, cell size, or genomic DNA integrity are unfavourable for DNA replication, G1 checkpoint is activated to prevent progression to S phase (Killander and Zetterberg, 1965). The most familiar component of G1 checkpoint is p53, which promotes the expression of p21 (El-Deiry et al., 1993) that inhibits G1 CDKs (Harper et al., 1993; Harper et al., 1995; Deng et al., 1995). After passing G1 checkpoint, cells undergo DNA replication in S phase. Disturbances within the replication process (e.g. by DNA lesions or insufficient supply of deoxynucleotide triphosphates) result in replicative stress. This goes along with abundant ssDNA formation that triggers ATR-CHK1-mediated intra-S-phase checkpoint (Longhese et al., 1996). As a further barrier, G2 checkpoint prohibits entry into mitosis until damaged DNA or incompletely replicated DNA is sufficiently repaired. The main kinase involved in G2 checkpoint is CHK1 (Liu et al., 2000). Besides executing inactivating phosphorylation of CDC25 (Peng et al., 1997; Sanchez et al., 1997), CHK1 phosphorylates the tyrosine-specific protein kinase WEE1, thus triggering its stabilisation (O'Connell et al., 1997). WEE1 mediates cell cycle arrest via phosphorylation and thus inactivation of CDK1 (Parker and Piwnica-Worms, 1992). Moreover, sustained G2 arrest is enforced by p53 upon persistent DNA damage via up-regulation of E2F7 (Carvajal et al., 2012) and down-regulation of the CDC25C gene (St. Clair et al., 2004). Last but not least, the mitotic kinase aurora B activates spindle assembly checkpoint in the middle of M phase to prevent anaphase onset until each chromosome is properly attached to the spindle apparatus (Hauf et al., 2003). Although it is generally accepted that all cell cycle checkpoints are reversible and cell cycle proceeds when the damage signal fades, however, prolonged cell cycle arrest can trigger apoptosis (Orth et al., 2011) and cellular senescence (Demidenko and Blagosklonny, 2008), thus changing the cellular fate permanently.

1.8 Current state of research linking CX-5461 with the DDR

Initially, the RNAP I inhibitor CX-5461 was suggested to inhibit rRNA synthesis selectively without affecting DNA, mRNA or protein synthesis (Drygin et al., 2011). However, this concept was challenged by some following studies that had observed DDR activation upon CX-5461 treatment (Negi and Brown, 2015; Quin et al., 2016; Xu et al., 2017). The first study reporting DDR activation upon CX-5461 treatment was published by Negi and Brown in 2015. Their experiments had revealed ATM-CHK2- and ATR-CHK1-pathway activations with subsequent G2 arrest in CX-5461 treated acute lymphoblastic leukaemia (ALL) cells (Negi and Brown, 2015). This finding was supported by another study showing accumulation of ATM, ATR, CHK1 and CHK2 proteins in CX-5461 treated primary immortalised human fibroblasts (BJ-T) (Quin et al., 2016). Paradoxically, the authors suggested that CX-5461 activates ATM-CHK2- and ATR-CHK1-pathways in the absence of DNA breaks since they neither observed γH2AX foci in immunofluorescence nor extended comet tail moments in single cell gel electrophoresis (Quin et al., 2016). Quite the opposite, Xu et al. proposed that CX-5461 provokes SSBs or gaps and to a minor degree also DSBs based on their experiments showing statistically increased comet tail moments 30 minutes after CX-5461 treatment in HCT116 cells (Xu et al., 2017). Further, they observed formation of γH2AX, as well as RAD51, RPA2 and 53BP1 foci 24 hours after CX-5461 treatment in HCT116 and U2OS cells (Xu et al., 2017). Intriguingly, CX-5461 was more toxic in various BRCA2 deficient cell lines than in BRCA2 proficient ones, and cells absent of functional BRCA2 acquired more often 53BP1 foci and stronger H2AX and RPA phosphorylation upon drug treatment (Xu et al., 2017). Moreover, HCT116 cells deficient for BRCA2, but not BRCA2 wild type cells, acquired chromosomal abnormalities 48 hours after CX-5461 treatment (Xu et al., 2017). Since other methods of rDNA transcription inhibition (BMH-21, siRNA for POLR1B) did not cause γH2AX and 53BP1 foci formation (Xu et al., 2017), the authors suggested that CX-5461 might trigger DNA damage independent from its main function in rDNA transcription inhibition (Xu et al., 2017).

However, co-treatment strategies with CX-5461 and DDR inhibitors revealed conflicting results. While pre-treatment with the ATR kinase inhibitor VE-822 allowed overcoming CX-5461 induced G2 arrest and increased the apoptotic fraction in two different leukaemia cell lines, this was not the case for the ATM inhibitor KU-60019 (Negi and Brown, 2015). Further, combination therapy with CX-5461 and dual DDR inhibition (ATM (KU-55933) and ATR (VE-821) inhibitors) caused abnormal mitosis and cell death in BJ-T p53sh (expressing a short hairpin RNA targeting p53) but not BJ-T p53 wild type cells (Quin et al., 2016), and knocking down BRCA2 or DNA-PK, but not 53BP1, enhanced the lethality of CX-5461 in HCT116 cells (Xu et al., 2017). Altogether, the discrepancies of pre-existing data leave a lot of questions unanswered, and this work mainly aimed to examine the interplay between CX-5461 triggered DDR activation and senescence induction.

2 Aim Of This Work

Unpublished work by the Zender laboratory (K. Wolter) has demonstrated CX-5461 as potent inducer of a novel type of cellular senescence, designated ribosomal checkpoint induced senescence (RCIS). Since senescence in general was shown to be linked to DDR activation, we wondered if RCIS induction is accompanied by DDR signalling as well. Previous publications reporting DDR activation upon CX-5461 treatment were limited on the first hours upon drug treatment, thus letting long-term effects and senescence induction unnoticed. This work goes beyond previous studies by performing parallel in-depth time course analysis of DDR and senescence markers during the whole process between initial CX-5461 treatment and final RCIS establishment in murine Nras^{G12V} p19$^{-/-}$ HCC cells. Besides being the first work reporting correlations between pharmaceutical RCIS induction and DDR activation, this work is the first characterising DDR activation upon CX-5461 treatment in a hepatocellular carcinoma (HCC) cell line in general.

Previous work by the Zender laboratory has demonstrated the use of two-step anticancer strategies with senescence induction by CX-5461 followed by senolytic therapy as promising strategy to improve therapeutic outcome (K. Wolter, unpublished). Yet, so far, a lack of efficient senolytic drugs with favourable clinical safety profile prevents translation of such two punch concepts into clinical application. Although DDR protraction was determined as hallmark of cellular senescence, however, nothing is known about the potential of using DDR inhibitors as senolytic drugs. Therefore, it was the main aim of this work to investigate if DDR inhibitors are senolytic and thus effective in such two-step anticancer treatment strategies. Moreover, this work aimed to improve current knowledge how CX-5461 induces DDR activation in general. We analysed how cell cycle and genomic stability change during pharmaceutical RCIS establishment, determined how p53 status influences the cellular drug response, and finally proposed a new mechanism how CX-5461 might trigger DDR activation.

3 Material and Methods

3.1 Material

3.1.1 Equipment

Equipment	Company
Apotome	Zeiss
Biofuge fresco	Heraeus
Blot paper	Bio-Rad
Cell scraper, 16 cm	Sarstedt
Centrifuge Heraeus™ Pico™ 17	Thermo Fisher Scientific
Centrifuge Megafuge 2.0R	Thermo Fisher Scientific
Centrifuge tubes (TubeOne 1.5 ml, 2.0 ml)	Starlab
ChemiDoc Imaging System	Bio-Rad
CO_2 incubator	Sanyo
Coverslips	R. Langenbrinck
Cryo tubes	Corning Incorporated
Culture plates 6-, 12-, 24-, 96-well	Thermo Fisher Scientific
Falcons 15 ml, 50 ml	Greiner Bio-One
Flasks 50 ml, 100 ml, 500 ml, 1000 ml	Schott Duran
Flow cytometer (Guava Easy Cyte plus)	Guava Technologies
Fluorescence microscope	Olympus
Freezer (Igloo GreenLine VIP insulation 830L)	Telstar
GELoader™ Tips	Hartenstein
Immersion oil	Cargille
Neubauer chamber	Assistent
Microplate reader (Infinite® M Plex)	Tecan
Microscope (CKX41)	Olympus
Microscope slides	R. Langenbrinck
Milli-Q® Integral Water Purification System	Merck Millipore
Mini-Protean® Tetra Cell	Bio-Rad

Mini Trans-Blot® Module	Bio-Rad
Multichannel pipet (2-20 µl, 20-200 µl)	Gilson
Multichannel pipet (100 µl, 300 µl)	Eppendorf
pH meter	SI analytics
Pipet (2 µl, 20 µl, 100 µl, 200 µl, 1000 µl)	Gilson
Pipet (10 µl, 100 µl)	Eppendorf
Pipetboy	IBS Integra Biosciences
Pipet tips (TipOne 10 µl, 200 µl, 1000 µl)	Starlab
Power Pack™ Basic Power Supply (P25T)	Biometra
Polyvinylidene difluoride (PVDF) transfer membrane	Merck Millipore
Reagent reservoir, 60 ml	Brand
Rocking shaker (DRS-12)	Neolab
Sonication System	Biorupter
Sterile bench	Heraeus Instruments
Stripette™ serological pipets (5 ml, 10 ml, 25 ml, 50 ml)	Corning
Thermomixer comfort	Eppendorf
Tissue culture chambers, 4- and 8-well	Sarstedt
Tissue culture dish, 100 mm	Sarstedt
Tissue culture flask, T-25	Sarstedt
Transfer pipets	Biologix Research Company
Vortex mixer (Reax 2000)	Heidolph
Waterbath	Memmert

3.1.2 Chemicals

Chemical	Company
Aceton	ROTH
Acrylamide/Bis-acrylamide Rotiophorese Gel	ROTH
Albumin fraction V, protease-free (BSA)	ROTH
Ammonium persulfate (APS)	Sigma Aldrich
β-mercaptoethanol	ROTH
Bromophenol blue	Sigma Aldrich
Colcemid solution in HBSS, Gibco, KaryoMAX	Thermo Fisher Scientific
Crystal violet	Sigma Aldrich
Distilled water, invitrogen, DNase/RNase free	Thermo Fisher Scientific
Dulbecco’s Modified Eagle Medium (DMEM), Gibco	Thermo Fisher Scientific
Dimethylsulfoxide (DMSO)	Sigma Aldrich
Ethylenediaminetetraacetic acid (EDTA)	ROTH
Ethyleneglycoltetraacetic acid (EGTA)	ROTH
Ethanol	PanReac AppliChem
Fetal bovine serum (FBS)	PAN Biotech
Glacial acetic acid (GAA)	SAFC Pharma
Glutaraldehyde	Serva
Glycine	ROTH
Glycerol	ROTH
HCl	VWR Chemicals
Hydrogen peroxide solution	Sigma Aldrich
Isopropanol	Honeywell
$K_3FE(CN)_6$	Sigma Aldrich
$K_4FE(CN)_6$	Sigma Aldrich
KCl	AppliChem
KH_2PO_4	ROTH
MEM-NEAA (100x), Gibco	Thermo Fisher Scientific
Methanol	VWR Chemicals
$MgCl_2$	ROTH
Mounting medium with DAPI, Vectashield HardSet	Vector Laboratories
Na_2HPO_4 $2H_2O$	ROTH

NaCl	VWR Chemicals
Normal goat serum (NGS)	abcam
N-N-dimethylformamide (DMF)	Sigma Aldrich
Phosphate-buffered saline (PBS), pH 7.4, Gibco	Thermo Fisher Scientific
Penicillin-streptomycin (PenStrep), Gibco	Thermo Fisher Scientific
Paraformaldehyde (PFA)	Sigma Aldrich
Phosphatase inhibitor (PhosSTOP, EASYpack)	Roche
Phenazine methosulfate (PMS)	Sigma Aldrich
Ponceau S solution	Sigma Aldrich
Powdered milk	ROTH
Propidium iodide (PI)	Sigma Aldrich
Protease inhibitor (cOmplete Tablets Mini, EDTA-free)	Roche
Protein assay reagent A/B/S	Bio-Rad
Protein ladder, broad range, Spectra, Multicolour	Thermo Fisher Scientific
Protein ladder, high range, Spectra, Multicolour	Thermo Fisher Scientific
Sodium dodecyl sulfate (SDS), ultrapure	ROTH
RNAse	Qiagen
Sodium pyruvate 100 mM (100x), Gibco	Thermo Fisher Scientific
Stripping buffer	Thermo Fisher Scientific
Tetramethylethylenediamine (TEMED)	ROTH
Tris base (Trizma®)	Sigma Aldrich
Triton-X100	ROTH
Trypsin-EDTA 0.05%, Gibco	Thermo Fisher Scientific
Tween-20	ROTH
Urea	AppliChem
Western ECL substrate, luminol/enhancer solution	Bio-Rad
Western ECL substrate, peroxide solution	Bio-Rad
X-Gal (5-bromo-4-chloro-3-indolyl-β-D-galactopyranoside)	PeqLab
XTT (2,3-bis-(2-methoxy-4-nitro-5-sulfophenyl)-2H-tetrazolium-5-carboxanilide), invitrogen	Thermo Fisher Scientific

3.1.3 Antibodies

Abbreviations used in the following tables: species (Sp), mouse (M), rabbit (Rb), goat (Go).

Tab. 1 | Primary antibodies for western blotting

Antigen	Company	Number	Sp
α-Tubulin	CST	2125S	Rb
Aurora A	abcam	ab13824	M
Aurora B	abcam	ab2254	Rb
β-Actin	ICN Biomedicals	lab intern	M
c-MYC	abcam	ab32072	Rb
Cyclin A2	abcam	ab38	M
Cyclin B1	CST	4138S	Rb
Cyclin D1	CST	2922S	Rb
FANCD2	abcam	ab108928	Rb
FANCI	abcam	ab74332	Rb
FANCM	abcam	ab95014	Rb
HMGA2	abcam	ab97276	Rb
Lamin B1	CST	13435S	Rb
p16	Santa Cruz	sc-1207	Rb
p21	BD Biosciences	556431	M
p53	CST	2524S	M
PARP1	CST	9542S	Rb
pATM (S1987)	invitrogen	PA5-37346	Rb
pATR (S428)	CST	2853S	Rb
pCHK1 (S345)	CST	2348S	Rb
pCHK2 (T383)	abcam	ab59408	Rb
pKAP1 (S824)	abcam	ab70369	Rb
pRPA32 (S4/S8)	Bethyl	A300-245A-M	Rb
RAD51	abcam	ab63801	Rb
Vinculin	Sigma Aldrich	V9131	M

Tab. 2 | Secondary antibodies for western blotting

Antigen	Company	Conjugation	Sp
Mouse (115-035-062)	Dianova	Peroxidase	Go
Rabbit (111-035-045)	Dianova	Peroxidase	Go

Tab. 3 | Primary antibodies for immunofluorescence

Antigen	Company	Number	Sp
Ki67	abcam	ab15580	Rb
γH2AX (S139)	Merck Millipore	M05-636	M
p53BP1 (S1778)	CST	2675S	Rb
DNA:RNA hybrids [S9.6]	Kerafast	ENH001	M

Tab. 4 | Secondary antibodies for immunofluorescence

Antigen	Company	Conjugation	Sp
Mouse IgG (H+L)	Life Technologies	Alexa 488	Go
Rabbit IgG (H+L)	Life Technologies	Alexa 594	Go

3.1.4 Inhibitors

Target	Company	Number	Name
ATM	AstraZeneca	AZD-0156	-
ATR	AstraZeneca	AZD-6738	-
Bcl-2	Selleckchem	ABT-263	Navitoclax
CHK1	Selleckchem	LY-2603618	Rabusertib
CHK2	Tocris	CCT-241533	-
DNA-PK	Selleckchem	NU-7441	-
PARP	Selleckchem	AZD-2281	Olaparib
PARP	Selleckchem	AG-014699	Rucaparib
PARP	Selleckchem	MK-4827	Niraparib
RNA polymerase I	Adooq Bioscience	CX-5461	-
RPA	lab intern	unpublished	-

3.1.5 Buffers and solutions

Buffer / Solution	Composition
TBS	50 mM TrisBase, 150 mM NaCl; in H_2O
TBS-T	0.1% Tween-20 in TBS
PBS (pH 7.4)	10 mM Na_2HPO_4 x 2 H_2O, 2 mM KH_2PO_4, 0.137 mM NaCl, 2.7 mM KCl; in H_2O
PBS/$MgCl_2$ (pH 5.5)	1 mM $MgCl_2$ in PBS
X-Gal staining solution	5 mM $K_3Fe(CN)_6$, 5 mM $K_4Fe(CN)_6$ x 3 H_2O, 1 mg/ml X-Gal; in PBS/$MgCl_2$ (pH 5.5)
IF antibody dilution	1% NGS, 0.2% Triton X-100, 0.1% Tween-20; in PBS
IF blocking solution	5% NGS, 0.2% Triton X-100, 0.1% Tween-20; in PBS
Laemmli buffer [4x]	200 mM Tris-HCl (pH 6.8), 277 mM SDS, 40% glycerol, 20% β-mercaptoethanol, 3 mM bromophenol blue; in H_2O
Cell lysis buffer	20 mM Tris-HCl (pH 7.5), 150 mM NaCl, 1 mM EDTA (pH 8.0), 1 mM EGTA (pH 8.0), 1% Triton X-100; in H_2O; 1 pill protease inhibitor (Roche, cOmplete Tablets Mini, EDTA-free) and 1 pill phosphatase inhibitor (Roche, PhosSTOP, EASYpack) are dissolved in 15 ml cell lysis buffer
SDS running buffer	25 mM TrisBase, 192 mM glycine, 0.1% SDS; in H_2O
WB transfer buffer	25 mM TrisBase, 192 mM glycine, 0.01% SDS, 20% methanol; in H_2O

3.1.6 Cell culture media

Medium	Composition
Growth medium	10% FBS, 1% MEM-NEAA, 1% PenStrep, 1% sodium pyruvate; in DMEM
Freezing medium	40% FBS, 10% DMSO; in growth medium

3.1.7 Cell lines

Name	Tissue	Species
$Nras^{G12V}$ $p19^{-/-}$	Hepatocellular carcinoma	murine
$Nras^{G12V}$ $p19^{-/-}$ $p53^{-/-}$	Hepatocellular carcinoma	murine
SMMC-7721	Hepatocellular carcinoma	human

3.1.8 Software

Topic	Category	Software
Experimental work	Flow cytometry	Guava CytoSoft 5.2
	Microplate reader	i-control 2.0
	Microscope	Olympus cellSens
	Fluorescence microscope	Olympus cellSens
	Apotome	AxioVision Imaging Software
	Western blot analysis	Image Lab Software
Data analysis	Statistical analysis	GraphPad Prism 6
	Graphical illustration	GraphPad Prism 6
	Picture editing	Image J
Data presentation	Figure design	Microsoft PowerPoint
	Writing program	Microsoft Word
Literature research	Literature programs	EndNote X8 and JabRef

3.2 Methods

3.2.1 Cell culture

Cells were cultivated in growth medium (see chapter 3.1.6) within Petri dishes at 37 °C in a CO_2 incubator. Cellular subconfluence was maintained by regularly passaging cells in 1:10 ratio. To this end, cells were washed with PBS, detached via incubation with 1 ml trypsine for five minutes at 37 °C, and resuspended in fresh growth medium. To determine the cell density, 10 µl of the cell suspension was put on a Neubauer chamber and cells were counted manually. The cell density was calculated with the following formula: cell number per ml = (cell count within four big squares / 4) x 10,000.

Cryoconservation at - 80 °C was used for long-term preservation of cell lines. For freezing, cells were detached by trypsinisation, transferred to a 15 ml cell culture tube and centrifuged for five minutes at 800 rpm. After resuspending the pellet in 5 ml of freezing medium (see chapter 3.1.6), the cell suspension was filled in cryo tubes and stored at - 80 °C. For thawing, cryo tubes were held in a 37 °C water bath for 30 seconds. The defrosted cells were diluted with 5 ml of pre-warmed growth medium and centrifuged for five minutes at 800 rpm. After resuspending the pellet in fresh growth medium, the cell suspension was transferred to a cell culture bottle and stored in a 37 °C CO_2 incubator.

3.2.2 Treatment with CX-5461

For most experiments, cells were treated with the RNAP I inhibitor CX-5461. The drug was stored as 1 mM stock at - 20 °C. Prior to treatment, cells were stored for 36 hours in cell culture dishes in a 37 °C CO_2 incubator. Immediately before treatment, CX-5461 was defrosted and diluted with fresh growth medium to a final concentration of 500 nM (if not explicitly stated different). The growth medium within the cell culture dishes was replaced by the freshly prepared medium containing 500 nM of CX-5461. After incubating for 24 hours in a CO_2 incubator at 37 °C, the CX-5461 containing medium was removed, cells were washed once with PBS, and fresh growth medium without CX-5461 was added.

Finally, cells were cultivated in a 37 °C CO_2 incubator up to the indicated treatment time point.

3.2.3 Crystal violet colony formation assay

For crystal violet colony formation assay, cells were cultivated in 24 well plates and treated in different ways as illustrated in Tab. 5. For fixation, cells were washed two times with PBS and incubated with 10% PFA for 20 minutes at room temperature. After a washing step with Milli-Q® water, cells were incubated with 0.5% crystal violet for 20 minutes, washed two more times with Milli-Q® water, and air-dried under a fume hood.

Tab. 5 | Experimental set-up for crystal violet colony formation assay

Abbreviations used in this table: plating (P), inhibitor treatment (I), CX-5461 treatment (C), fixation (F). Settings are labelled by a-e as used in the results part of this work.

	Setting	Timeline
a	inhibitor on growing cells	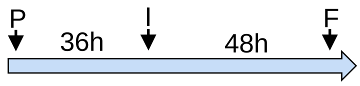
b	pre-treatment with inhibitor	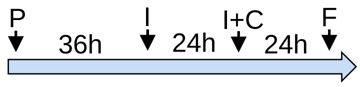
c	simultaneous treatment	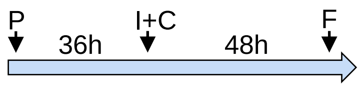
d	inhibitor on RCIS cells (2 days)	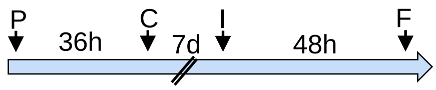
e	inhibitor on RCIS cells (9 days)	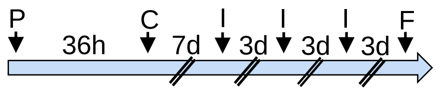

3.2.4 XTT cell viability assay

For XTT cell viability assay, cells were cultivated in 96 well plates for 36 hours. Next, the prepared cells were treated with a dilution series of different drug concentrations for 48 hours (100 µl of liquid per well). Each treatment setting was conducted in triplicates and three wells were filled with pure growth medium without cells to measure background activity. Immediately before labelling cells, 10 µl of PMS solution (10 mM PMS in PBS) was mixed with 4 ml of XTT solution (0.1% XTT in pre-warmed growth medium) and 25 µl of this mixture was added to each well. After incubating for two hours at 37 °C, absorbance was measured at 450 nm using Tecan Microplate Reader.

3.2.5 Senescence-associated β-galactosidase staining

For SA-β-Gal staining, cells were plated in 10 cm dishes and treated with CX-5461 as described in chapter 3.2.2. To stain all different treatment time points simultaneously, plating and treatment were performed individually for each sample, so that finally all samples were ready for fixation all at once. For fixation, cells were washed with PBS, incubated with 0.5% glutaraldehyde in PBS (pH 7.4) for five minutes at room temperature, washed once more with PBS, and two more times with 1 mM $MgCl_2$ in PBS (pH 5.5) for five minutes each at room temperature. Next, cells were incubated with X-Gal staining solution (see chapter 3.1.5) at 37 °C until the cells without CX-5461 (negative control) started to adopt blue staining. At this time point, reaction was stopped for all the samples by washing all dishes three times with PBS for five minutes each before treating them with 37% formaldehyde for 30 minutes at room temperature. After three final washing steps with PBS for five minutes each, coloured pictures were taken using Zeiss Apotome.

3.2.6 Protein extraction and quantification

For protein extraction, cells were plated in 10 cm Petri dishes and treated with CX-5461 as described in chapter 3.2.2. For the untreated control sample, as well as the early CX-5461 treatment time points up to one day, two dishes were prepared and pooled to receive approximately the same amount of cellular material for all the samples. Before harvesting, cells were washed two times with PBS and got diluted in 0.6 ml of PBS. Detachment was done mechanically using a cell scraper. The cell suspension was transferred to a 1.5 ml Eppendorf cup and centrifuged at 13,000 rpm for three minutes. The pellets were stored at - 80 °C. To generate whole cell lysates, cell lysis buffer (see chapter 3.1.5) was freshly prepared, diluted in 4:1 ratio with 8 M Urea, and added to the defrosted pellets. Next, samples were sonicated (Biorupter Sonication System) for ten minutes and centrifuged at 13,000 rpm for ten more minutes. The supernatants were transferred to new Eppendorf cups and stored again at - 80 °C. To measure protein densities of the whole cell lysates, Bradford protein assay kit was used according to the manufacturer’s instructions. In doing so, absorbance was measured at 690 nm using Tecan Microplate Reader.

3.2.7 SDS gel electrophoresis

SDS gel electrophoresis was used to separate the whole cell lysates (see chapter 3.2.6) in a molecular weight dependent fashion. To this end, running gels were poured as listed in Tab. 6. While high percentage running gels were favoured for analysing small proteins, low percentage running gels were preferred for bigger ones. The poured running gels were topped with 500 µl of isopropanol during drying. After gels had solidified, the isopropanol topping was replaced by the stacking gel solution (Tab. 7) and 15 well combs were used to form gel pockets. For each sample, the protein lysate volume containing 50 µg of protein was diluted in PBS up to a total volume of 20 µl. For denaturation, 6.7 µl of the Laemmli buffer stock [4x] (see chapter 3.1.5) was added to each sample, followed by an incubation step at 95 °C for ten minutes. The first gel pocket was loaded with a protein ladder while all the further pockets were loaded with the prepared sample materials. Finally, protein separation took place in running buffer (see chapter 3.1.5) at 100 - 120 V.

Tab. 6 | Running gel composition

Chemical		5%	7%	10%	12%	15%
Milli-Q®	ml	17.2	15.3	12.3	10.2	7.2
1.5 M Tris-HCl (pH 8.8)	ml	7.5	7.5	7.5	7.5	7.5
SDS 20% (w/v)	µl	150	150	150	150	150
Acrylamide/Bis-acrylamide 30%, 0.8% (w/v)	ml	5.0	6.9	9.9	12.0	15.0
APS 10% (w/v)	µl	150	150	150	150	150
TEMED	µl	20	20	20	20	20

Tab. 7 | Stacking gel composition

Chemical		
Milli-Q®	ml	6.15
0.5 M Tris-HCl (pH 6.8)	ml	2.5
SDS 20% (w/v)	µl	50
Acrylamide/Bis-acrylamide 30%, 0.8% (w/v)	ml	1.34
APS 10% (w/v)	µl	50
TEMED	µl	10

3.2.8 Western blotting

Western blotting was used to transfer the separated proteins (see chapter 3.2.7) from the gel to a PVDF membrane. To this end, the PVDF membrane was pre-incubated with 75% methanol for two minutes, followed by two minutes with Milli-Q® water and two more minutes with transfer buffer (see chapter 3.1.5). After preparing the transfer box in accordance with the manufacturer's instructions, the transfer process took place in transfer buffer at 4 °C either at 120 V for approximately two hours or at 25 V overnight. The exact transfer time varied amongst different analyses depending on the molecular weight of the investigated protein (extended duration for bigger proteins, shortened duration for smaller ones). To ensure that the transfer process was successful, the PVDF membrane was incubated with Ponceau S staining solution, thus colouring the transferred proteins in red. For blocking, the PVDF membrane was incubated with either 5% milk powder or 5% BSA (listed in Tab. 8) in TBS-T for 90 minutes at room temperature. This and all the further steps were conducted under slightly shaking conditions at 35 rpm. After three washing steps with TBS-T, the blocked PVDF membrane was incubated with the primary antibody (diluted in TBS-T, concentrations are listed in Tab. 8) for twelve hours (small and unphosphorylated proteins) up to three days (huge and phosphorylated proteins) at 4 °C. After three more washing steps for ten minutes each, the PVDF membrane was incubated with the secondary antibody (diluted in TBS-T at 1:3000) for 40 minutes at room temperature. Again, the membrane was washed three times with TBS-T for ten minutes each before it was finally incubated with a 1:1 mixture of luminol/enhancer and peroxide solutions (BioRad® Western Blot ECL Kit) for approximately five minutes under light-protected conditions. In the end, the blots were developed using Western Blot Imaging System and Image Lab Software.

Tab. 8 **|** Primary antibody concentrations and blocking for western blotting

Antigen	MW [kDa]	Concentration	Blocking
α-Tubulin	50	1:1000	Milk
Aurora A	46	1:1000	Milk
Aurora B	39	1:1000	Milk
β-Actin	42	1:1000	Milk
c-MYC	49	1:1000	Milk
Cyclin A2	60	1:200	Milk
Cyclin B1	55	1:1000	Milk
Cyclin D1	36	1:1000	Milk
FANCD2	166	1:1000	Milk
FANCI	149	1:2000	Milk
FANCM	227	1:5000	Milk
HMGA2	17	1:1000	Milk
Lamin B1	70	1:1000	Milk
p16	16	1:200	Milk
p21	18	1:333	Milk
p53	53	1:1000	Milk
PARP1	116	1:1000	Milk

pATM (S1987)	351	1:1000	BSA
pATR (S428)	301	1:1000	BSA
pCHK1 (S345)	54	1:1000	BSA
pCHK2 (T383)	61	1:1000	BSA
pKAP1 (S824)	110	1:1000	BSA
pRPA32 (S4/S8)	34	1:5000	Milk
RAD51	37	1:1000	BSA
Vinculin	124	1:5000	Milk

3.2.9 Immunofluorescence

For immunofluorescence stainings, cells were plated in either 4- or 8-well tissue chambers with detachable walls and treated with CX-5461 as described in chapter 3.2.2. To stain all the different drug treatment time points simultaneously, plating and treatment were performed individually for each sample, so that finally all samples were ready for fixation all at once. Equal cell densities at fixation were reached by plating out only half as many cells for the late drug treatment time points (three, five and seven days) than for the untreated control sample and the early CX-5461 treatment time points (up to one day after treatment). Just prior to fixation, growth medium was removed carefully with a pipet and cells were washed once with either 0.1% Triton X-100 in PBS (used for all washing steps in Ki67, γH2AX (S139) and p53BP1 (S1778) stainings) or pure PBS (used for all washing steps in DNA:RNA hybrid [S9.6] and pure DAPI stainings). For Ki67, γH2AX (S139), p53BP1 (S1778) and pure DAPI stainings, cells were fixed with 4% PFA in PBS for 30 minutes at room temperature. For DNA:RNA hybrid [S9.6] staining, fixation was done with ice-cold methanol for 15 minutes at - 20 °C. Except for the DNA:RNA hybrid [S9.6] staining, cells were washed two times after fixation before getting permeabilized by 0.5% Triton X-100 in PBS for 15 minutes at room temperature, followed by four more washing steps. In contrast, no permeabilization step was performed in the DNA:RNA hybrid [S9.6] staining. Instead of that, only three normal washing steps were conducted. Next, cells were incubated with blocking solution (see chapter 3.1.5) for 15 minutes at room temperature. For staining, the antibodies were thinned with dilution solution (see chapter 3.1.5) as listed in Tab. 9. Cells were incubated with the primary antibody at 4 °C overnight, washed three times for five minutes each at room temperature, and finally got incubated with the secondary antibody for 45 minutes at room temperature under light-protected conditions. After three more washing steps for five minutes each, the walls of the culture chamber were removed. Mounting medium with DAPI was added on the remaining microscope slide before it was coated by a coverslip. Finally, the slides were analysed using Zeiss fluorescence microscope. For quantification, 'positive' cells were counted manually with the help of Image J. The total cell count was determined by counting all nuclei stained with DAPI. Ki67 staining was pan-nuclear so that all stained nuclei were interpreted as Ki67 'positive' cells. In contrast, thresholds were set to classify cells as 'positive' for γH2AX (≥ 5 foci) or p53BP1 (≥ 3 foci).

Tab. 9 **|** Antibody concentrations for immunofluorescence

Primary Antibody		Secondary Antibody	
Antigen	Concentration	Antigen	Concentration
Ki67	1:1000	rabbit (Alexa 594)	1:1000
γH2AX (S139)	1:1000	mouse (Alexa 488)	1:500
p53BP1 (S1778)	1:100	rabbit (Alexa 594)	1:500
DNA:RNA hybrid [S9.6]	1:200	mouse (Alexa 488)	1:500

3.2.10 Flow cytometric cell cycle analysis with propidium iodide

For cell cycle analysis, cells were cultivated in 10 cm dishes, treated with CX-5461 (see chapter 3.2.2) up to the indicated time point, detached chemically via trypsinisation, and resuspended in fresh growth medium. Next, 10^6 cells per sample were transferred to a 15 ml falcon and spun down at 1200 rpm for five minutes. The pellet was washed once with PBS before it was resuspended in 250 µl of PBS. For fixation, 750 µl of pure ethanol (- 20 °C) was added drop by drop while vortexing and cells were stored in fixative at 4 °C. Just prior to the staining with the fluorescent DNA intercalating agent propidium iodide (PI), cells were washed with 1% BSA in PBS. For staining, the pellet was resuspended in

1 ml of PI-RNase-solution (50 µg/ml PI and 250 µg/ml RNase in PBS) and incubated at 4 °C overnight. After that, cells were resuspended and transferred to a 96-well plate (250 µl per well). Finally, Guava Easy Cyte plus flow cytometer and CytoSoft 5.2 software were used to measure the DNA content per cell. Cells with 2N DNA content (single chromosome set) were interpreted as G1 phase cells, while cells with 4N DNA content (doubled chromosome set) were classified as G2/M phase cells. Cells with a DNA content between these two fractions were determined as S phase cells, while cells with more than 4N DNA content were classified as hyperploid.

3.2.11 Chromosome spread assay

For chromosome spread assay, cells were cultivated in 10 cm dishes and treated with CX-5461 (see chapter 3.2.2) up to the indicated time point. Just prior to trypsin-based detachment, cells were treated with 500 µg/ml colcemid for two hours to enhance the fraction of metaphase cells. The detached cells were centrifuged at 1000 rpm for 4 minutes. After aspirating most of the supernatant, cells were resuspended in some residual liquid. Next, 5 ml of ice cooled 0.56% KCl solution was added drop by drop while vortexing. After incubating for six minutes at room temperature, cells were centrifuged at 1000 rpm for six minutes, and the pellet was again resuspended in some residual liquid of the supernatant. For fixation, 5 ml of fixative (consisting of three parts methanol and one part GAA) was added drop by drop while vortexing and cells were again centrifuged at 1000 rpm for six minutes. This fixation step was repeated two more times. After having aspirated the supernatant, the pellet was finally resuspended in 1 ml of fixative. For each sample, three microscope slides (cleaned with alcohol) were sprinkled with three drops of the prepared cell suspension released from about 50 cm distance to spread as wide as possible. After drying for at least one hour at room temperature, mounting medium with DAPI was added, and the microscope slides were sealed with coverslips. For analysis, Zeiss fluorescence microscope and cellSens software were used.

4 Results

4.1 Senescence marker analysis upon CX-5461 treatment

We used crystal violet colony formation and XTT cell viability assays to measure how the RNAP I inhibitor CX-5461 affects cell viability in murine $Nras^{G12V}$ $p19^{-/-}$ HCC cells (Fig. 1 A-B). As established by K. Wolter (unpublished), CX-5461 treated cells showed strong reduction of blue dots in crystal violet colony formation assay, consistent with less viable cells (Fig. 1 A). However, this cell viability reducing effect was observed for all the three concentrations that have been tested in this experiment (250 nM, 500 nM, 1 µM). In line with previous data from our laboratory presenting that CX-5461 induces senescence rather than cell death in murine $Nras^{G12V}$ $p19^{-/-}$ HCC cells (K. Wolter, unpublished), even very high drug doses did not completely eradicate murine $Nras^{G12V}$ $p19^{-/-}$ HCC cells (Fig. 1 B). This saturation effect observed for high drug doses supports once more the findings of K. Wolter that CX-5461 reduces cell viability by arresting cellular proliferation rather than provoking apoptosis.

To characterise the kinetics of this growth arrest in more detail, we did immunofluorescence staining with the proliferation marker Ki67 in untreated cells as well as three hours, twelve hours, three days and seven days after CX-5461 treatment in murine $Nras^{G12V}$ $p19^{-/-}$ HCC cells (Fig. 1 E-F). As expected, untreated cells were highly proliferating with 99.06% (95% CI = 97.75 - 100.4%, SD = 1.82) of them being positive for Ki67. The rate of Ki67 positive cells just slightly declined three and twelve hours after CX-5461 treatment, but significantly ($P < 0.0001$) dropped after three (mean 26.39%, 95% CI = 24.55 - 28.22%, SD = 2.57) and seven (mean 2.06%, 95% CI = 0.41 - 3.72%, SD = 2.31) days, thus indicating that loss of proliferative activity mainly occurs between twelve hours and three days after CX-5461 treatment in murine $Nras^{G12V}$ $p19^{-/-}$ HCC cells.

The finding that CX-5461 is a potent inducer of RCIS was, amongst other things, based on high ß-galactosidase levels in fully established RCIS cells – a cellular state that has been defined for murine Nras^{G12V} p19$^{-/-}$ HCC cells one week after CX-5461 treatment (K. Wolter, unpublished). However, SA-β-Gal staining at earlier treatment time points was not yet examined. Here, I used SA-β-Gal staining at different drug treatment time points to visualise the process of RCIS induction upon CX-5461 treatment in murine Nras^{G12V} p19$^{-/-}$ HCC cells (Fig. 1 C & G). Intriguingly, the fraction of SA-β-Gal positive cells significantly (P < 0.0001) increased already one day after drug treatment (mean 28.37%, 95% CI = 24.72 - 32.02%, SD = 5.10). Within the following days, the fraction of SA-β-Gal positive cells continuously rose to 90.93% (95% CI = 88.94 - 92.93%, SD = 2.79) at the seven days time point. Therefore, this experiment unveils rising SA-β-Gal enzyme activity as a dynamic and time-consuming process during RCIS induction that starts already one day after CX-5461 treatment.

Given that SA-β-Gal staining alone is not sufficient to confirm senescence, I did in-depth time-course analysis of multiple proteins that have been proposed as senescence markers to characterise the kinetics of RCIS induction in murine Nras^{G12V} p19$^{-/-}$ HCC cells in more detail. To this end, I compared cellular protein contents of untreated and nine different CX-5461 treated samples (ranging from one hour to seven days after drug treatment) using SDS gel electrophoresis and western blotting techniques (Fig. 1 D). While p53 protein was not measurable in untreated cells as well as one hour after drug treatment, it strongly amassed after three hours and reached its maximum at the five hours time point. Although p53 protein levels decreased in the further course, they stayed higher than in the untreated sample at all the late treatment time points. Quite similarly, the CDK inhibitors p21 and p16 started to accumulate three hours after CX-5461 treatment. For p21, highest protein levels were measured between five hours and one day after drug treatment, while p16 protein peaked one day after treatment. Afterwards, cellular protein contents of both declined. Together, these results show that the senescence marker proteins p53, p21 and p16 accumulate transiently during CX-5461 mediated RCIS induction with reaching highest protein levels between five hours and one day after treatment.

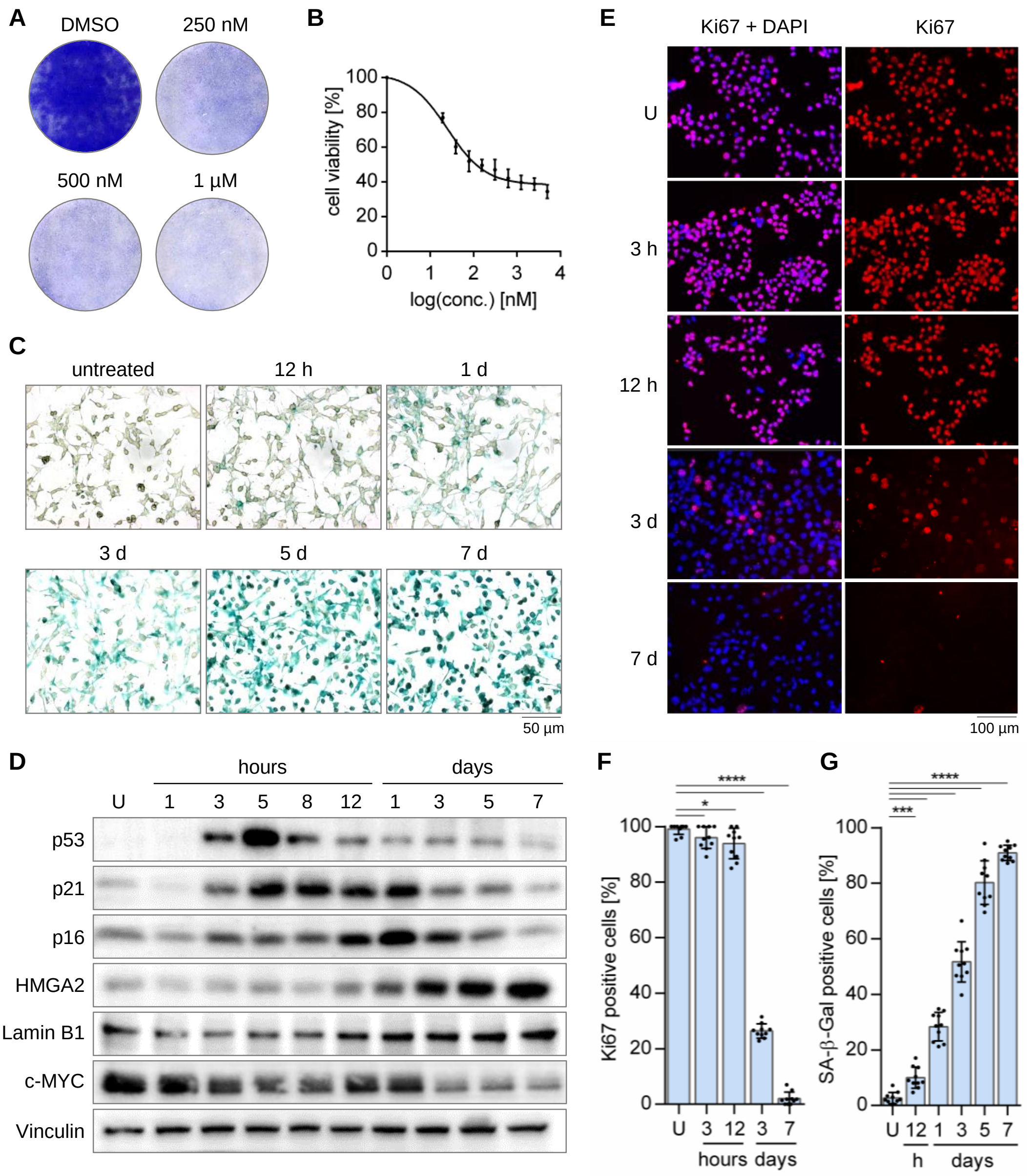

Fig. 1 | Senescence marker analysis upon CX-5461 treatment

A-G Experiments were done with murine Nras^{G12V} p19$^{-/-}$ HCC cells. CX-5461 was used at 500 nM if not explicitly stated different. **A** Crystal violet colony formation assay of cells treated with either DMSO or CX-5461 for 48 hours. **B** XTT assay of cells treated with CX-5461 for 48 hours. Data show mean ± SD (n = 3 replicates). **C & G** SA-β-Gal staining of untreated and CX-5461 treated cells. **D** Western blot analyses of senescence markers in untreated (U) and CX-5461 treated cells. CX-5461 treatment was investigated at nine time points after initial drug treatment. Vinculin is illustrated as representative loading control. All further loading controls are shown in Supplementary Figure 2 A. **E-F** Immunofluorescence staining of the proliferation marker Ki67 (red) and DAPI (blue) in untreated (U) and CX-5461 treated cells. Exposure time: DAPI 2 ms, TRITC 600 ms. Two independent experiments were performed. **F-G** For quantification, positive cells were counted in ten random optical fields per sample. Data are mean ± SD (n = 10 random optical fields). Unpaired t test with Welch's correction, * $P < 0.05$, *** $P = 0.0001$, **** $P < 0.0001$.

In contrast, cellular protein levels of HMGA2 and lamin B1 – that were both just slightly available in untreated cells or cells treated with CX-5461 for up to twelve hours – were constantly high in all the later treatment time points (one, three, five and seven days after drug treatment). This ongoing accumulation of HMGA2 and lamin B1 proteins suggests them as markers of established RCIS cells. Oppositional kinetics were observed for the transcription factor c-MYC. Its expression was high in untreated cells as well as up to one day after CX-5461 treatment, but clearly reduced after three, five and seven days, thus indicating suppression of c-MYC in RCIS cells.

4.2 DDR protein analysis upon CX-5461 treatment

As mounting evidence indicates cellular senescence as an outcome of a protracted DDR (Fagagna, 2008), we set out to investigate if CX-5461 mediated RCIS is accompanied by DDR signalling as well. To this end, immunofluorescence and western blotting techniques were used to analyse numerous DDR proteins in a time-dependent manner in CX-5461 treated murine Nras^{G12V} p19$^{-/-}$ HCC cells (Fig. 2). In the immunofluorescence assay, we stained untreated cells and four different CX-5461 treatment time points (three hours, twelve hours, three days and seven days) for the DSB marker proteins γH2AX (S139) and p53BP1 (S1778) (Fig. 2 A-B). However, 74.07% (95% CI = 63.65 - 84.50%, SD = 14.57) of the untreated cells were positive for γH2AX (S139). Nonetheless, the fraction of γH2AX (S139) positive cells significantly (P = 0.0011) increased after CX-5461 treatment and peaked at the twelve hours time point (mean 95.65%, 95% CI = 93.73 - 97.57%, SD = 2.68). Afterwards, the rate of γH2AX (S139) positive cells decreased so that it was even lower at the three and seven days time points than in the untreated sample. Different to γH2AX (S139), only 3.63% (95% CI = 2.55 - 4.72%, SD = 1.52) of the untreated cells were positive for p53BP1 (S1778). After CX-5461 treatment, the fraction of p53BP1 (S1778) positive cells impressively increased up to 90.79% (95% CI = 84.56 - 97.03%, SD = 8.71) at the twelve hours time point. Moreover, the rate of p53BP1 (S1778) positive cells stayed significantly (P < 0.0001) higher in all the CX-5461 treated samples and therefore also in RCIS cells than in the untreated sample. In summary, this immunofluorescence staining shows rapid accumulation of the DSB marker proteins γH2AX (S139) and p53BP1 (S1778) after CX-5461 treatment in murine $Nras^{G12V}$ $p19^{-/-}$ HCC cells with highest protein levels twelve hours after drug treatment.

Next, SDS gel electrophoresis and western blotting were used to visualise a larger spectrum of DDR proteins during the time course of CX-5461 mediated RCIS induction (Fig. 2 C). To draw conclusions on temporal contexts between senescence and DDR processes, I analysed the same treatment time points than in the previous senescence marker analysis (Fig. 1 D). Amongst others, I checked for phosphorylated and therefore activated proteins taking part in ATR-CHK1- (activated by ssDNA (Zou and Elledge, 2003)) and ATM-CHK2- (activated by DSBs (Lee and Paull, 2005)) pathways. While pATR (S428) was not measurable in untreated cells, it was clearly present in all the CX-5461 treated samples. However, pATR (S428) protein levels were quite equally high between one hour and eight hours after drug treatment but fluctuated at the later treatment time points. Its downstream target pCHK1 (S345) was also only slightly measurable in untreated cells, but clearly traceable between one hour and three days after CX-5461 treatment. However, five and seven days after drug treatment, cellular pCHK1 (S345) protein levels were as low as in the untreated sample. In summary, both pATR (S428) and pCHK1 (S345) proteins accumulated already one hour after CX-5461 treatment, thus indicating rapid ATR-CHK1-pathway activation upon CX-5461 treatment. The other important kinase, pATM (S1987), was also not measurable in untreated cells, but present in all the investigated treatment time points between one hour and one day after drug treatment, having its peak at the eight hours time point. However, pATM (S1987) was not observed three, five and seven days after treatment. Its downstream kinase pCHK2 (T383) also accumulated upon CX-5461 treatment and reached highest protein levels between five hours and one day after therapy. Next to CHK2, the heterochromatin protein KAP1, that is suggested to mediate gene silencing and chromatin relaxation upon DNA damage, is another downstream target of ATM (Ziv et al., 2006). While pKAP1 (S824) was not found in untreated cells, it was at high levels in all the CX-5461 treated samples without any exception. In line with the immunofluorescence results of the DSB marker proteins γH2AX (S139) and p53BP1 (S1778) (Fig. 2 A-B), the observed ATM-CHK2-pathway activation supports rapid DSB response after CX-5461 treatment. Further, the DSB repair protein RAD51 strongly amassed within the first twelve hours after CX-5461 treatment before it dramatically dropped one and three days after treatment so that it was not even measurable at the five and seven days time points. Quite similarly, cellular protein content of the ICL repair protein FANCD2 was low in untreated cells, raised between one hour and one day after drug treatment, started to decline at the three days time point and was not traceable five and seven days after treatment. FANCI, another DDR protein taking part in the FA pathway, also accumulated upon CX-5461 treatment and reached its maximum after one day. Just like FANCD2, FANCI was not measurable five and seven days after treatment. In contrast, however, FANCM protein stayed at high levels in all the late treatment time points after it had started to accumulate three hours after drug treatment. Such an ongoing protein accumulation was further observed for pRPA32 (S4/S8), a subunit of the heterotrimeric ssDNA-binding protein complex RPA (Wold and Kelly, 1988). While pRPA32 (S4/S8) was only slightly measurable in untreated cells and cells treated for up to five hours with CX-5461, it amassed in a continuous manner from eight hours to seven days after drug treatment.

Altogether, these results show that CX-5461 mediated RCIS induction is accompanied by remarkable DDR activation in murine Nras^{G12V} p19$^{-/-}$ HCC cells. While most of the analysed DDR proteins amassed transiently with having their peaks within the first 24 hours after drug treatment, however, some others (like pKAP1 (S824), pRPA32 (S4/S8) and FANCM) stayed at high levels at the later drug treatment time points and therefore in RCIS cells. Together, these results indicate that CX-5461 triggers complex DDR activation processes that are partly transient and partly permanent.

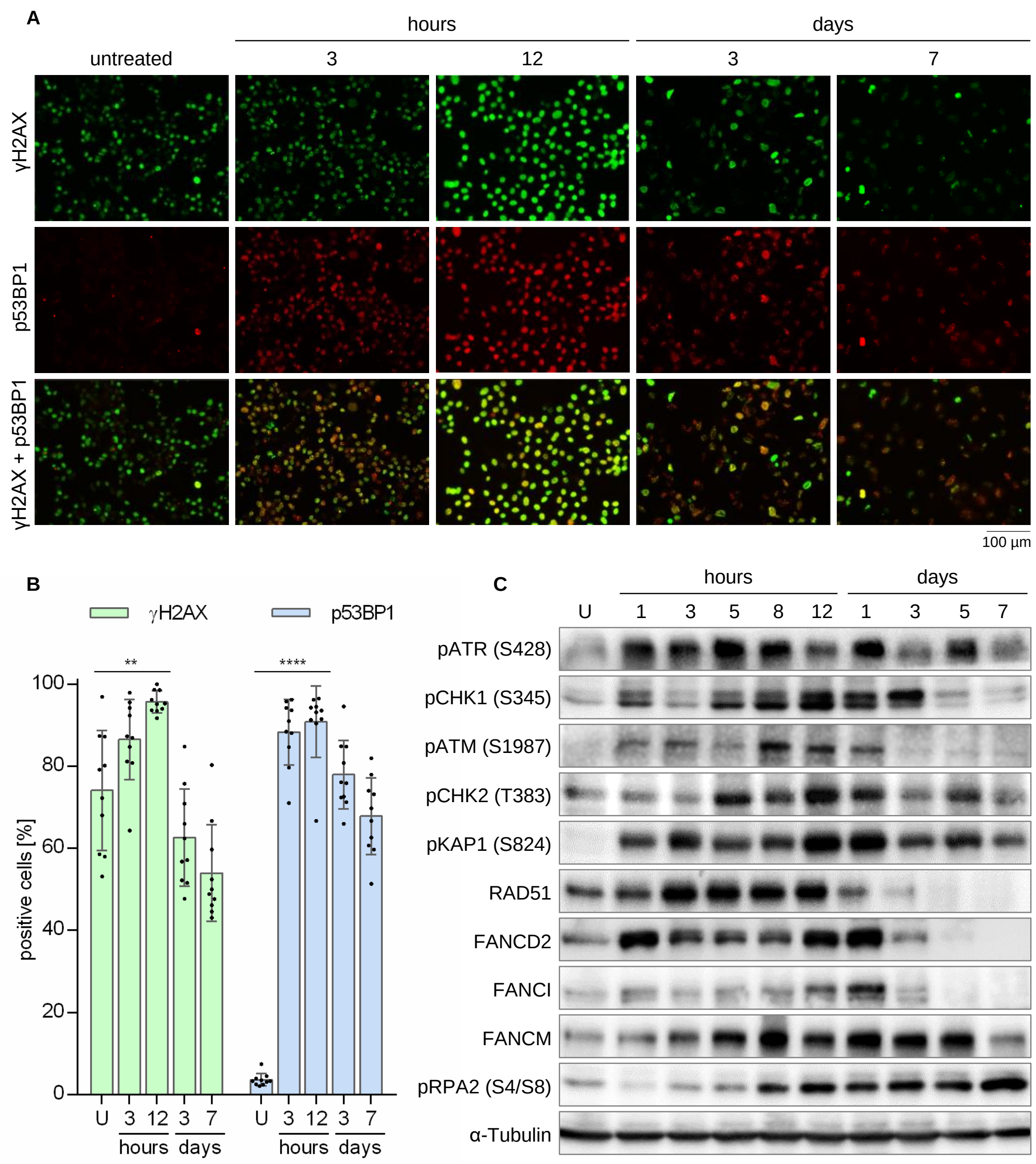

Fig. 2 | DDR protein analysis upon CX-5461 treatment

A-C Experiments were done with murine Nras^{G12V} p19$^{-/-}$ HCC cells. CX-5461 was used at 500 nM. **A-B** Immunofluorescence co-staining with γH2AX (green) and p53BP1 (red) in untreated and CX-5461 treated cells. Exposure time: DAPI 2 ms, FITC 130 ms, TRITC 500 ms. For quantification, positive cells (γH2AX ≥ 5 foci, p53BP1 ≥ 3 foci) were counted manually in ten random optical fields per sample. Data are mean ± SD (n = 10 random optical fields). Unpaired t test with Welch's correction, ** $P = 0.0011$, **** $P < 0.0001$. **C** Western blot analyses of several DDR proteins in untreated (U) and CX-5461 treated cells. CX-5461 treatment was investigated at nine time points after initial drug treatment. However, two different protein bands were observed for pCHK1 (S345), most likely due to hyperphosphorylation. α-Tubulin is illustrated as representative loading control. All further loading controls are shown in Supplementary Figure 2 B.

4.3 Combination therapy of CX-5461 and DDR inhibitors

Although a protracted DDR has been identified as hallmark of senescent cells (Fagagna, 2008), however, no data is available concerning the efficacy of DDR inhibitors as senolytic drugs. To provide first data relating to this unanswered research topic, we treated CX-5461 induced RCIS cells with several DDR inhibitors (Fig. 3, Fig. 4). Based on my previous experiments having shown that most DDR proteins accumulate transiently upon CX-5461 treatment but are absent in RCIS cells (Fig. 2), I further did co-treatment with CX-5461 and DDR inhibitors to target the DDR proteins at the time of their accumulation (Fig. 3, Fig. 4). First, IC_{50} was measured by XTT cell viability assay to choose appropriate drug concentrations for the experiment. Next, crystal violet colony formation assay was used to visualise the cell viability reducing effect of the DDR inhibitors upon the following treatment settings: a) single DDR inhibitor treatment, b) pre-treatment with DDR inhibitor followed by CX-5461 treatment, c) simultaneous treatment with DDR inhibitor and CX-5461, and d) DDR inhibitor treatment in CX-5461 induced RCIS cells. Since previous results from the Zender laboratory (K. Wolter, unpublished) have demonstrated that the senolytic agent navitoclax (Zhu et al., 2016) potently eradicates CX-5461 induced RCIS cells, navitoclax (ABT-263) was chosen as positive control. As expected, 2 µM of navitoclax sufficiently eliminated RCIS cells, or cells treated with CX-5461 and navitoclax simultaneously, without affecting non-senescent cells, thus evidencing the appropriateness of the experimental setting in detecting synergistic and senolytic effects. Next, the same procedure was executed for different DDR protein inhibitors (ATRi AZD-6738, ATMi AZD-0156, DNA-PKi NU-7441, CHK1i LY-2603618, CHK2i CCT-241533, PARPi AZD-2281, and an unpublished RPA inhibitor designed by the Zender (S. Zwirner and A. Moschopoulou) and Laufer (G.-S. Haase and G. Schmidberger) laboratories). All in all, the results were quite similar for the tested DDR inhibitors. While single DDR inhibitor treatment clearly affected the viability of growing cells, however, simultaneous treatment with CX-5461 and the DDR inhibitors was less effective in reducing cell viability. Likewise, pre-treatment with a DDR inhibitor followed by CX-5461 treatment did not cause a synergistic cell viability reducing effect. Intriguingly, CX-5461 induced RCIS cells were even fully resistant against the tested DDR inhibitors, and even dual therapy with ATM (AZD-0156) and ATR (AZD-6738) inhibitors, that was highly toxic in non-senescent cells, had nearly no effect on RCIS cells (Fig. 4 I). Together, this experiment clearly shows that the investigated DDR inhibitors are not senolytic in CX-5461 induced RCIS cells – and that they are not even capable to reduce cell viability in a synergistic manner in co-treatment strategies with CX-5461.

However, unpublished work by Oliver Bischof (Institut Pasteur, Nuclear Organisation and Oncogenesis Unit, Department of Cell Biology and Infection, Paris, France) has revealed a senolytic effect for long-term PARP inhibitor treatment in doxorubicin induced senescent fibroblasts. To test the transferability of his findings to our model of CX-5461 induced RCIS, I treated RCIS cells for nine (long-term treatment) or two (short-term treatment) days with the PARP inhibitor olaparib (Fig. 5). Non-senescent cells were treated for only two but not nine days with the PARP inhibitor since longer treatment duration was not feasible due to overgrowing of the control samples. However, 40 µM of olaparib moderately reduced cell viability in non-senescent murine $Nras^{G12V}$ $p19^{-/-}$ HCC cells but did not at all affect RCIS cells – no matter if the treatment was conducted for two or nine days. Since this outcome was unexpected regarding the promising results from Oliver Bischof, we decided to repeat the experiment with two other PARP inhibitors, namely rucaparib and niraparib. Indeed, both reduced cell viability in RCIS cells after long-term but not short-term treatment. Though, it must be mentioned that the same drug doses of rucaparib and niraparib were highly toxic in non-senescent cells already two days after treatment. Further, non-senescent cells were slightly (rucaparib) or moderately (niraparib) susceptible to lower drug doses (10 µM and 20 µM) while these doses had no effect on RCIS cells. In summary, this experiment shows that nine days PARP inhibitor treatment with rucaparib and niraparib, but not olaparib, successfully reduces cell viability in CX-5461 induced RCIS cells, but it must be emphasised that this effect is not selective since non-senescent cells are even more sensitive to PARP inhibitor treatment than RCIS cells.

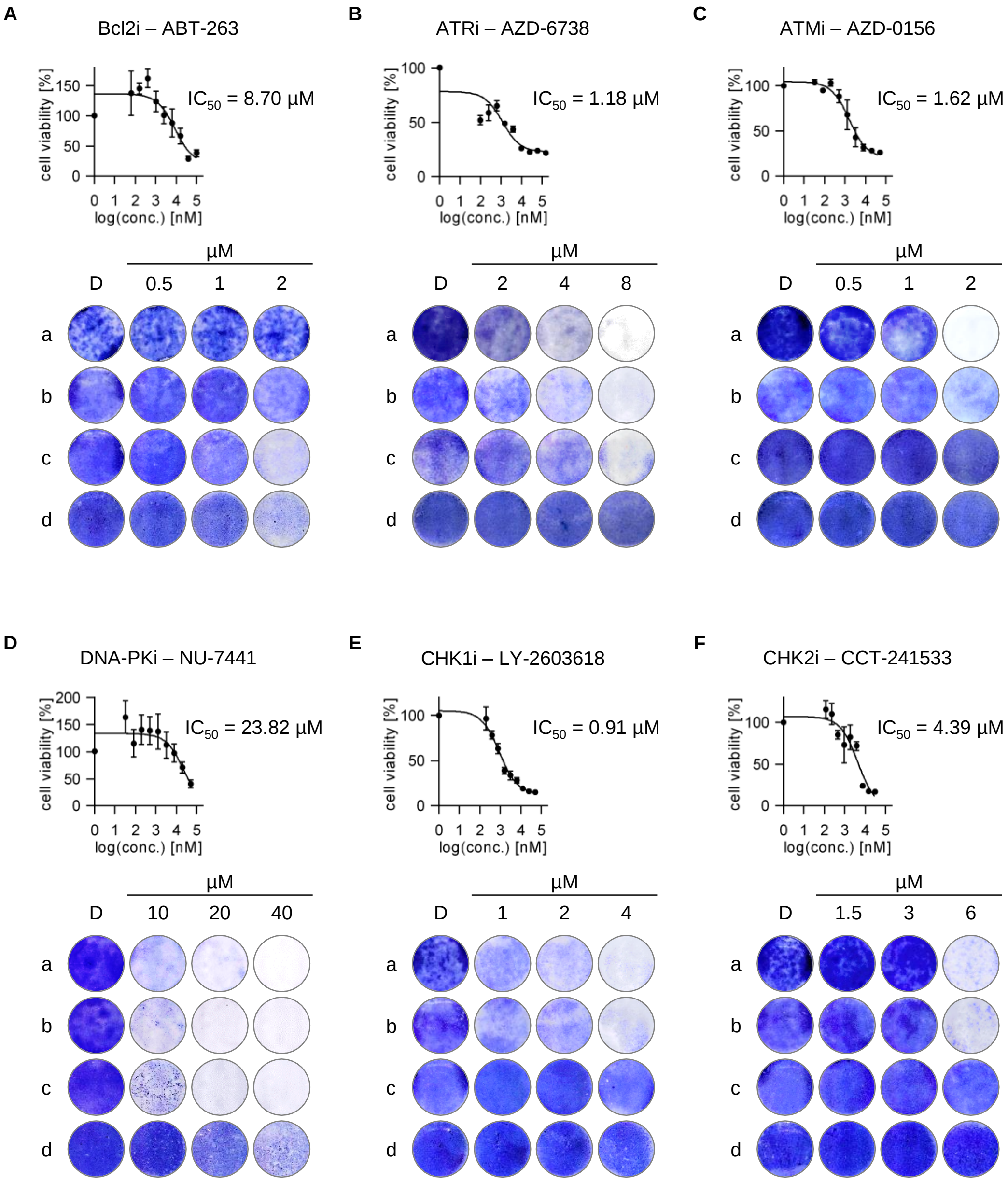

Fig. 3 | Combination therapy of CX-5461 and DDR inhibitors (1)

Detailed subscription is placed below the second part of this figure on the following page.

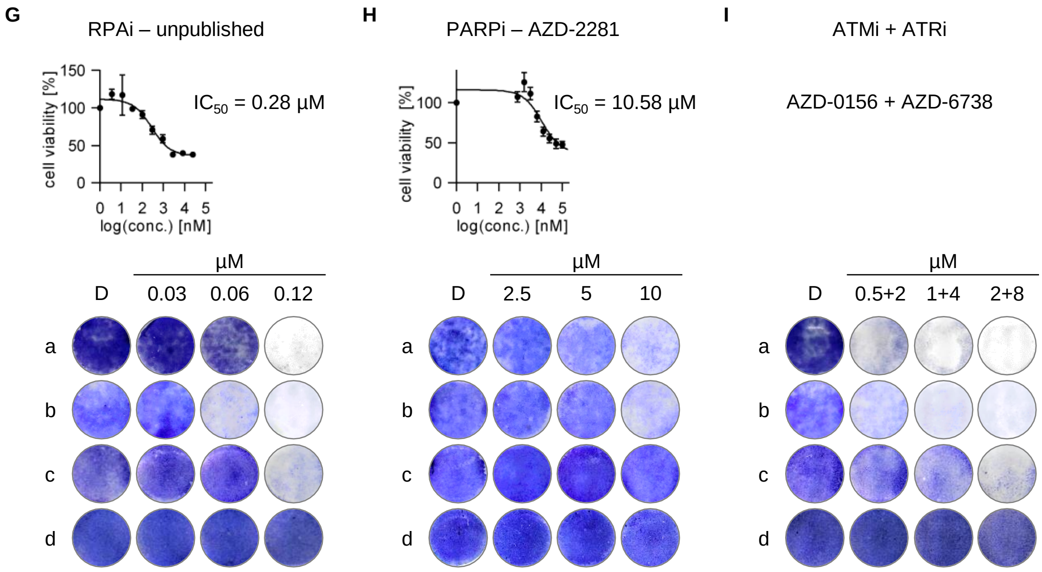

Fig. 4 | Combination therapy of CX-5461 and DDR inhibitors (2)

A-I Experiments were done with murine Nras^{G12V} p19$^{-/-}$ HCC cells. CX-5461 was used at 500 nM. IC_{50} measurements on growing cells were performed by XTT assay. Data show mean ± SD (n = 3 replicates). Crystal violet colony formation assay was used to analyse the inhibitory effect upon different treatment settings. Different settings are labelled as following: a) inhibitor on growing cells, b) pre-treatment with inhibitor, c) simultaneous treatment, and d) inhibitor on RCIS cells (for more detailed description see chapter 3.2.3). Control treatment was done with DMSO (D). For each setting, one representative out of triplicates is illustrated. **A** The senolytic agent ABT-263 (navitoclax) was used as positive control. **B-H** Different DDR inhibitors as labelled within the figure. **I** Dual treatment with ATM and ATR inhibitors.

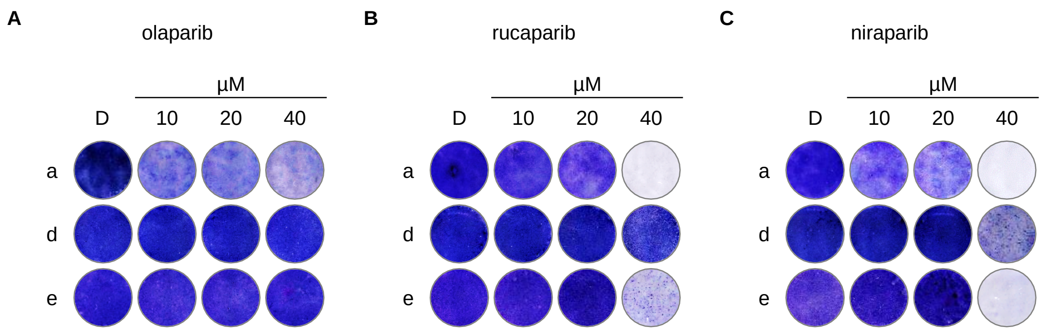

Fig. 5 | Combination therapy of CX-5461 and PARP inhibitors

A-C Experiments were done with murine Nras^{G12V} p19$^{-/-}$ HCC cells. CX-5461 was used at 500 nM. Crystal violet colony formation assay was used to analyse the inhibitory effect of three different PARP inhibitors (olaparib, rucaparib and niraparib) upon different treatment settings. Different settings are labelled as following: a) inhibitor on growing cells (treatment duration: 2 days), d) inhibitor on RCIS cells (treatment duration: 2 days), and e) inhibitor on RCIS cells (treatment duration: 9 days) (for more detailed description see chapter 3.2.3). Control treatment was done with DMSO (D). For each setting, one representative out of triplicates is illustrated.

4.4 Combination therapy of CX-5461 and cisplatin

Based on my previous results showing total absence of the DNA repair proteins FANCD2, FANCI and RAD51 in RCIS cells (Fig. 2 C), I hypothesised that restricted repair mechanisms might make RCIS cells vulnerable to newly generated DNA damage. I used the chemotherapeutic agent cisplatin, that generates mainly intrastrand but also interstrand crosslinks (Eastman, 1987), to test this hypothesis. Since previous experiments have indicated long-term treatment as more promising in affecting cell viability in RCIS cells (Fig. 5), RCIS cells were treated for either two or nine days with cisplatin. As shown in Fig. 6 C, cisplatin indeed reduced viability of CX-5461 induced RCIS cells. While 7.5 µM of cisplatin just slightly affected RCIS cell viability in the two days treatment setting, it was highly toxic after nine days of treatment. Analogous to the PARP inhibitor experiments (Fig. 5), non-senescent cells were treated for only two but not nine days with cisplatin since longer treatment duration was prohibited by overgrowing of the control sample. Comparing the two days treatment of non-senescent and RCIS cells, it must be noticed that cisplatin was more toxic in growing than in senescent cells, thus symbolising that cisplatin does not affect RCIS cell viability selectively. Nonetheless, this experiment provides proof of principle that RCIS cells are not resistant against newly generated DNA damage and remain targetable by DNA damaging drugs.

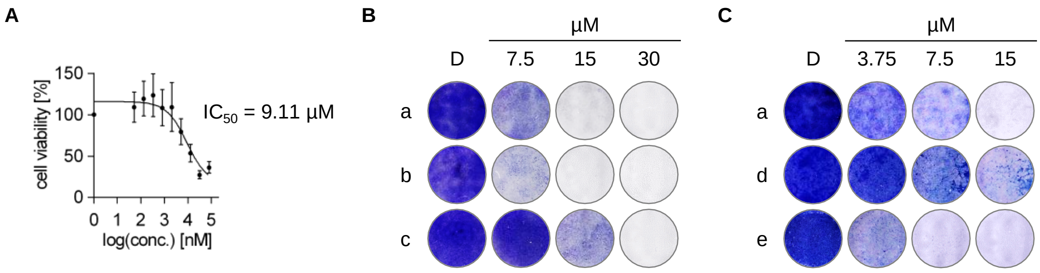

Fig. 6 | Combination therapy of CX-5461 and cisplatin

A-C Experiments were done with murine Nras^{G12V} p19$^{-/-}$ HCC cells. CX-5461 was used at 500 nM. **A** IC_{50} measurement of cisplatin on growing cells was performed by XTT assay. Data show mean ± SD (n = 3 replicates). **B-C** Crystal violet colony formation assay was used to analyse the effect of cisplatin upon different treatment settings. Different settings are labelled as following: a) cisplatin on growing cells (treatment duration: 2 days), b) pre-treatment with cisplatin, c) simultaneous treatment, d) cisplatin on RCIS cells (treatment duration: 2 days), e) cisplatin on RCIS cells (treatment duration: 9 days) (for more detailed description see chapter 3.2.3). Control treatment was done with DMF (D). For each setting, one representative out of triplicates is illustrated.

4.5 Cell cycle analysis upon CX-5461 treatment

As a relevant part of the DDR, cell cycle checkpoint activation prohibits cell cycle progression and cell division in the presence of DNA damage (Barnum and O'Connell, 2014). Here, I used flow cytometric cell cycle analysis with PI to investigate cell cycle alterations upon CX-5461 treatment in murine Nras^{G12V} p19$^{-/-}$ HCC cells (Fig. 7 A-B). In the untreated sample, 46.9% of all cells were in G1 phase, while 23.1% were in G2/M, and 21.0% in S phase. After CX-5461 treatment, the S phase fraction increased up to 35.8% at the five hours treatment time point. However, this early S phase peak was replaced by an impressive raise of the G2/M phase fraction at subsequent time points. The G2/M fraction included 48.9% of all cells eight hours after drug treatment, 66.0% after one day, and stayed at high levels in all the following time points. Unexpectedly, a further peak – corresponding to cells with more than 4N DNA content – raised attention in all the late treatment time points. While this fraction of hyperploid cells was only 8.9% in the untreated sample, it was 16.5% after five, 17.1% after seven and 22.7% after 14 days. Together, these results show rapid accumulation of S phase cells followed by permanent G2/M phase arrest in CX-5461 treated cells. Moreover, hyperploidy was observed in a remarkable part of RCIS cells.

To exclude that the observed hyperploid DNA contents (Fig. 7 A-B) were caused by artificial cell agglutination, I next wanted to visualise the individual chromosomes within single cells by chromosome spread assay (Fig. 7 D). While this assay worked quite nicely in non-senescent cells, however, it was not feasible in RCIS cells. As a possible explanation, it seems plausible that RCIS cells might be unassailable to colcemid due to their cell cycle arrest. Though, colcemid treatment is critical in this assay as it inhibits spindle formation, thus stopping mitosis and enhancing the fraction of metaphase cells with maximally condensed and therefore countable chromosomes (Howe et al., 2014). Nevertheless, analysing the DAPI stained cells microscopically revealed an interesting observation. A subfraction of RCIS cells owned conspicuous small DAPI fragments next to the main nucleus that were not observed in untreated cells (Fig. 7 D). The shape of these DAPI fragments suggests them to be micronuclei – a sign of genomic instability (Lewis and Golsteyn, 2016).

Furthermore, I used western blotting technique to measure cellular protein contents of cyclins and aurora kinases during the time-course of CX-5461 mediated RCIS induction in murine Nras^{G12V} p19$^{-/-}$ HCC cells (Fig. 7 C). The cellular protein content of cyclin A2, that binds CDK2 in S phase and CDK1 during G2/M transition (Pagano et al., 1992), continuously rose within the first 24 hours after drug treatment. After peaking at the twelve hours and one day time points, it dropped and was just slightly measurable three, five and seven days after treatment. Cyclin B1, taking part in the mitosis-promoting cyclin B1-CDK1 complex (O'Farrell, 2001), was not traceable in untreated cells, but started to accumulate three hours after drug treatment and reached its maximum at the twelve hours and one day time points. Like cyclin A2, cyclin B1 was not measurable three, five and seven days after CX-5461 treatment. However, the expression of cyclin D1, that dimerises with CDK4 and CDK6 to promote G1/S transition (Massagué, 2004), did not undergo comparable changes upon CX-5461 treatment. Even seven days after drug treatment, it was just slightly less available than in untreated cells. The mitotic kinase aurora A, that promotes G2/M transition (Dutertre et al., 2004) by recruiting CDK1-cyclin B1 complexes to centrosomes (Hirota et al., 2003), was just faintly measurable in untreated cells but started to amass five hours after drug treatment. Like cyclin B1, aurora A peaked at the twelve hours and one day time points. The other mitotic kinase, aurora B, which regulates chromosome segregation and cytokinesis (Goto et al., 2002; Tapia et al., 2006), was widely available in untreated cells and cells treated with CX-5461 for up to 24 hours. However, it disappeared three, five and seven days after drug treatment, thus indicating downregulation of aurora B as a feature of RCIS. Altogether, the experiments show extensive cell cycle alterations during CX-5461 mediated RCIS induction in murine Nras^{G12V} p19$^{-/-}$ HCC cells. Moreover, the varying expression of cyclins and aurora kinases suggests them to be involved in piloting cell cycle changes upon CX-5461 treatment.

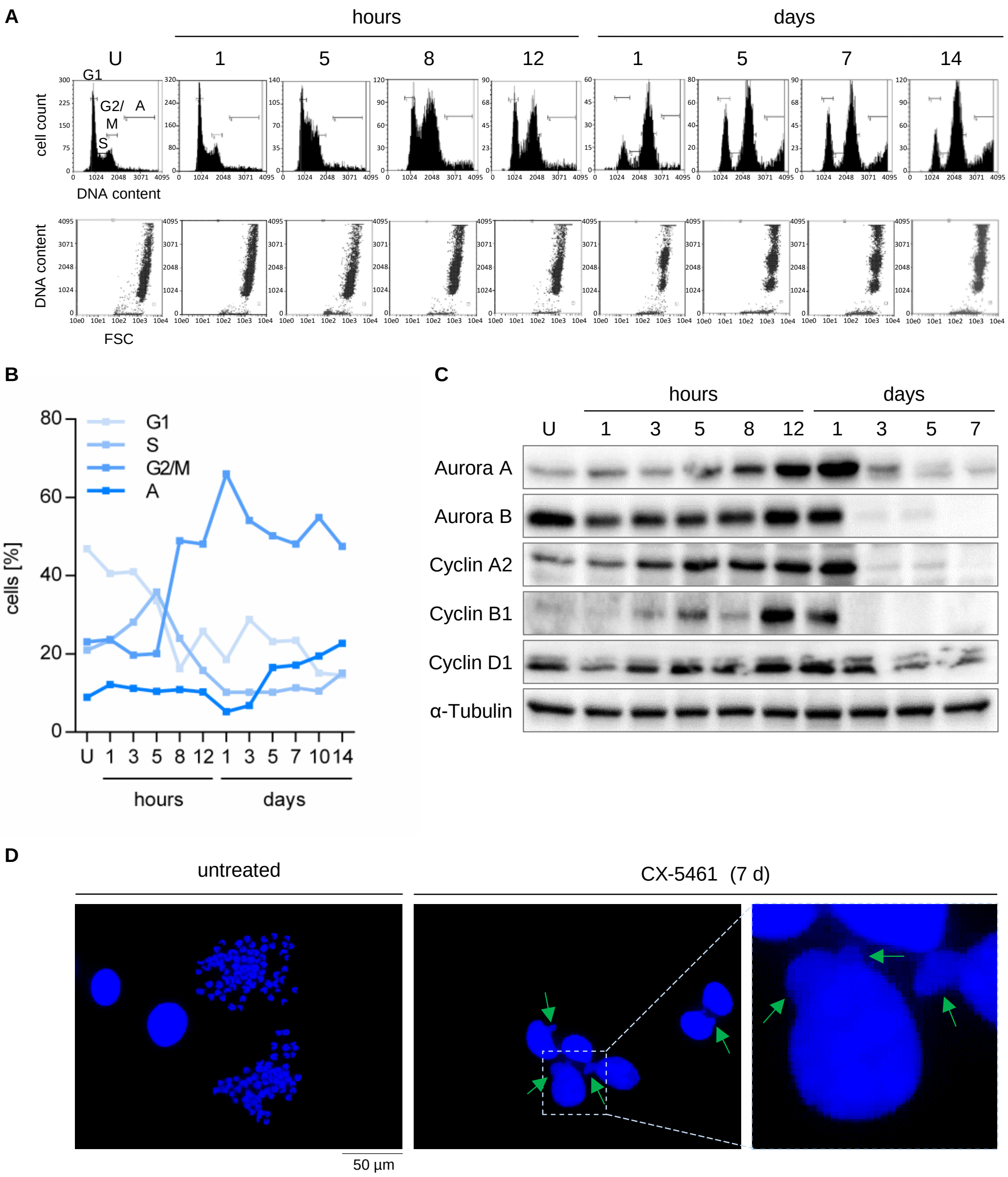

Fig. 7 | Cell cycle analysis upon CX-5461 treatment

A-D Experiments were done with murine Nras^{G12V} p19$^{-/-}$ HCC cells. CX-5461 was used at 500 nM. **A-B** Flow cytometric cell cycle analysis with PI in untreated (U) and CX-5461 treated cells. CX-5461 treatment was investigated at eleven time points after initial drug treatment. For lack of space, original data of the three hours, three days and ten days samples are shown in Supplementary Figure 1 B. For graphical illustration, thresholds for cell cycle phases were set as depicted in A and percentages of each phase were plotted in B. **C** Western blot analyses of several cell cycle proteins in untreated (U) and CX-5461 treated cells. CX-5461 treatment was investigated at nine time points after initial drug treatment. α-Tubulin is illustrated as representative loading control. All further loading controls are shown in Supplementary Figure 2 C. **D** Chromosome spread assay of untreated and CX-5461 treated cells. CX-5461 treatment was analysed seven days after drug treatment. Green arrows point to micronuclei. A representative picture detail with micronuclei is magnified.

4.6 Senescence and DDR analysis in CX-5461 treated p53 deficient cells

Unpublished work by the Zender laboratory (S. Zwirner and K. Wolter) has indicated that murine Nras^{G12V} p19$^{-/-}$ p53$^{-/-}$ HCC cells are undergoing more often cell death upon CX-5461 treatment than murine Nras^{G12V} p19$^{-/-}$ HCC cells. However, the underlying mechanism remained to be elucidated. To characterise the cellular drug response in murine Nras^{G12V} p19$^{-/-}$ p53$^{-/-}$ HCC cells, I analysed cellular protein contents of selected senescence and DDR markers in a time-course setting by western blotting (Fig. 8 A) and compared it to my previous results from murine Nras^{G12V} p19$^{-/-}$ HCC cells (Fig. 1 D, Fig. 2 C, Fig. 7 C). In principle, the senescence marker proteins p21, p16 and HMGA2 accumulated in both cell lines upon CX-5461 treatment, thus supporting previous data from our laboratory (K. Wolter, unpublished) suggesting that CX-5461 induces senescence not only in murine Nras^{G12V} p19$^{-/-}$ HCC cells but also in the surviving fraction of murine Nras^{G12V} p19$^{-/-}$ p53$^{-/-}$ HCC cells. While p21 protein levels dropped three days after CX-5461 treatment in murine Nras^{G12V} p19$^{-/-}$ HCC cells (Fig. 1 D), however, they stayed at high levels up to seven days after treatment in the murine Nras^{G12V} p19$^{-/-}$ p53$^{-/-}$ HCC cell line (Fig. 8 A). Likewise, enhanced protein contents of the DNA repair proteins RAD51 and FANCD2, as well as the cell cycle regulating protein cyclin A2, were clearly visible in both cell lines but longer-lasting in the p53 deficient one, thus indicating that CX-5461 triggers prolonged DDR activation in p53 deficient cells. Only pKAP1 (S824) accumulation was similar in both cell lines. Like already described for murine Nras^{G12V} p19$^{-/-}$ HCC cells, pKAP1 (S824) protein was not measurable in untreated cells but clearly amassed in all the CX-5461 treated samples no matter if they were analysed one hour or seven days after drug treatment.

Since cell cycle checkpoint activation is one of the most important functions of p53 (Hafner et al., 2019), I hypothesised that p53 deficient cells might be unable to undergo cell cycle arrest upon CX-5461 treatment. To test this assumption, flow cytometric cell cycle analysis with PI was compared in CX-5461 treated murine Nras^{G12V} p19$^{-/-}$ and Nras^{G12V} p19$^{-/-}$ p53$^{-/-}$ HCC cell lines (Fig. 8 C-D).

Based on my previous experiments showing that the five hours, one day and seven days treatment time points are most critical in detecting cell cycle alterations upon CX-5461 treatment (Fig. 7 A-B), the comparison was limited to these treatment time points. For murine Nras^{G12V} p19$^{-/-}$ HCC cells, results were quite equal to the detailed analysis shown in Fig. 7 A-B and described in chapter 4.5. In the murine Nras^{G12V} p19$^{-/-}$ p53$^{-/-}$ HCC cell line, the untreated sample contained 39.1% of G1 phase cells, while 25.5% were in G2/M and 20.7% in S phase, thus resembling the cell cycle distribution shown for Nras^{G12V} p19$^{-/-}$ HCC cells. Moreover, CX-5461 caused an early S phase peak (28.9% at the five hours time point) followed by a second G2/M phase peak (61.1% at the one day and 42.4% at the seven days treatment time point) not only in p53 proficient but also in murine Nras^{G12V} p19$^{-/-}$ p53$^{-/-}$ HCC cells. In contrast to these drug-induced cell cycle alterations that were in principle similar for both cell lines, however, the cell lines tremendously differed in their fractions of hyperploid cells upon CX-5461 treatment. Seven days after drug treatment, this hyperploid fraction included 21.0% of the p53 proficient but 50.9% of the p53 deficient cells. In summary, this comparison shows that both cell lines experience early S phase shift followed by stable G2/M arrest upon CX-5461 treatment, and that p53 deficient cells are much more vulnerable to become aneuploid after CX-5461 treatment than p53 wild type ones.

To visualise the nuclear structure of these aneuploid cells, immunofluorescence staining with DAPI was done in untreated cells and seven days after CX-5461 treatment for murine Nras^{G12V} p19$^{-/-}$ and Nras^{G12V} p19$^{-/-}$ p53$^{-/-}$ HCC cell lines (Fig. 8 B & E). For quantification, the fraction of cells containing at least two DAPI fragments was determined. In murine Nras^{G12V} p19$^{-/-}$ HCC cells, this fraction increased from 3.7% (95% CI = 0.80 - 6.54%, SD = 1.16) to 17.3 % (95% CI = 7.29 - 27.37%, SD = 4.04) upon CX-5461 treatment (*P* = 0.0212). Strikingly, this increase was much stronger (*P* = 0.0006) in murine Nras^{G12V} p19$^{-/-}$ p53$^{-/-}$ HCC cells where it rose from 10.0% (95% CI = 7.52% - 12.48%, SD = 1.00) to 81.0% (95% CI = 71.06% - 90.94%, SD = 4.00).

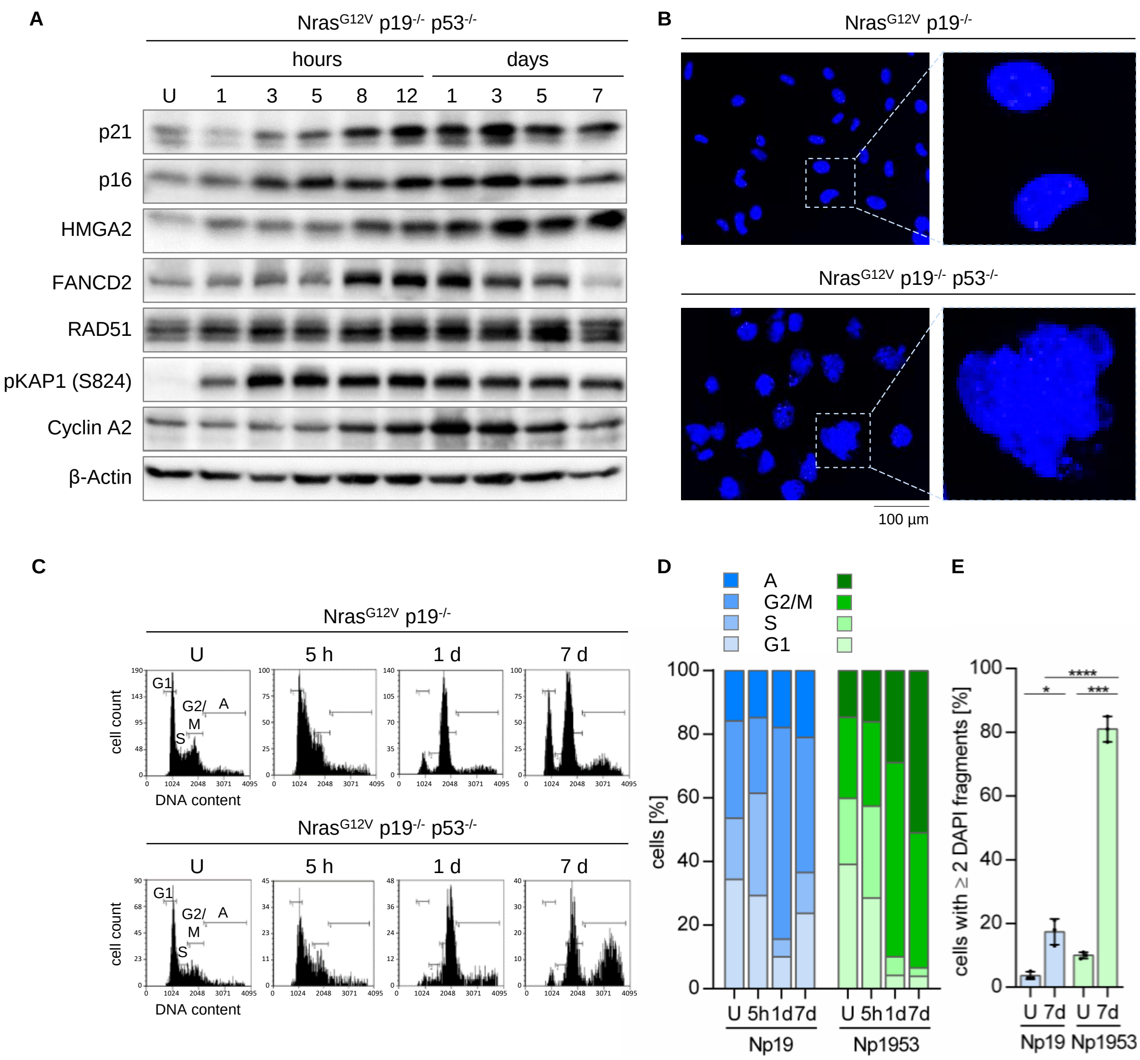

Fig. 8 | Senescence and DDR analysis in CX-5461 treated p53 deficient cells

A-E Experiments were done with the murine HCC cell lines Nras^{G12V} p19$^{-/-}$ (Np19) and Nras^{G12V} p19$^{-/-}$ p53$^{-/-}$ (Np1953). CX-5461 was used at 500 nM. **A** Western blot analyses of several senescence markers and DDR proteins in untreated (U) and CX-5461 treated murine Nras^{G12V} p19$^{-/-}$ p53$^{-/-}$ HCC cells. Analogous to previous western blot analyses of murine Nras^{G12V} p19$^{-/-}$ HCC cells (Fig. 1 D, Fig. 2 C, Fig. 7 C), the samples contained only adherent cells that did not undergo cell death upon CX-5461 treatment. CX-5461 treatment was investigated at nine time points after initial drug treatment. β-Actin is illustrated as representative loading control. All further loading controls are shown in Supplementary Figure 2 D. **B & E** Immunofluorescence staining with DAPI (blue) showing nuclear shapes of murine Nras^{G12V} p19$^{-/-}$ and Nras^{G12V} p19$^{-/-}$ p53$^{-/-}$ HCC cells seven days after CX-5461 treatment. For quantification, the fraction of cells with two or more DAPI fragments was determined in untreated (U) and CX-5461 treated (7d) cells. For each setting, triplicates were analysed with 100 nuclei respectively. Data are mean ± SD (n = 3 replicates). Unpaired t test with Welch's correction, * $P = 0.0212$, *** $P = 0.0006$, **** $P < 0.0001$. **C-D** Flow cytometric cell cycle analysis with PI in untreated (U) and CX-5461 treated murine Nras^{G12V} p19$^{-/-}$ and Nras^{G12V} p19$^{-/-}$ p53$^{-/-}$ HCC cells. CX-5461 treatment was investigated at three time points after initial drug treatment. The stacked bar charts visualise the percentage of cells within each cell cycle phase (thresholds for cell cycle phases are marked in C).

4.7 Analysis of DNA:RNA hybrids upon CX-5461 treatment

Although my work (Fig. 2, Fig. 7, Fig. 8) and others (Negi and Brown, 2015; Quin et al., 2016; Xu et al., 2017) have shown pronounced DDR activation upon CX-5461 treatment, however, the origin of CX-5461 induced DDR activation is not yet understood. Based on the working mechanism of CX-5461 as an RNAP I inhibitor (Drygin et al., 2011), we hypothesised that its disturbance of the DNA transcription process might result in DNA:RNA hybrid formation. Moreover, we assumed that the damaging event must occur very early after drug treatment since previous experiments have shown first signs of DDR activation already one hour after treatment (Fig. 2).

To test our hypothesis, I did immunofluorescence staining of DNA:RNA hybrids in untreated murine $Nras^{G12V}$ $p19^{-/-}$ HCC cells and compared it to cells treated with CX-5461 for three hours (Fig. 9). Intriguingly, the number of DNA:RNA hybrid foci per cell significantly ($P < 0.0001$) increased from 0.24 (95% CI = 0.09 - 0.39, SD = 0.78) to 2.64 (95% CI = 2.42 - 2.87, SD = 1.13) upon CX-5461 treatment. The fraction of cells without any DNA:RNA hybrid focus diminished from 86% to 3% while two or more DNA:RNA hybrid foci were detected in only 5% of the untreated but 87% of the CX-5461 treated cells. In summary, this experiment clearly proves DNA:RNA hybrid formation upon CX-5461 treatment, thus supporting our hypothesis that DNA:RNA hybrids might be the origin of CX-5461 induced DDR activation.

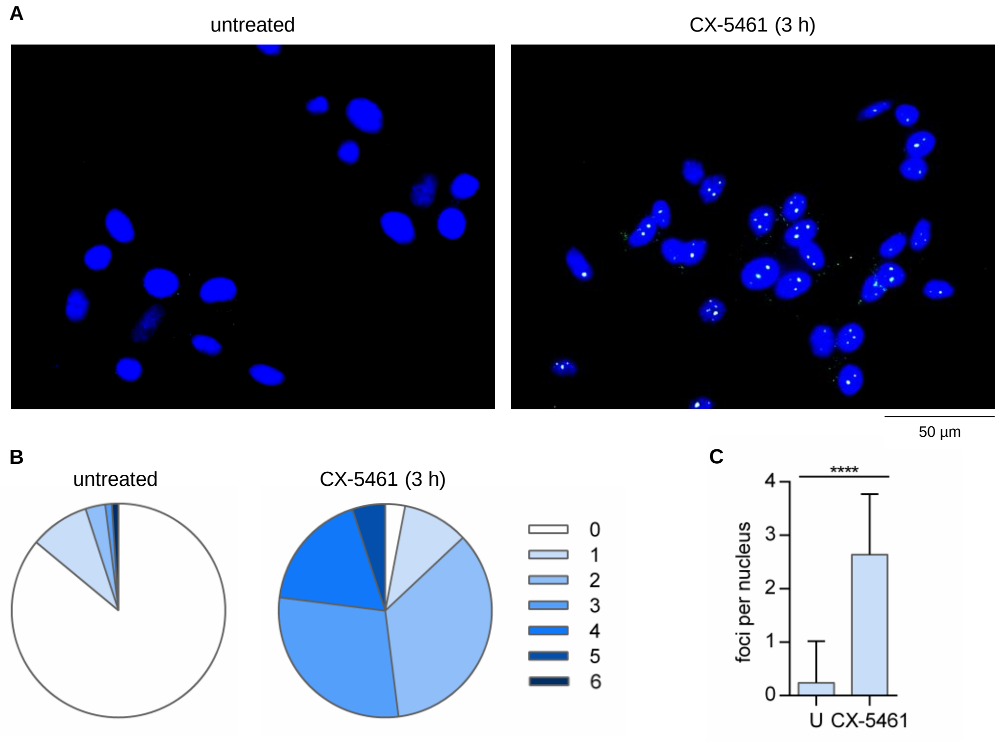

Fig. 9 | Analysis of DNA:RNA hybrids upon CX-5461 treatment

A-C Immunofluorescence analysis of DNA:RNA hybrid antibody [S9.4] in untreated and CX-5461 treated cells. Experiment was done with murine Nras^{G12V} p19$^{-/-}$ HCC cells. CX-5461 was used at 500 nM. Exposure time: FITC 350 ms, DAPI 8 ms. **B-C** For quantification, 100 nuclei per sample were analysed. Circular charts show percentages of nuclei containing the labelled number of DNA:RNA hybrid foci. Bar charts show average foci per nucleus. Data are mean ± SD (n = 100 nuclei). Unpaired t test with Welch's correction, **** *P* < 0.0001.

5 Discussion

5.1 RCIS induction is a dynamic and time-dependent process

Previous work by the Zender laboratory (K. Wolter, unpublished) has shown CX-5461 as potent inducer of growth arrest and RCIS in a broad range of murine and human solid cancer cell lines. In this work, the time-dependent kinetics of CX-5461 induced growth arrest and senescence were analysed in more detail in murine Nras^{G12V} p19$^{-/-}$ HCC cells (Fig. 1). As expected, the proliferation marker Ki67 (Gerdes et al., 1983) was nearly extinguished seven days after CX-5461 treatment, thus indicating proliferation arrest in RCIS cells (Fig. 1 E-F). More interestingly, analysing Ki67 in earlier treatment time points offered new insights in the initiation of this proliferation arrest. While Ki67 activity was clearly reduced three days after drug treatment, the very high rates of Ki67 positive cells at the three and twelve hours treatment time points imply that CX-5461 does not affect cellular proliferation within the first hours. However, it has been reported that CX-5461 reduces EdU (5-ethynyl-2'-deoxyuridine) staining already two hours after drug treatment in human HCT116 cells (Xu et al., 2017). In contrast to Ki67 that is continuously produced from the start of S phase until mitotic exit before it steadily decays during G0 and G1 phases (Miller et al., 2018), halogenated nucleotides – such as the thymidine analogue EdU – incorporate into newly synthesised DNA only during active DNA replication in S phase (Cavanagh et al., 2011). Although comparing my results with those from Xu et al. must be considered critically (e.g. due to the use of different cell lines), combining both results might indicate that CX-5461 reduces active DNA replication already within the first hours after treatment while it takes several days until a rested cellular state is established.

However, previous studies (K. Wolter, unpublished) based on the assumption that cells are in RCIS approximately one week after CX-5461 treatment without having analysed the time-course of the senescence induction process.

Strikingly, my experiments recorded rising SA-β-Gal activity already one day after CX-5461 treatment, followed by a continuous increase within the subsequent days until nearly all cells were positive for SA-β-Gal one week after drug treatment (Fig. 1 C & G). Therefore, increasing SA-β-Gal activity was nearly reciprocally proportional to decreasing Ki67 activity. Together, these two experiments suggest RCIS induction as a dynamic and time-dependent process that starts already within the first hours after CX-5461 treatment although it takes nearly a week to entirely evolve.

In line with this, the senescence marker proteins p53, p21 and p16 accumulated within the first hours after drug treatment in murine Nras^{G12V} p19$^{-/-}$ HCC cells (Fig. 1 D). Since the familiar tumour suppressor protein p53 (Finlay et al., 1989; Baker et al., 1989) has reams of cellular functions (Hafner et al., 2019), a reliable interpretation of its accumulation in the context of CX-5461 triggered RCIS induction is quite challenging. However, p53 is known to facilitate a senescence program in cells exposed to stresses such as oncogene activation or DNA damage (Bond et al., 1996). The current working model based on lab internal and published data suggests that CX-5461 enhances cellular p53 levels in the framework of nucleolar stress pathway activation (Rubbi and Milner, 2003). In this regard, nucleolar stress triggers the binding of ribosomal proteins (e.g. L5, L11, L23) to the E3 ubiquitin-protein ligase MDM2. This binding prohibits MDM2-mediated p53 ubiquitination and degradation (Haupt et al., 1997; Kubbutat et al., 1997), thus resulting in rising p53 levels that trigger cell cycle arrest (Dai et al., 2004; Dai and Lu, 2004; Lohrum et al., 2003). Since CX-5461 inhibits the nucleolar enzyme RNAP I (Drygin et al., 2011), nucleolar stress pathway activation by CX-5461 seems to be quite plausible. Moreover, proof-of-principle that disturbance of RNAP I can trigger nucleolar stress pathway activation was demonstrated for actinomycin D (Dai et al., 2004; Dai and Lu, 2004; Lohrum et al., 2003), a DNA intercalating agent that inhibits RNAP I at the elongation step (Fetherston et al., 1984). Altogether, the peak of p53 protein levels five hours after drug treatment might indicate nucleolar stress pathway activation in CX-5461 treated murine Nras^{G12V} p19$^{-/-}$ HCC cells.

Though, it must be considered that rising p53 protein levels were reported in multiple other contexts as well (Hafner et al., 2019). In the context of DNA damage, ATM-mediated phosphorylation of p53 at S15 inhibits its binding to MDM2 (Banin et al., 1998), thus prohibiting its degradation (Sakaguchi et al., 2000). According to my experiments showing enhanced pATM (S1987) levels in CX-5461 treated murine $Nras^{G12V}$ $p19^{-/-}$ HCC cells (Fig. 2 C), DDR signalling offers a further explanation for the observed p53 protein accumulation. However, p53 promotes transcription of the CDK inhibitor p21 (El-Deiry et al., 1993) that mediates cell cycle arrest. Primarily, p21 has been suggested as trigger for G1 cell cycle checkpoint arrest, but mounting evidence indicates an involvement in G2 checkpoint as well (Dulić et al., 1998; Bunz et al., 1998). Strikingly, my experiments revealed highest p21 protein levels between five hours and one day after CX-5461 treatment and therefore simultaneously and shortly after maximal p53 protein accumulation that was observed at the five hours time point (Fig. 1 D). This temporal correlation supports a p53-dependent p21 activation in CX-5461 treated cells. However, raising p21 protein levels upon CX-5461 treatment were observed not only in murine $Nras^{G12V}$ $p19^{-/-}$ but also in $Nras^{G12V}$ $p19^{-/-}$ $p53^{-/-}$ HCC cells (Fig. 8 A). Although this does not exclude p53-dependent p21 activation in CX-5461 treated p53 wild type cells, it shows that p21 protein accumulation upon CX-5461 treatment can occur in a p53-independent manner. Anyway, the accumulation of p21 protein was just transient in CX-5461 treated murine $Nras^{G12V}$ $p19^{-/-}$ HCC cells (Fig. 1 D). Even though p21 is a well-established mediator of cellular senescence (Fang et al., 1999; Herbig et al., 2008), its role in preserving the senescent state is controversial. On the one hand, p21 has been suggested as an essential player in maintaining viability of senescent cells, especially in DNA damage-induced senescence (Yosef et al., 2017). On the other hand, another study has reported that p21 protein levels increase when cells near the senescent state but decline when senescence has fully established (Alcorta et al., 1996). Consistent with the latter publication, my results suggest an involvement of p21 in mediating RCIS induction without being crucial in RCIS maintenance.

Just like p53 and p21, also p16 protein levels accumulated transiently upon CX-5461 treatment with having its peak between twelve hours and three days after drug treatment in murine Nras^{G12V} p19$^{-/-}$ HCC cells (Fig. 1 D). Concerning the role of p16 in senescence, a study has shown gradually rising p16 protein levels during the process of senescence induction resulting in an amassing of p16 protein in senescent HDFs (Alcorta et al., 1996). Moreover, high levels of p16 protein were even suggested to prevent senescence reversal upon p53-inactivation (Beauséjour et al., 2003). However, the transient accumulation of p16 protein during RCIS induction and its absence in fully established RCIS cells is still not implausible since some other studies have indicated that p16 is not obligatory for the senescent state (Sundar et al., 2018; Haferkamp et al., 2009). Like discussed for p53 and p21, these results indicate an involvement of p16 in RCIS induction without being obligatory for RCIS maintenance.

In contrast, expression of HMGA2 was exclusively upregulated at the last CX-5461 treatment time points that have been analysed – namely three, five and seven days – and therefore in RCIS cells (Fig. 1 D). According to previous unpublished data from the laboratory (K. Wolter) that had shown HMGA2 accumulation in other types of RCIS, this data confirms augmented HMGA2 protein content also in CX-5461 induced RCIS. The non-histone protein HMGA2 is a component of SAHFs that repress proliferation-associated genes, thus stabilising proliferation arrest and senescence (Narita et al., 2006). Accordingly, the delayed but ongoing accumulation of HMGA2 after CX-5461 treatment might correlate with SAHFs that could be responsible for RCIS maintenance. At the same time, c-MYC protein levels were clearly depleted (Fig. 1 D). The transcription factor c-MYC participates in numerous cellular processes including cell cycle progression, proliferation, apoptosis and metabolism (Pelengaris et al., 2002). Moreover, suppression of the c-MYC oncogene has been shown to provoke cellular senescence in diverse tumour types including hepatocellular carcinoma, lymphoma and osteosarcoma (Wu et al., 2007). In summary, I suggest the enhancement of HMGA2 and the decline of c-MYC as features of CX-5461 induced RCIS that might be crucial in maintaining the senescent state. Further, there is a direct link between p21, p16 and HMGA2. p21 and p16 prevent RB hyperphosphorylation (Sherr and McCormick, 2002) and hypophosphorylated RB prohibits transcription of E2F target genes needed for cell cycle progression (Sherr and McCormick, 2002). However, E2F target gene repression itself has been suggested to trigger chromatin reorganisation and SAHF formation (Narita et al., 2003). Hence, I assume that upon CX-5461 treatment, p53, p21 and p16 pilot a rapid but transient stress response resulting in an initial repression of E2F target genes that provokes SAHF formation and that SAHFs are responsible for long-term E2F target gene repression and RCIS maintenance.

The last senescence marker that has been analysed in this work is lamin B1 (Fig. 1 D). Lamin B1 is involved in building up the matrix of the nuclear lamina, and its loss was proposed as a hallmark of senescence (Freund et al., 2012). Surprisingly, my experiments revealed an increase of lamin B1 protein levels between one and seven days after CX-5461 treatment and therefore in RCIS cells (Fig. 1 D). In accordance with another study that has reported overexpression of lamin B1 in oxidative stress induced senescence (OIS) (Barascu et al., 2012), I assume that loss of lamin B1 cannot be claimed as general hallmark of senescence. Instead of that, overexpression of lamin B1 is found in both, OIS and RCIS, and maybe also in other types of senescence.

5.2 RCIS induction is accompanied by a DNA damage response

According to previous publications that have suggested a strong link between cellular senescence and DDR activation (Fagagna, 2008), this work clearly shows that also CX-5461 induced RCIS is accompanied by DDR signalling (Fig. 2). The time-course analysis of both, senescence and DDR markers, allows drawing conclusions of temporal correlations between senescence induction and DDR activation in CX-5461 treated murine Nras^{G12V} p19$^{-/-}$ HCC cells (Fig. 1, Fig. 2). While several DDR proteins (e.g. pATM (S1987), pATR (S428), and FANCD2) were increased already one hour after drug treatment (Fig. 2 C), first signs of senescence induction (like enhanced levels of p53, p21 and p16 proteins) were observed at the three hours treatment time point. Based on these results, I suggest that CX-5461 triggers DDR activation before the senescence induction process starts. However, it must be considered that the underlying mechanisms of CX-5461 induced senescence are not yet fully understood, so that there might be further signs of early senescence induction that have not been assessed in this study. Moreover, the results of this work are limited on showing correlation without proofing causation, thus making further research necessary to prove causation between DDR activation and RCIS induction. However, most of the analysed DDR proteins accumulated just transiently upon CX-5461 treatment so that their subsequent decline was in coincidence with the rise of senescence markers like HMGA2 or positive SA-β-Gal staining. In short, DDR signal fades when cells near the RCIS state. In line with this conclusion, a previous study regarding replicative senescence has shown ATM activation and γH2AX nuclear focus formation in pre-senescent primary human fibroblasts that disappeared once cells became fully senescent (Bakkenist et al., 2004). Although most of the analysed DDR proteins were absent seven days after drug treatment and therefore in RCIS cells, pKAP1 (S824), pRPA32 (S4/S8) and FANCM were clearly present at these late treatment time points. However, they might indicate ongoing DDR signalling in RCIS cells and it remains unclear if they are involved in maintaining the RCIS state.

Taking a closer look on the functions of the accumulating DDR proteins, they do not infer to a specific kind of DNA damage since some of them are involved in DSB repair, while others take part in ICL repair or ssDNA signalling. In response to DSBs, ATM and ATR kinases immediately phosphorylate H2AX at S139 (γH2AX) (Rogakou et al., 1998; Burma et al., 2001; Ward and Chen, 2001) and 53BP1 at S1778 (Lee et al., 2009). In my immunofluorescence staining, however, many of the untreated cells were positive for γH2AX while only a few cells were positive for p53BP1 (S1778) (Fig. 2 A-B). This might be explained by the cell cycle dependent expression of γH2AX and its involvement in other cellular processes that limit its specificity as DSB marker (MacPhail et al., 2003). De Feraudy et al. have classified three different types of γH2AX formation: γH2AX foci co-localizing with 53BP1 foci depicting DSBs, γH2AX foci not co-localizing with 53BP1 being of unknown significance, and pan-nuclear γH2AX staining representing a preapoptotic signal (Feraudy et al., 2010). Based on this classification, most of the γH2AX foci observed in untreated cells might represent by-products of normal replication rather than DSBs. In line with this assumption, the murine $Nras^{G12V}$ $p19^{-/-}$ HCC cell line that has been used for this experiment has tremendous proliferative activity (Fig. 1 E-F). Since the analysed samples mark different time points during CX-5461 mediated RCIS induction and therefore vary in their proliferation rates (Fig. 1 E-F), a reliable interpretation of the cell cycle dependent γH2AX staining is challenging. Therefore, I suggest p53BP1 (S1778) as a better marker for comparing DSB signalling in samples with varying proliferation rates as it is the case in senescing cells. However, the fraction of both γH2AX and p53BP1 (S1778) positive cells clearly increased upon CX-5461 treatment and reached its peak at the twelve hours time point (Fig. 2 A-B), thus indicating DSB formation within the first hours after drug treatment. While the rate of p53BP1 (S1778) positive cells was still significantly higher seven days after drug treatment than in untreated cells, this was not the case for γH2AX. Considering the cell-cycle dependent expression of γH2AX (MacPhail et al., 2003), the low levels of γH2AX observed in RCIS cells might result from proliferation arrest (Fig. 1 E-F). Yet, the remaining γH2AX foci might mark real DSBs, and – together with the ongoing enhancement of p53BP1 (S1778) foci – indicate prolonged DSB signalling in RCIS cells. Further, the phosphorylated and therefore activated forms of two other DSB marker proteins, ATM and CHK2, also accumulated upon CX-5461 treatment with reaching their maxima eight and twelve hours after treatment (Fig. 2 C) and therefore approximately at the same time as γH2AX and p53BP1 (S1778). Altogether, my results support strong DSB signalling following CX-5461 treatment that peaks after twelve hours and diminishes but not extinguishes when cells become senescent.

A further downstream target of ATM is the heterochromatin-associated protein KAP1 which is phosphorylated upon discovery of damaged or broken DNA (Ziv et al., 2006). Intriguingly, pKAP1 (S824) was not even measurable in untreated cells, but remarkably amassed in all the CX-5461 treated samples quite independent of the investigated time point (Fig. 2 C), thus demonstrating strong and long-lasting KAP 1 activation upon CX-5461 treatment. Phosphorylation of KAP1 induces its release from the chromatin, thereby promoting DNA relaxation that simplifies the assembly of DDR proteins onto DSBs (Goodarzi and Jeggo, 2011). The permanent accumulation of pKAP1 (S824) in CX-5461 treated cells might indicate long-term chromatin relaxation upon CX-5461 treatment. Paradoxically, my previous results have suggested that CX-5461 triggers formation of SAHFs (as indicated by HMGA2 accumulation (Fig. 1 D)) which are compacted heterochromatin structures. While solely pKAP1 (S824) was measurable during the first hours after CX-5461 treatment, simultaneous accumulation of pKAP1 (S824) and HMGA2 was observed at later treatment time points and therefore in RCIS cells. Based on these findings, I hypothesise that CX-5461 treatment might result in rapid KAP1-mediated chromatin relaxation to facilitate DDR processes (which are maximally active during the first hours after drug treatment) followed by complex chromatin reorganisation processes during RCIS establishment. Moreover, I suggest that in RCIS cells, some DNA regions are characterised by pKAP1 (S824) dependent chromatin relaxation, while others are forming SAHFs to maintain cell cycle arrest and senescence via permanent repression of E2F target regions. However, immunofluorescence co-staining of pKAP1 (S824) and HMGA2 in RCIS cells might be helpful to strengthen this hypothesis.

Next to the activated DSB response pathways, also proteins taking part in ATR-CHK1-pathway accumulated in CX-5461 treated murine Nras^{G12V} p19$^{-/-}$ HCC cells (Fig. 2 C). ATR-CHK1-pathway is predominantly triggered by free ssDNA (Zou and Elledge, 2003) that arises for instance at stalled replication forks (Dobbelstein and Sørensen, 2015) or as an intermediate during DSB repair (Shiotani and Zou, 2009). Hence, the accumulation of pATR (S428) and its downstream kinase pCHK1 (S345) indicate the presence of free ssDNA upon CX-5461 treatment. Since free ssDNA is usually recognised by RPA (Chen and Wold, 2014), it was unexpected that pATR (S428) and pRPA32 (S4/S8) did not accumulate simultaneously in my experiments. While pATR (S428) amassed already one hour after drug treatment, the increment of pRPA32 (S4/S8) started not until the eight hours time point. Anyway, RPA is not the only protein that binds ssDNA. RAD51 competes with RPA by forming nucleoprotein filaments with ssDNA that are essential for homology search and strand exchange in HR (Shinohara et al., 1992). Since cellular protein levels of RAD51 were enhanced between three and twelve hours after drug treatment (Fig. 2 C), CX-5461 might cause free ssDNA that is bound by RAD51 rather than RPA within the first hours after treatment. Intriguingly, my results would fit to a shift from RAD51 to pRPA32 (S4/S8) at later time points, indicating that ssDNA molecules resulting from CX-5461 treatment might be protected by RPA in the long run.

However, augmented RAD51 expression suggests that HR participates in DNA damage repair upon CX-5461 treatment. Since HR is involved in processing DSB intermediates arising from ICL repair (De Silva et al., 2000), the accumulation of RAD51 might correlate not only with DSBs but also ICLs. In support of this notion, the time courses of FANCD2 and FANCI protein accumulations upon CX-5461 treatment resembled those of RAD51 (Fig. 2 C). Although FA pathway has some non-canonical functions like replication fork stabilisation (Wang et al., 2008) and cytokinesis regulation (Chan et al., 2009; Vinciguerra et al., 2010), its canonical role in ICL repair suggests that CX-5461 might provoke such faulty genomic links. Since ICL repair causes DSBs (De Silva et al., 2000) and free ssDNA as intermediates (Shiotani and Zou, 2009), ICLs would not only explain FA pathway activation but also DSB and ssDNA signalling upon CX-5461 treatment.

Altogether, my work clearly demonstrates that CX-5461 mediated RCIS induction is accompanied by strong DDR activation, which is partly transient and partly permanent. Yet, it must be considered that DDR activation is just an indirect sign of DNA damage. For instance, ATR signalling was postulated to drive cells into senescence in the absence of DNA breaks (Toledo et al., 2008). Thus, measuring DNA damage directly (e.g. by comet assay) would be obligatory to confirm DNA damage as source of the observed DDR activation.

5.3 RCIS cells are resistant against DDR inhibitors

Based on the proposition that ongoing DDR activation is a feature of senescence (Fagagna, 2008), I have hypothesised that DDR inhibitors might act as senolytic drugs. In line with unpublished results from the Zender laboratory (K. Wolter), CX-5461 induced RCIS cells were selectively killed by the senolytic agent navitoclax (ABT-263) (Zhu et al., 2016) (Fig. 3 A), thus proving that RCIS cells are in general susceptible for senolytic therapy. However, a comparable senolytic effect was observed for none of the investigated DDR protein inhibitors (ATRi AZD-6738, ATMi AZD-0156, DNA-PKi NU-7441, CHK1i LY-2603618, CHK2i CCT-241533, PARPi AZD-2281) (Fig. 3 B-F, Fig. 4). Quite the contrary, RCIS cells became resistant against the examined DDR inhibitors. This resistance phenomenon might be explainable by proliferation arrest of RCIS cells (Fig. 1 E-F). Since replicating cells are constantly acquiring replication-associated DNA damage that triggers DDR activation, rapidly proliferating cell lines, like murine Nras^{G12V} p19$^{-/-}$ HCC (Fig. 1 E-F), depend on proper DDR functionality to ensure genomic stability. In contrast, senescent cells do not replicate and therefore do not generate this kind of DNA damage. This link might make senescent cell viability less dependent on functional DDR activity than it is the case in replicating cells. In line with this assumption, most DDR proteins (e.g. pATM (S1987), pATR (S428), pCHK1 (S345) and pCHK2 (T383)) accumulated in a transient manner upon CX-5461 treatment and were nearly absent in RCIS cells (Fig. 2). However, this was not the case for pRPA32 (S4/S8) that was widely available in RCIS cells (Fig. 2 C). Although its ongoing increase predisposes RPA as target structure for senolytic therapy, however, pharmaceutical RPA inhibition by an unpublished, highly efficient RPA inhibitor (designed by the Zender (S. Zwirner and A. Moschopoulou) and Laufer (G.-S. Haase and G. Schmidberger) laboratories) was not senolytic in RCIS cells (Fig. 4 G).

Since most of the analysed DDR proteins accumulated just temporarily upon CX-5461 treatment (Fig. 2), I assumed that simultaneous treatment with CX-5461 and DDR inhibitors might be more promising. In this context, I supposed that DDR inhibitors might disturb the process of RCIS induction, thus changing cellular fate from senescence to cell death. However, co-treatment with CX-5461 and the previously listed DDR inhibitors did not reduce cell viability in a synergistic way (Fig. 3 B-F, Fig. 4). First, I suspected the redundancy of the DDR system as responsible for the ineffectiveness of the investigated combination therapy concepts. Although ATM-CHK2- and ATR-CHK1-pathways are conventionally thought to be active in different contexts, mounting evidence suggests this model as less strict than primarily thought and attests them to cross talk with each other to a certain extent (Maréchal and Zou, 2013). Therefore, I assumed that blocking only one of these pathways might be compensated by the other one. Yet, even dual-therapy with ATM (AZD-0156) and ATR (AZD-6738) inhibitors did neither cause senolytic cell death in RCIS cells nor synergistic cell viability reduction in simultaneous treatment with CX-5461 (Fig. 4 I). Next, I supposed that species or cell line specific problems might be responsible for the ineffectiveness of the investigated combination therapies – but repeating the experiment for ATR (AZD-6738) and PARP (AZD-2281) inhibitors in human HCC cells (SMMC-7221) did not reveal any synergistic or senolytic effect as well (Supplementary Figure 1 C). However, the reason why simultaneous CX-5461 and DDR inhibitor treatment does not synergistically reduce cell viability although the targeted DDR proteins clearly amass upon CX-5461 treatment (Fig. 2 C) remains elusive.

5.4 Long-term PARP inhibition reduces cell viability in RCIS cells

Within the last years, PARP inhibitors came into focus of modern cancer therapy and are already approved for some indications, most notably for BRCA mutated ovarian and breast cancers (Bryant et al., 2005). Although PARP inhibitors primarily aim PARP1, some of them – for instance niraparib – target PARP2 as well (Knezevic et al., 2016). Since PARP1 is critical in SSB restoration (Chaudhuri and Nussenzweig, 2017), PARP inhibition results in abundant SSBs that impede replication forks, thus triggering HR for repair

(Bryant et al., 2005). The involvement of BRCA proteins in HR is suggested as underlying mechanism for the high effectiveness of PARP inhibitors in BRCA1/2 mutant tumours (Bryant et al., 2005; Farmer et al., 2005). However, unpublished work by Oliver Bischof (Institut Pasteur, Nuclear Organisation and Oncogenesis Unit, Department of Cell Biology and Infection, Paris, France) has uncovered a senolytic effect for long-term PARP inhibitor treatment in doxorubicin induced senescent fibroblasts. According to his discovery, my results revealed that CX-5461 induced RCIS cells undergo cell death after nine days of treatment with either 40 µM of the PARP inhibitors niraparib or rucaparib, but not olaparib (Fig. 5). Therefore, the senolytic therapy concept suggested from O. Bischof seems to be transferable to our model of CX-5461 induced RCIS. Yet, some limitations must be discussed critically. Overgrowing of the untreated control sample prohibited to treat non-senescent cells for nine days with the PARP inhibitors. Hence, it was not feasible to compare drug responses in RCIS and non-senescent cells for the nine days PARP inhibitor treatment. Comparing just the two days PARP inhibitor treatment, which was feasible in RCIS and non-senescent cells, revealed higher efficiency in non-senescent cells (Fig. 5). This observation strongly argues against a selective senolytic effect of PARP inhibitors in CX-5461 induced RCIS cells. Nonetheless, my work supports that highly dosed rucaparib and niraparib, but not olaparib, eliminate next to non-senescent tumour cells also senescent ones, thereby improving current knowledge how PARP inhibitors affect tumour tissue in the long run.

Since my experiments revealed an RCIS eliminating effect for rucaparib and niraparib, but not olaparib, we questioned if niraparib and rucaparib might affect RCIS cell viability via another target than PARP. In contrast to olaparib, that is suggested to inhibit PARP1 and PARP2 high specifically, rucaparib and niraparib have further molecular target structures (rucaparib: hexose-6-phosphate dehydrogenase, niraparib: deoxycytidine kinase) (Knezevic et al., 2016). Although further experiments will be necessary to investigate if rucaparib and niraparib eliminate senescent cells via another target structure than PARP, some hints are already pointing in this direction. First, western blotting did not show heightened PARP1 protein levels upon CX-5461 treatment in murine $Nras^{G12V}$ $p19^{-/-}$ HCC cells (Supplementary Figure 1 A), thus arguing against a critical role of PARP1 in maintaining RCIS cell viability. Second, it is suggested that PARP inhibitors cause cell death via abundant SSBs that impede replication forks, thus disturbing the active replication process (Bryant et al., 2005). Since senescent cells do not replicate (Fig. 1 E-F), it seems unlikely that they are susceptible to SSB mediated replication disturbances. In this regard, it is peculiar that PARP inhibitors affect non-replicating senescent cells, and further research will be needed to examine the underlying mechanisms.

5.5 RCIS cells are predominantly arrested at G2 cell cycle checkpoint

Cell cycle checkpoint activation is an important part of the DDR as it prohibits cell cycle progression in the presence of defective DNA or other cellular damages, thus protecting genomic integrity (Barnum and O'Connell, 2014). Flow cytometric cell cycle analysis with PI revealed a remarkable peak of S phase cells five hours after CX-5461 treatment in murine $Nras^{G12V}$ $p19^{-/-}$ HCC cells (Fig. 7 A-B). Since S phase is characterised by DNA replication (Barnum and O'Connell, 2014), this peak might reflect disturbances during the DNA replication process resulting in an early intra-S-phase checkpoint arrest. Together with the rapid accumulation of DDR proteins (Fig. 2), this early S phase peak indicates that CX-5461 might trigger a DNA damaging event during replication. In line with this conclusion, a previous study has reported that CX-5461 induces DNA damage foci predominantly in S phase in human HCT116 cells (Xu et al., 2017). However, this early S phase peak was replaced by a subsequent rise of G2/M phase cells (Fig. 7 A-B). Given that flow cytometric cell cycle analysis with PI is based on measuring DNA contents within single cells, it does not allow to differentiate between G2 and M phase since both are characterised by a doubled chromosome set. Nonetheless, I suppose that these cells with 4N DNA content are more likely G2 than M phase cells. For instance, the mitotic kinase aurora B, that regulates chromosome segregation and cytokinesis (Goto et al., 2002; Tapia et al., 2006), was at high levels in untreated cells and cells treated with CX-5461 for up to 24 hours, but absent three, five and seven days after drug treatment, thus arguing against M phase status in RCIS cells (Fig. 7 C). Further, a previous study has shown no increase of cellular pH3 levels in CX-5461 treated ALL cells (Negi and Brown, 2015). Since histone H3 is phosphorylated by aurora B at the onset of mitosis (Hsu et al., 2000; Goto et al., 2002; Tapia et al., 2006), the authors did also suggest G2 rather than M phase arrest 24 hours after CX-5461 treatment in ALL cells (Negi and Brown, 2015). However, they did not check for later time points and a following study has indicated transient G2 arrest upon CX-5461 treatment (Quin et al., 2016). Their experiments have revealed G2 arrest 24 and 48, but not 96, hours after CX-5461 treatment in BJ-T cells (Quin et al., 2016). In BJ-T p53sh cells, G2 arrest was still measurable 96 hours after treatment, but also less pronounced than at the 24 or 48 hours time points (Quin et al., 2016). In contrast, my work showed permanent G2 arrest in CX-5461 treated murine $Nras^{G12V}$ $p19^{-/-}$ HCC cells, thus indicating stable G2 arrest in RCIS (Fig. 7 A-B). Moreover, I assume that this G2 arrest results from G2 cell cycle checkpoint activation caused by unrepairable DNA damage. In line with this assumption, the simultaneous amassing of aurora A and cyclin B1 proteins at the twelve hours and one day treatment time points (Fig. 7 C) might correlate with cell accumulation at a premitotic state. Aurora A promotes centrosome maturation during late G2 phase (Barretta et al., 2016), phosphorylates CDC25B to promote G2/M transition (Dutertre et al., 2004), recruits CDK1-cyclin B1 complexes (that accumulate just prior to mitosis but remain inactive until dephosphorylation by CDC25 (Strausfeld et al., 1991)) to centrosomes to promote early mitotic events like chromosome condensation (Hirota et al., 2003), and ensures adequate spindle assembly during prometaphase (Glover et al., 1995). Hence, both aurora A and cyclin B1 take part in G2/M transition (Tanaka et al., 2002; Marumoto et al., 2002) and their simultaneous amassing twelve hours and one day after CX-5461 treatment might indicate cell accumulation just prior to mitosis and therefore at G2 cell cycle checkpoint.

However, interpreting cellular protein levels of cyclin A2 is more challenging since it has dual function in the cell cycle: it binds CDK1 during G2/M transition, and CDK2 during S phase (Pagano et al., 1992). Cyclin A2 accumulated almost continuously within the first 24 hours after CX-5461 treatment, but was nearly absent at the three, five and seven days time points (Fig. 7 C). Like discussed for aurora A and cyclin B1, the amassing of cyclin A2 twelve hours and one day after CX-5461 treatment might correlate with its function in G2/M transition. However, cyclin A2 was upregulated already three, five and eight hours after CX-5461 treatment, maybe due to its function in S phase.

In contrast to cyclin B1 and cyclin A2 protein levels that clearly varied during CX-5461 mediated RCIS induction, cyclin D1 was only slightly reduced five and seven days after treatment (Fig. 7 C). The most common function of cyclin D1 is to dimerise with CDK4 and CDK6 to promote G1/S transition (Massagué, 2004). However, this task cannot explain the stable expression of cyclin D1 during RCIS induction since previous results have shown G2 arrest already eight hours after treatment (Fig. 7 A). In general, interpreting cyclins as direct signs of specific cell cycle phases must be considered critically since mounting evidence indicates overlapping functions for CDKs and cyclins, thus challenging the traditional model of cell-cycle control in which each transition is regulated by pairing of specific CDKs and cyclins (Hochegger et al., 2008). Among the analysed cyclins, cyclin D1 was the only one that was still traceable seven days after CX-5461 treatment and therefore in RCIS. Intriguingly, previous publications have reported enhanced expression of cyclin D1 in senescent human fibroblasts (Fukami et al., 1995; Brown et al., 2012), but the interplay between cyclin D1 and senescence remains poorly understood.

Altogether, I suggest that CX-5461 provokes a DNA damaging event rapidly after drug treatment that occurs during DNA replication and triggers tremendous DDR signalling (Fig. 2). As the general model of cell cycle checkpoints states reversibility if the damage is sufficiently repaired (Shaltiel et al., 2015), I assume that the generated DNA damage is not sufficiently repaired, thus triggering permanent G2 cell cycle checkpoint arrest to prevent mitotic entry. In this case, however, I would expect ongoing amassing of DNA repair proteins, but most of the analysed DDR proteins accumulated just transiently upon CX-5461 treatment (Fig. 2). Therefore, I suppose that CX-5461 provokes an initial DNA damaging event that activates superior cellular mechanisms to preserve permanent cell cycle arrest. In accordance with published literature concerning the mechanisms that ensure stable cell cycle arrest in other types of senescence (Narita et al., 2006), I suggest that the permanent cell cycle arrest in CX-5461 induced RCIS is maintained by persistent chromatin modifications like SAHFs that prevent transcription of genes needed for cell cycle progression.

5.6 CX-5461 provokes genomic instability

Flow cytometric cell cycle analysis with PI revealed hyperploidy in a relevant fraction of CX-5461 induced RCIS murine Nras^{G12V} p19$^{-/-}$ HCC cells (Fig. 7 A-B). However, the underlying mechanism remains unknown. Since unequal chromosome distribution during mitosis is the most common source of aneuploidy (Gordon et al., 2012), I hypothesise that a subfraction of CX-5461 treated cells undergo mitosis instead of cell cycle arrest despite drug-induced DNA damage. This hypothesis is supported by the finding that more than 25% of CX-5461 treated cells were still positive for Ki67 three days after drug treatment (Fig. 1 E-F). As Ki67 positivity indicates ongoing proliferative activity (Gerdes et al., 1983), those cells might have undergone mitosis despite CX-5461 induced DNA damage, thereby risking faulty chromosome distribution and thus aneuploid daughter cells. However, I assume that those aneuploid daughter cells undergo cell cycle checkpoint arrest prior to the next mitotic event since the rate of Ki67 positive cells dropped to 2% seven days after drug treatment (Fig. 1 E-F).

Another mechanistic explanation for the observed aneuploid cells might be endoreplication or endomitosis. Endoreplication, which occurs for instance upon ongoing DDR activation, describes that cells exit cell cycle in G2 phase, skip M phase completely, and undergo S phase instead (Zielke et al., 2013). Hence, endoreplication generates a single giant polyploid nucleus (Zielke et al., 2013), but analysing RCIS cells microscopically has revealed only a few giant nuclei while most cells were multinucleated (data not shown). Under the assumption that these multinucleated cells are the aneuploid ones, it seems more likely that those cells might have undergone endomitosis rather than endoreplication. In endomitosis, mitosis is initiated but not completed, so that the hyperploid cell is either mononucleated or binucleated depending on how far mitosis has progressed (Zielke et al., 2013). However, further research will be necessary to prove the underlying mechanism of CX-5461 induced aneuploidy.

Visualising single chromosomes in RCIS cells would have been helpful to further characterise these aneuploid cells. Though, chromosome spread assay failed in RCIS cells (Fig. 7 D) – probably due to a lack of metaphase cells with maximally condensed and therefore countable chromosomes. As a side effect, the lack of metaphase cells supports once more that RCIS cells are arrested at G2 rather than mitotic spindle assembly checkpoint. Moreover, analysing the DAPI stained samples microscopically led to the discovery of micronuclei in RCIS cells (Fig. 7 D). Since micronuclei are a sign of genomic instability (Lewis and Golsteyn, 2016), they display an indirect hint for chromosomal instability and aneuploidy in RCIS. Hence, the observed micronuclei support my hypothesis that some of the CX-5461 treated cells progress cell cycle despite drug-induced DNA damage, thus suffering genomic instability and aneuploidy. Although chromosomal instability itself has been postulated as a trigger of premature senescence (Andriani et al., 2016), I do not suggest aneuploidy as predominant trigger of RCIS since only a subfraction of CX-5461 treated cells became aneuploid while nearly all cells developed the senescent state.

5.7 p53 protects genomic stability upon CX-5461 treatment

Murine Nras^{G12V} p19$^{-/-}$ p53$^{-/-}$ HCC cells undergo more often cell death upon CX-5461 treatment than murine Nras^{G12V} p19$^{-/-}$ HCC cells (S. Zwirner and K. Wolter, unpublished). Though, the surviving fraction of p53 deficient cells is thought to acquire a senescent phenotype as well (K. Wolter, unpublished).

However, the reason for the different drug responses has not yet been explored and current literature is discordant about the role of p53 in the working mechanism of CX-5461. First, it has been published that CX-5461 induces autophagic cell death with features of a senescent phenotype in a p53-independent manner in solid tumour cell lines (Drygin et al., 2011). This assumption was based on just slightly increased p53 protein levels 24 and 48 hours after CX-5461 treatment in human melanoma A375 cells as well as similar drug sensitivities in p53 wild type and p53 mutant solid cancer cell lines (Drygin et al., 2011). In line with this work, another one has claimed that p53 inhibition does not influence caspase-dependent apoptosis although p53 and p21 expressions were increased one day after CX-5461 treatment in three out of four ALL cell lines (Negi and Brown, 2015). However, this concept was challenged by another study that has suggested p53-dependent apoptotic signalling as main therapeutic effect of CX-5461 in human leukaemia and lymphoma cell lines (Bywater et al., 2012). Based on my own results showing pronounced accumulation of p53 protein within the first hours after CX-5461 treatment (Fig. 1 D), I supposed a critical role for p53 in DDR activation and cell cycle checkpoint arrest upon CX-5461 treatment, for instance via upregulation of p21 transcription (El-Deiry et al., 1993). Yet, p21 protein did not only accumulate in murine Nras^{G12V} p19$^{-/-}$ (Fig. 1 D) but also Nras^{G12V} p19$^{-/-}$ p53$^{-/-}$ (Fig. 8 A) HCC cells, thus demonstrating that p21 activation upon CX-5461 treatment is at least partially independent of p53. Moreover, also p16 and HMGA2 proteins accumulated in the p53 deficient cell line upon CX-5461 treatment (Fig. 8 A), thereby strengthen our assumption that surviving murine Nras^{G12V} p19$^{-/-}$ p53$^{-/-}$ HCC cells undergo senescence just like their p53 proficient counterparts. Further, CX-5461 induced amassing of the CDK inhibitors p21 and p16 as well as the DNA repair proteins FANCD2 and RAD51 was longer-lasting in p53 deficient than p53 wild type cells, thus indicating prolonged DDR activation in the murine Nras^{G12V} p19$^{-/-}$ p53$^{-/-}$ HCC cell line. Together, these results support an involvement of p53 in preventing or repairing DNA damage upon CX-5461 treatment.

Based on its critical role in cell cycle checkpoint activation (Hafner et al., 2019), I hypothesised that p53 deficient cells might be unable to establish stable cell cycle arrest upon CX-5461 treatment, thus entering mitosis despite DNA damage and finally becoming prone to mitotic catastrophe and apoptosis. However, CX-5461 caused early accumulation of S phase cells followed by stable G2 arrest not only in p53 proficient (Fig. 7 A-B) but also p53 deficient (Fig. 8 C-D) cells. Yet, the cell lines remarkably differed in their fraction of aneuploid cells and their amount of micronuclei seven days after drug treatment that were much higher in the p53 deficient cell line (Fig. 8 B-E). Accordingly, murine Nras^{G12V} p19$^{-/-}$ p53$^{-/-}$ HCC cells are more endangered to suffer genomic instability upon CX-5461 treatment than their p53 proficient counterpart, thus supporting a critical role for p53 in protecting genomic integrity upon CX-5461 treatment. Further, the higher risk of genomic instability might explain why murine Nras^{G12V} p19$^{-/-}$ p53$^{-/-}$ HCC cells are undergoing more often cell death upon CX-5461 treatment than murine Nras^{G12V} p19$^{-/-}$ HCC cells. Since another study has reported CX-5461 induced chromosomal abnormalities in BRCA2$^{-/-}$ but not BRCA2 wild type HCT116 cells (Xu et al., 2017), it seems likely that both p53 and BRCA2 are guardians of genomic integrity upon CX-5461 treatment.

5.8 CX-5461 causes formation of DNA:RNA hybrids

Based on my experiments showing DNA:RNA hybrid formation upon CX-5461 treatment (Fig. 9), I hypothesised that those might be the mediators of CX-5461 induced DDR activation. Most commonly, DNA:RNA hybrids form co-transcriptionally when newly synthesised RNA reanneals to its template DNA strand, thus generating a DNA:RNA hybrid and a displaced non-template DNA strand (Thomas et al., 1976). These three-stranded nucleic acid structures are called R-loops due to their similarity to D-loops (known from HR) differing in their RNA moiety (Thomas et al., 1976). While physiological R-loops are thought to perform co-transcriptional regulatory functions and support DNA repair, evidence is mounting that R-loop misregulation results in DNA damage and genomic instability (Niehrs and Luke, 2020). The abundance of DNA:RNA hybrids in CX-5461 treated cells (Fig. 9) suggests that CX-5461 provokes formation of R-loops. At first glance, it seems quite plausible that RNAP I inhibition causes R-loop formation since R-loops are by-products of transcription (Thomas et al., 1976) and their accumulation has been already reported upon RNAP II arrest (Zhang et al., 2017). Though, considering the working mechanism of CX-5461 in more detail (Drygin et al., 2011) is not in line with the common model of co-transcriptional R-loop formation. While co-transcriptional R-loops are formed during elongation (Aguilera and García-Muse, 2012), CX-5461 inhibits transcription at the initiation stage (Drygin et al., 2011). However, there are some possible explanations how R-loops might still form upon CX-5461 treatment. First, CX-5461 might affect bonds between rDNA and RNAP I molecules that are already at elongation stage at the time of treatment, thus provoking co-transcriptional R-loops. Second, CX-5461 might arrest RNAP I after DNA unwinding had already happened, thus making rDNA molecules vulnerable for RNA annealing. In this context, the annealing RNA molecules might be transcribed by another RNAP molecule. Although DNA:RNA hybrid formation requires sequence homology, however, some studies have reported DNA:RNA hybrids containing RNA moieties synthesised elsewhere in the genome, called *in trans* DNA:RNA hybrids (Wahba et al., 2013; Nadel et al., 2015) – and some hints are indicating that CX-5461 might form such DNA:RNA hybrids *in trans*. First, RAD51 protein, that accumulates rapidly after CX-5461 treatment (Fig. 2 C), has a non-canonical function in promoting hybridisation of RNA to homologous chromosomal loci distinct from their site of synthesis (Wahba et al., 2013). Moreover, DNA:RNA hybrid formation is markedly facilitated by non-template DNA strand sequences with high G/C ratio (Roy and Lieber, 2009; Ginno et al., 2012) – and rDNA genes, whose transcription is disturbed by CX-5461, have G-rich regions downstream their promoters, thus making them predilection sites for R-loop formation (Roy and Lieber, 2009; Lindström et al., 2018). Further, it has been published that CX-5461 increases the frequency of G-quadruplexes (Xu et al., 2017) which are secondary structures forming at G-rich sequences.

Based on the assumption that CX-5461 provokes DNA:RNA hybrids *in trans,* the RNA moiety might be synthesised by RNAP II or RNAP III instead of RNAP I. However, it is suggested that CX-5461 inhibits RNAP I without affecting RNAP II (Drygin et al., 2011), but no data is available concerning if CX-5461 manipulates RNAP III. In ribosomal biogenesis, 5 S rRNA is synthesised by RNAP III, while all the other rRNA molecules are cleaved from a 45 S precursor transcribed by RNAP I (Russell and Zomerdijk, 2006). If CX-5461 inhibits RNAP I but not RNAP III, CX-5461 might disequilibrate the cellular rRNA content so that 5 S rRNA molecules amass. These redundant 5 S rRNA molecules might serve as RNA moieties in DNA:RNA hybrid formation. Yet, it must be emphasised that this is only a hypothesis since up to now no data is available if 5 S rRNA molecules indeed accumulate in CX-5461 treated cells. Moreover, it would be interesting to test if CX-5461 impacts the activity of extracellular-signal-regulated kinase (ERK) that co-regulates RNAP I and RNAP III to ensure coordinated rRNA synthesis (White, 2005).

Although the mechanism how CX-5461 generates DNA:RNA hybrids remains a bit enigmatic, however, my experiments clearly show their formation upon CX-5461 treatment (Fig. 9). Therefore, it arises the question in what way DNA:RNA hybrids are impacting the cellular fate in the context of CX-5461 treatment. The two-faced nature of R-loops – beneficial ‘physiological’ R-loops and detrimental ‘unscheduled' R-loops (Niehrs and Luke, 2020) – implies that the abundant DNA:RNA hybrids observed in CX-5461 treated cells might contribute to drug induced DDR activation and genomic instability. Intriguingly, DNA:RNA hybrids can, if not resolved quickly, lead to clashes between transcription and replication machineries (García-Muse and Aguilera, 2016). I hypothesise that CX-5461 treated cells acquire DNA:RNA hybrids that subsequently provoke such transcription-replication collisions (TRCs). This hypothesis is in line with the assumption that CX-5461 disturbs the replication process (discussed in chapter 5.5) as supported by the S phase peak observed five hours after drug treatment (Fig. 7 A-B) as well as the results from another study indicating that CX-5461 induces DNA damage during replication (Xu et al., 2017). Further, p53 has been shown to participate in preventing interferences between replication and transcription – and this non-canonical function of p53 is independent of p21-driven cell cycle arrest (Yeo et al., 2016). Based on that, I hypothesise that p53 deficient cells have a higher risk to suffer TRCs upon CX-5461 treatment than p53 wild type cells, thus offering an explanatory approach why murine $Nras^{G12V}$ $p19^{-/-}$ $p53^{-/-}$ HCC cells undergo more often aneuploidy (Fig. 8 B-E) and cell death (S. Zwirner and K. Wolter, unpublished) upon CX-5461 treatment than their p53 proficient counterparts. Since this feature of p53 is independent of p21-driven cell cycle arrest (Yeo et al., 2016), this hypothesis is in line with the finding that both cell lines experience p21 activation and cell cycle checkpoint arrest (Fig. 1 D, Fig. 7 A-B, Fig. 8).

TRCs pose tremendous threats to genomic stability since they trigger replication fork stalling (Gan et al., 2011). I assume that CX-5461 treated cells acquire DNA:RNA hybrids that provoke TRCs with subsequent replication fork stalling. As RPA is commonly known to coat ssDNA at stalled replication forks (Branzei and Foiani, 2010), the accumulation of pRPA32 (S4/S8) upon CX-5461 treatment (Fig. 2 C) might support this hypothesis. However, accumulation of pRPA32 (S4/S8) is not specific, and visualising progression of individual replication forks by DNA fibre technique is superior to prove replication fork stalling (Nieminuszczy et al., 2016). Strikingly, this assay has been performed by another group and they have reported substantially shortened replication track length – indicating blocked replication forks – in HCT116 cells treated with CX-5461 for 30 minutes (Xu et al., 2017). This effect was more prominent in BRCA2 deficient than BRCA2 proficient HCT116 cells and BRCA2 knockout HCT116 cells showed enhanced lethality upon CX-5461 treatment (Xu et al., 2017). Although the underlying mechanisms are poorly understood, it is known that BRCA1 and BRCA2 proteins are involved in R-loop restoration (Bhatia et al., 2014; Hatchi et al., 2015; Tan et al., 2017; Shivji et al., 2018). Therefore, I assume that the hypersensitivity of BRCA2 deficient cells to CX-5461 observed by Xu et al. might be based on impaired R-loop repair. Although the exact mechanisms of R-loop restoration are not yet entirely identified, it is suggested that pathways known from resolving other types of transcriptional stress might be involved (Crossley et al., 2019). For instance, NER factors that are known to remove bulky DNA lesions are thought to actively process R-loops into DSBs (Sollier et al., 2014). These DSBs might trigger ATM activation that, together with ATR activation by RPA, might orchestrate broad DDR signalling in response to R-loops (Sollier and Cimprich, 2015). Further, it has been proposed that RPA stimulates RNase H1 to remove RNA moieties in DNA:RNA hybrids (Nguyen et al., 2017). Although it seems more likely that the accumulation of pRPA32 (S4/S8) upon CX-5461 treatment (Fig. 2 C) is due to its ssDNA stabilising function at stalled replication forks, it might also indicate DNA:RNA hybrid repair. Moreover, different cell lines defective in FANCD2 or FANCA have been shown to accumulate R-loops (Schwab et al., 2015; García-Rubio et al., 2015), thus suggesting an involvement of FA pathway in R-loop repair. FANCM protein has been even shown to resolve R-loops directly via its translocase activity (Schwab et al., 2015). In this context, amassing of FANCD2, FANCI and FANCM proteins in CX-5461 treated cells (Fig. 2 C) might be a sign of R-loop repair. Therefore, I hypothesise that not only BRCA2 (synonymous name: FANCD1) deficiency (Xu et al., 2017) but also deficiencies in other FA pathway proteins might enhance the lethality of CX-5461. Since no potent FA protein inhibitor is currently available to test this hypothesis pharmacologically, a starting point for further research projects might be using RNAi technique to determine the lethality of CX-5461 upon different FA protein deficiencies.

All in all, I assume that CX-5461 treated cells acquire DNA:RNA hybrids that provoke TRCs and replication fork stalling. However, replication fork stalling itself might be responsible for aneuploidy observed in a part of CX-5461 treated cells (Fig. 7, Fig. 8). This linkage is inspired by Saada et al. who have established a mechanistic model how replication fork stalling causes aneuploidy. They have suggested that temporarily paused forks are stabilised by intra-S-phase checkpoint activation and protected by RAD51 (Saada et al., 2017). In the absence of recombination proteins, large ssDNA gaps arise behind these forks and lead to mitotic sister chromatid bridging that results in aneuploidy and cell death (Saada et al., 2017). Strikingly, my experiments showed RAD51 accumulation (Fig. 2 C) and rise of S phase cells (Fig. 7 A-B) within the first hours after CX-5461 treatment that might correlate to temporarily paused forks. Further, formation of large ssDNA gaps at permanently stalled forks might explain the delayed but ongoing accumulation of pRPA2 (S4/S8) that starts in temporal context with the drop of RAD51 protein levels (Fig. 2 C). Moreover, transition from transient to terminal fork arrest might trigger the observed shift from intra-S-phase to permanent G2 cell cycle checkpoint arrest (Fig. 7 A-B). Overcoming adequate G2 cell cycle checkpoint arrest despite terminal replication fork stalling might result in mitotic sister chromatid bridging and thus aneuploidy.

Altogether, I propose a novel mode of action for CX-5461 that is based on the formation of DNA:RNA hybrids causing TRCs in S phase cells, which lead to replication fork stalling and permanent G2 cell cycle arrest. Further, I assume that these events are crucial mediators of DDR activation and genomic instability upon CX-5461 treatment and that p53 is involved in preventing such TRCs. This novel hypothetic mode of action for CX-5461 offers a conceivable explanation for most of my observations, but further research will be needed for its verification.

6 Outlook

Understanding the working mechanism and side effects of CX-5461 at its molecular biological level is indispensable for ensuring drug safety and enabling powerful combination therapy strategies. In this work, I proposed a novel hypothetic mode of action for CX-5461 that bases on drug-induced DNA:RNA hybrids which provoke TRCs and replication fork stalling. To strengthen my hypothesis, the kinetics of CX-5461 induced DNA:RNA hybrid formation and replication fork stalling should be further analysed in a time-course setting. To this end, immunofluorescence could be used to monitor DNA:RNA hybrid formation, while DNA fibre technique is a good choice for visualising replication fork stalling. Further, following studies should be conducted in both p53 wild type and p53 mutant cells since my work has proposed p53 as guardian of genomic stability upon CX-5461 treatment.

Based on my results showing DNA:RNA hybrid formation upon CX-5461 treatment, I assume that DDR inhibitors targeting R-loop repair pathways might be synergistically lethal in combination therapy with CX-5461. Since previous studies have reported an involvement for BRCA1 and BRCA2 proteins in R-loop restoration (Bhatia et al., 2014; Hatchi et al., 2015; Tan et al., 2017; Shivji et al., 2018), I suggest that the hypersensitivity of BRCA2 deficient cells to CX-5461 (Xu et al., 2017) might result from impaired R-loop repair. As topoisomerase (Drolet et al., 1995; El Hage et al., 2010) and RAD51 (Wahba et al., 2013) were suspected to be involved in R-loop repair, topoisomerase inhibitors (e.g. topotecan or irinotecan) and the RAD51 inhibitor B02 should be tested in combination therapy with CX-5461. Further, an R-loop resolving function was proposed for FA pathway proteins (Schwab et al., 2015; García-Rubio et al., 2015). Since no potent FA protein inhibitor is currently available, it might be interesting to determine the lethality of CX-5461 upon different FA protein deficiencies using RNAi technique. Altogether, the novel hypothetic mode of action proposed in this work offers a promising starting point for further research projects and new combination therapy studies with CX-5461.

7 Summary

7.1 English

Cellular senescence is a phenomenon by which normal cells cease to divide but stay transcriptionally and metabolically active while their cell cycle is durably arrested. Although senescence functions as tumour suppressor mechanism during early tumourigenesis, accumulating evidence suggests that it poses a risk for tumour progression in pre-existing tumour cells. Ongoing research is done to identify agents that eliminate unwanted senescent cells selectively, so called senolytics. One of the features described for several types of senescence is an activated DNA damage response (DDR). In this work, we used murine $Nras^{G12V}$ $p19^{-/-}$ HCC cells to analyse DDR activation in a novel type of senescence induced by the RNA polymerase I inhibitor CX-5461 that has been recently characterised by the Zender laboratory (K. Wolter, unpublished) and termed ribosomal checkpoint induced senescence (RCIS). Although we observed pronounced DDR activation and permanent G2 cell cycle arrest upon CX-5461 treatment, we neither found a synergistic effect when treating cells with CX-5461 and DDR inhibitors simultaneously nor a senolytic effect by DDR inhibition in RCIS cells. Quite the contrary, cells became totally resistant against DDR inhibitors when nearing the senescent state. Further, we discovered that CX-5461 affects genomic stability, and that p53 wild type status serves as a key feature in preserving genomic integrity upon CX-5461 treatment. Last but not least, we observed DNA:RNA hybrid formation upon CX-5461 treatment, thus offering new insights in the molecular working mechanism of CX-5461. Based on that, I proposed a novel hypothetic mode of action for CX-5461 focusing on clashes between transcription and replication machineries. This new approach raises the question if DNA:RNA hybrids or such clashes might be critical in senescence induction. Further, targeting proteins involved in DNA:RNA hybrid repair displays a promising starting point for new combination therapy studies aiming to increase the effectiveness of CX-5461 for tumour therapy.

7.2 German

Die zelluläre Seneszenz beschreibt einen Zustand, bei dem Zellen transkriptionell und metabolisch aktiv bleiben, während ihr Zellzyklus stabil arretiert ist. Obwohl die Seneszenz in der Frühphase der Tumorentstehung als Tumorsuppressormechanismus dient, scheint sie bei bereits bestehendem Tumorgewebe ein Risikofaktor für einen Tumorprogress darzustellen. Daher zielen aktuelle Forschungsarbeiten darauf ab, Substanzen zu identifizieren, die ungewünschte seneszente Zellen gezielt eliminieren, sogenannte Senolytika. Ein für mehrere Seneszenztypen beschriebenes Merkmal ist die Aktivierung einer DNA Schadensantwort (DDR). In dieser Arbeit nutzten wir murine Nras^{G12V} p19$^{-/-}$ HCC Zellen, um die DDR-Aktivierung in einer neuen Form von Seneszenz zu untersuchen, die durch den RNA Polymerase I Inhibitor CX-5461 ausgelöst wird und kürzlich vom Zender Labor (K. Wolter, unveröffentlicht) charakterisiert und als ribosomal-induzierte Seneszenz (RCIS) benannt wurde. Obwohl wir nach CX-5461 Behandlung eine starke Aktivierung verschiedener DDR-Signalwege und die Etablierung eines permanenten G2-Zellzyklus-Arrests zeigen konnten, fand sich weder ein synergistischer Effekt bei simultaner Behandlung mit CX-5461 und DDR-Inhibitoren noch ein senolytischer Effekt von DDR-Inhibitoren in RCIS-Zellen. Seneszente Zellen entwickelten sogar eine komplette Resistenz gegenüber den getesteten DDR-Inhibitoren. Des Weiteren beobachteten wir, dass CX-5461 die genomische Struktur deutlich verändert und identifizierten den p53 Wildtyp Status als Schlüsseleigenschaft zum Erhalt der genomischen Integrität nach CX-5461 Behandlung. Abschließend stellten wir fest, dass es unter Behandlung mit CX-5461 zur Bildung von DNA:RNA Hybriden kommt. Darauf basierend stellte ich eine neue Hypothese bezüglich des Wirkmechanismus von CX-5461 auf, die auf dem Zusammenstoßen von Transkriptions- und Replikationsmechanismen beruht. Unklar bleibt, ob DNA:RNA Hybride eine funktionelle Relevanz bei der Seneszenzinduktion haben. Die in der Reparatur von DNA:RNA Hybriden beteiligten Proteine stellen jedoch vielversprechende Zielstrukturen für neue Kombinationstherapien mit CX-5461 dar, um dessen Wirksamkeit in der Tumortherapie zu verbessern.

Supplementary Figures

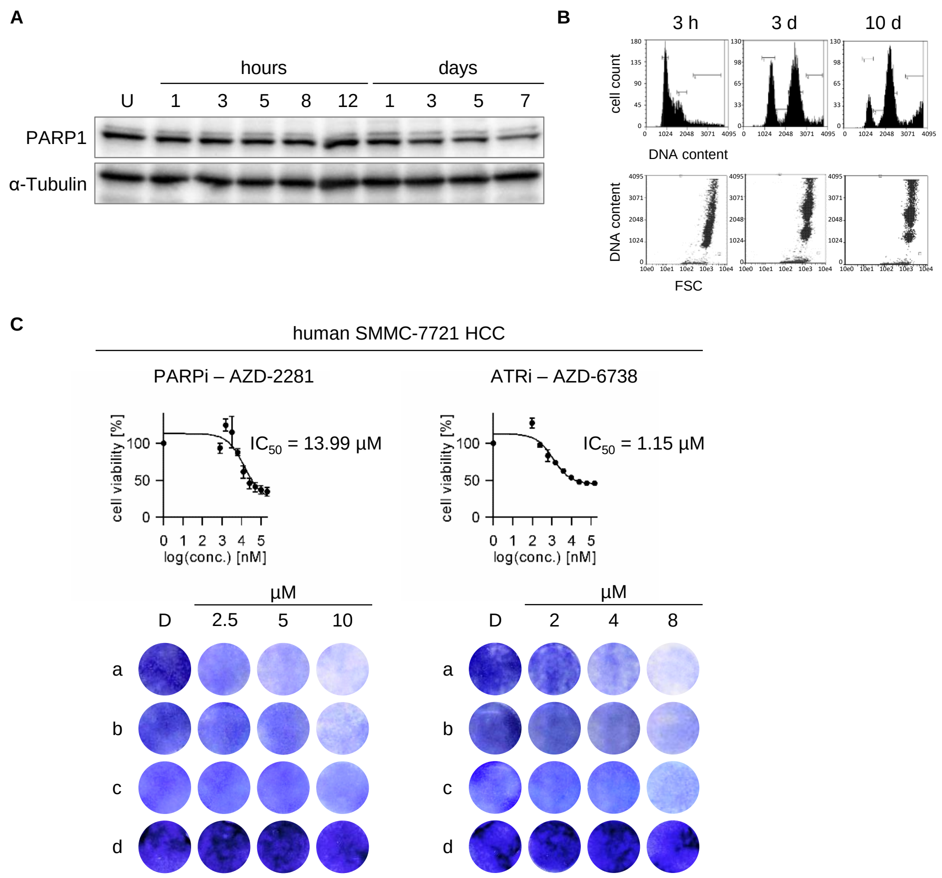

Supplementary Figure 1

A-C Experiments were done with murine Nras^{G12V} p19$^{-/-}$ HCC cells (A-B) and human SMMC-7721 HCC cells (C). CX-5461 was used at 500 nM. **A** Western blot analysis of PARP1 in untreated (U) and CX-5461 treated cells. CX-5461 treatment was investigated at nine time points after initial drug treatment. α-Tubulin was used as loading control. **B** Flow cytometric cell cycle analysis with PI in untreated and CX-5461 treated cells. CX-5461 treatment was investigated at eleven time points after initial drug treatment. For lack of space, original data of the three hours, three days and ten days samples are shown here. All other samples are shown in Fig. 7 A. **C** IC_{50} measurements on growing cells were performed by XTT assay. Data show mean ± SD (n = 3 replicates). Crystal violet colony formation assay was used to analyse the inhibitory effect upon different treatment settings. Different settings are labelled as following: a) inhibitor on growing cells, b) pre-treatment with inhibitor, c) simultaneous treatment, and d) inhibitor on RCIS cells (for more detailed description see chapter 3.2.3). Control treatment was done with DMSO (D). For each setting, one representative out of triplicates is illustrated.

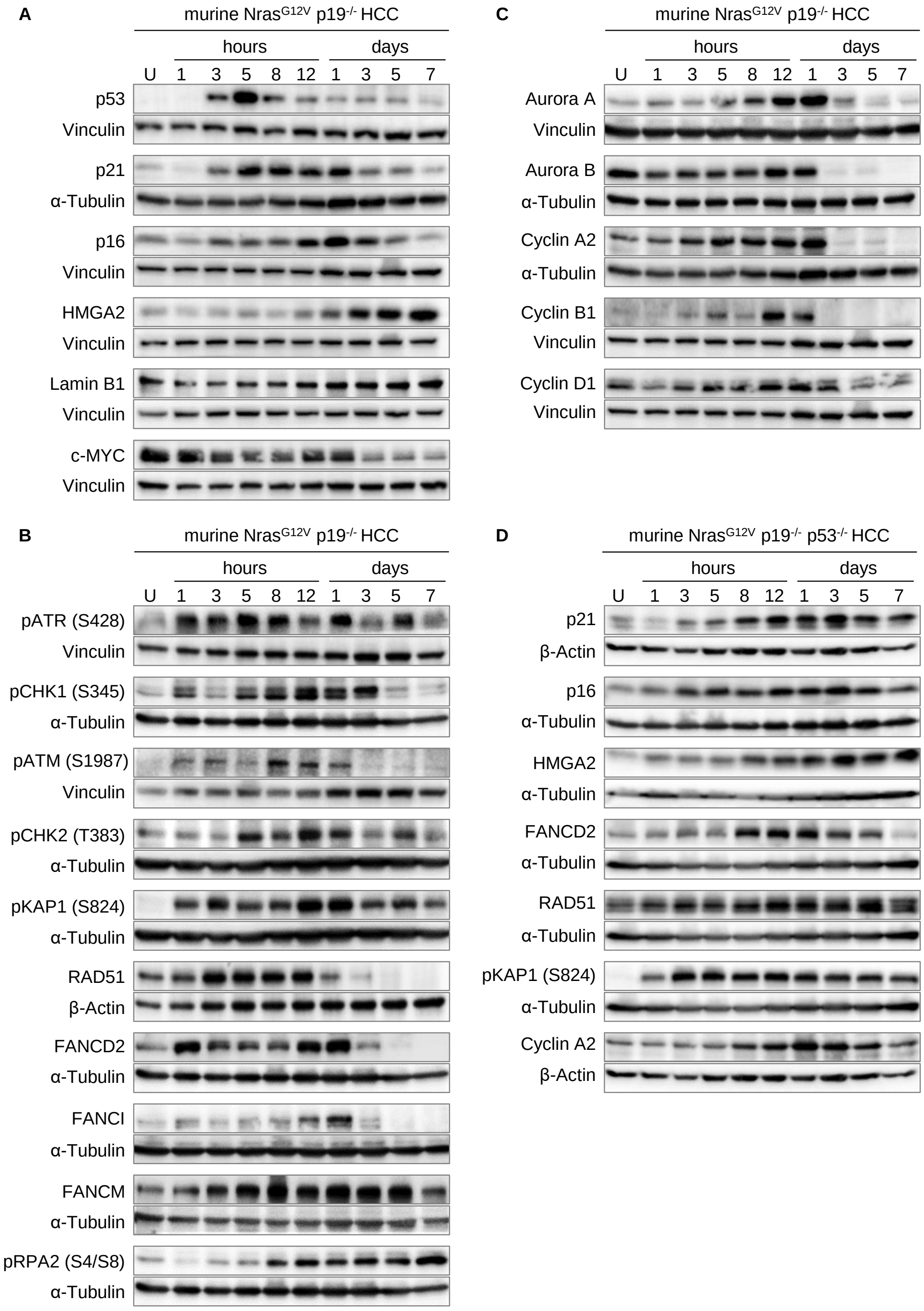

Supplementary Figure 2

A-D This figure includes all western blots shown in chapter 4 with their corresponding loading controls (**A** - Fig. 1 D, **B** - Fig. 2 C, **C** - Fig. 7 C, **D** - Fig. 8 A). Experiments were done with untreated (U) and CX-5461 treated cells. CX-5461 was used at 500 nM. CX-5461 treatment was investigated at nine time points after initial drug treatment as labelled within the figure.

References

Aguilera, A. and García-Muse, T. (2012) 'R Loops: From Transcription Byproducts to Threats to Genome Stability', *Molecular Cell*, vol. 46, pp. 115-124.

Alcorta, D., Xiong, Y., Phelps, D., Hannon, G., Beach, D. and Barrett, J. (1996) 'Involvement of the cyclin-dependent kinase inhibitor p16 (INK4a) in replicative senescence of normal human fibroblasts ', *Proceedings of the National Academy of Sciences*, vol. 93, pp. 13742-13747.

Andriani, G., Almeida, V., Faggioli, F., Mauro, M., Tsai, W., Santambrogio, L., Maslov, A., Gadina, M., Campisi, J., Vijg, J. and Montagna, C. (2016) 'Whole Chromosome Instability induces senescence and promotes SASP', *Nature*, vol. 6, pp. 1-17.

Baerlocher, G., Mak, J., Röth, A., Rice, K. and Lansdorp, P. (2003) 'Telomere shortening in leukocyte subpopulations from baboons', *Journal of Leukocyte Biology*, vol. 73, pp. 289-296.

Baker, S., Fearon, E., Nigro, J., Hamilton, S., Preisinger, A., Jessup, J., Tuinen, P., Ledbetter, D., Barker, D., Nakamura, Y., White, R. and Vogelstein, B. (1989) 'Chromosome 17 Deletions and p53 Gene Mutations in Colorectal Carcinomas', *Science*, vol. 244, pp. 217-221.

Baker, D., Wijshake, T., Tchkonia, T., LeBrasseur, N., Childs, B., Sluis, B., Kirkland, J. and Deursen, J. (2011) 'Clearance of p16Ink4a-positive senescent cells delays ageing-associated disorders', *Nature*, vol. 479, pp. 232-236.

Bakkenist, C., Drissi, R., Wu, J., Kastan, M. and Dome, J. (2004) 'Disappearance of the Telomere Dysfunction-Induced Stress Response in Fully Senescent Cells', *Cancer Research*, vol. 64, pp. 3748-3752.

Bakkenist, C. and Kastan, M. (2003) 'DNA damage activates ATM through intermolecular autophosphorylation and dimer dissociation', *Nature*, vol. 421, pp. 499-506.

Banin, S., Moyal, L., Shieh, S.Y., Taya, Y., Anderson, C., Chessa, L., Smorodinsky, N., Prives, C., Reiss, Y., Shiloh, Y. and Ziv, Y. (1998) 'Enhanced Phosphorylation of p53 by ATM in Response to DNA Damage', *Science*, vol. 281, pp. 1674-1677.

Barascu, A., Le Chalony, C., Pennarun, G., Genet, D., Imam, N., Lopez, B. and Bertrand, P. (2012) 'Oxidative stress induces an ATM-independent senescence pathway through p38 MAPK-mediated lamin B1 accumulation', *The EMBO Journal*, vol. 31, pp. 1080-1094.

Barnum, K. and O’Connell, M. (2014) 'Cell Cycle Regulation by Checkpoints', *Methods in Molecular Biology*, vol. 1170, pp. 29-40.

Barretta, M., Spano, D., D’Ambrosio, C., Cervigni, R., Scaloni, A., Corda, D. and Colanzi, A. (2016) 'Aurora-A recruitment and centrosomal maturation are regulated by a Golgi-activated pool of Src during G2', *Nature Communications*, vol. 7, pp. 1-13.

Bartkova, J., Rezaei, N., Liontos, M., Karakaidos, P., Kletsas, D., Issaeva, N., Vassiliou, L.-V., Kolettas, E., Niforou, K., Zoumpourlis, V., Takaoka, M., Nakagawa, H., Tort, F., Fugger, K., Johansson, F., Sehested, M., Andersen, C., Dyrskjot, L., Ørntoft, T., Lukas, J., Kittas, C., Helleday, T., Halazonetis, T., Bartek, J. and Gorgoulis, V. (2006) 'Oncogene-induced senescence is part of the tumorigenesis barrier imposed by DNA damage checkpoints', *Nature*, vol. 444, pp. 633-637.

Beauséjour, C., Krtolica, A., Galimi, F., Narita, M., Lowe, S., Yaswen, P. and Campisi, J. (2003) 'Reversal of human cellular senescence: roles of the p53 and p16 pathways.', *The EMBO Journal*, vol. 22, pp. 4212-4222.

Bhatia, V., Barroso, S., García-Rubio, M., Tumini, E., Herrera-Moyano, E. and Aguilera, A. (2014) 'BRCA2 prevents R-loop accumulation and associates with TREX-2 mRNA export factor PCID2', *Nature*, vol. 511, pp. 362-365.

Bond, J., Haughton, M., Blaydes, J., Gire, V., Wynford-Thomas, D. and Wyllie, F. (1996) 'Evidence that transcriptional activation by p53 plays a direct role in the induction of cellular senescence', *Oncogene*, vol. 13, pp. 2097-2104.

Bonetti, D., Colombo, C., Clerici, M. and Longhese, M. (2018) 'Processing of DNA Ends in the Maintenance of Genome Stability', *Frontiers in Genetics*, vol. 9, pp. 1-11.

Boyce, R. and Howard-Flanders, P. (1964) 'Release of ultraviolet light-induced thymine dimers from DNA in E. coli K-12', *Proceedings of the National Academy of Sciences*, vol. 51, pp. 293-300.

Braig, M., Lee, S., Loddenkemper, C., Rudolph, C., Peters, A., Schlegelberger, B., Stein, H., Dörken, B., Jenuwein, T. and Schmitt, C. (2005) 'Oncogene-induced senescence as an initial barrier in lymphoma development', *Nature*, vol. 436, pp. 660-665.

Branzei, D. and Foiani, M. (2010) 'Maintaining genome stability at the replication fork', *Nature Reviews Molecular Cell Biology*, vol. 11, pp. 208-219.

Bronner, D., Baker, S., Morrison, P., Warren G, Smith, L., Lescoe, M., Kane, M., Earabino, C., Lipford, J., Lindblom, A., Tannergård, P., Bollag, R., Godwin, A., Ward, D., Nordenskøld, M., Fishel, R., Kolodner, R. and Liskay, R. (1994) 'Mutation in the DNA mismatch repair gene homologue hMLH1 is associated with hereditary non-polyposis colon cancer', *Nature*, vol. 368, pp. 258-261.

Brown, N., Jeselsohn, R., Bihani, T., Hu, M., Foltopoulou, P., Kuperwasser, C. and Hinds, P. (2012) 'Cyclin D1 Activity Regulates Autophagy and Senescence in the Mammary Epithelium', *Cancer Research*, vol. 72, pp. 6477-6489.

Bryant, H., Schultz, N., Thomas, H., Parker, K., Flower, D., Lopez, E., Kyle, S., Meuth, M., Curtin, N. and Helleday, T. (2005) 'Specific killing of BRCA2-deficient tumours with inhibitors of poly(ADP-ribose) polymerase', *Nature*, vol. 434, pp. 913-917.

Bunz, F., Dutriaux, A., Lengauer, C., Waldman, T., Zhou, S., Brown, J., Sedivy, M., Kinzler, K. and Vogelstein, B. (1998) 'Requirement for p53 and p21 to Sustain G2 Arrest After DNA Damage', *Science*, vol. 282.

Burma, S., Chen, B., Murphy, M., Kurimasa, A. and Chen, D. (2001) 'ATM phosphorylates histone H2AX in response to DNA double-strand breaks', *The Journal of Biological Chemistry*, vol. 276, pp. 42462-42467.

Bywater, M., Poortinga, G., Sanij, E., Hein, N., Peck, A., Cullinane, C., Wall, M., Cluse, L., Drygin, D., Anderes, K., Huser, N., Proffitt, C., Bliesath, J., Haddach, M., Schwaebe, M., Ryckman, D., Rice, W., Schmitt, C., Lowe, S., Johnstone, R., Pearson, R., McArthur, G. and Hannan, R. (2012) 'Inhibition of RNA Polymerase I as a Therapeutic Strategy to Promote Cancer-Specific Activation of p53', *Cancer Cell*, vol. 22, pp. 51-65.

Bzymek, M., Thayer, N., Oh, S., Kleckner, N. and Hunter, N. (2010) 'Double Holliday junctions are intermediates of DNA break repair', *Nature*, vol. 464, pp. 937-941.

Cahu, J., Bustany, S. and Sola, B. (2012) 'Senescence-associated secretory phenotype favors the emergence of cancer stem-like cells', *Cell Death and Disease*, vol. 3, pp. 1-8.

Campisi, J. (2005) 'Senescent Cells, Tumor Suppression, and Organismal Aging: Good Citizens, Bad Neighbors', *Cell*, vol. 120, pp. 513-522.

Campisi, J. and Fagagna, F. (2007) 'Cellular senescence: when bad things happen to good cells', *Nature Reviews Molecular Cell Biology*, vol. 8, pp. 729-740.

Carvajal, L., Hamard, P.J., Tonnessen, C. and Manfredi, J. (2012) 'E2F7, a novel target, is up-regulated by p53 and mediates DNA damage-dependent transcriptional repression', *Genes & Development*, vol. 26, pp. 1533-1545.

Cavanagh, B., Walker, T., Norazit, A. and Meedeniya, A. (2011) 'Thymidine Analogues for Tracking DNA Synthesis', *Molecules*, vol. 16, pp. 7980-7993.

Ceccaldi, R., Parmar, K., Mouly, E., Delord, M., Kim, J., Regairaz, M., Pla, M., Vasquez, N., Zhang, Q.S., Pondarre, C., Latour, R., Gluckman, E., Cavazzana-Calvo, M., Leblanc, T., Larghero, J., Grompe, M., Socié, G., A. and Soulier, J. (2012) 'Bone Marrow Failure in Fanconi Anemia Is Triggered by an Exacerbated p53/p21 DNA Damage Response that Impairs Hematopoietic Stem and Progenitor Cells', *Cell Stem Cell*, vol. 11, pp. 36-49.

Chang, B.D., Broude, E., Dokmanovic, M., Zhu, H., Ruth, A., Xuan, Y., Kandel, E., Lausch, E., Christov, K. and Roninson, I. (1999) 'A Senescence-like

Phenotype Distinguishes Tumor Cells That Undergo Terminal Proliferation Arrest after Exposure to Anticancer Agents', *Cancer Research*, vol. 59, pp. 3761-3767.

Chang, H., Pannunzio, N., Adachi, N. and Lieber, M. (2017) 'Non-homologous DNA end joining and alternative pathways to double-strand break repair', *Nature Reviews Molecular Cell Biology*, vol. 18, pp. 495-506.

Chan, K., Palmai-Pallag, T., Ying, S. and Hickson, I. (2009) 'Replication stress induces sister-chromatid bridging at fragile site loci in mitosis', *Nature Cell Biology*, vol. 11, pp. 753-760.

Chaudhuri, A. and Nussenzweig, A. (2017) 'The multifaceted roles of PARP1 in DNA repair and chromatin remodelling', *Nature Reviews Molecular Cell Biology*, vol. 18, pp. 610-621.

Chen, Q. and Ames, B. (1994) 'Senescence-like growth arrest induced by hydrogen peroxide in human diploid fibroblast F65 cells', *Proceedings of the National Academy of Sciences*, vol. 91, pp. 4130-4134.

Chen, Z., Trotman, L., Shaffer, D., Lin, H.K., Dotan, Z., Niki, M., Koutcher, J., Scher, H., Ludwig, T., Gerald, W., Cordon-Cardo, C. and Pandolfi, P. (2005) 'Crucial role of p53-dependent cellular senescence in suppression of Pten-deficient tumorigenesis', *Nature*, vol. 436, pp. 725-730.

Chen, R. and Wold, M. (2014) 'Replication protein A: Single-stranded DNA’s first responder', *BioEssays*, vol. 36, pp. 1156-1161.

Ciccia, A., Ling, C., Coulthard, R., Yan, Z., Xue, Y., Meetei, A., Laghmani, E., Joenje, H., McDonald, N., Winter, J., Wang, W. and West, S. (2007) 'Identification of FAAP24, a Fanconi Anemia Core Complex Protein that Interacts with FANCM', *Molecular Cell*, vol. 25, pp. 331-343.

Cleaver, J. (1968) 'Defective Repair Replication of DNA in Xeroderma Pigmentosum', *Nature*, vol. 218, pp. 652-656.

Collado, M., Gil, J., Efeyan, A., Guerra, C., Schuhmacher, A., Barradas, M., Benguría, A., Zaballos, A., Flores, J., Barbacid, M., Beach, D. and Serrano, M. (2005) 'Senescence in premalignant tumours', *Nature*, vol. 436, p. 642.

Coppé, J.P., Desprez, P.Y., Krtolica, A. and Campisi, J. (2010) 'The Senescence-Associated Secretory Phenotype: The Dark Side of Tumor Suppression', *Annual Review of Pathology: Mechanisms of Disease*, vol. 5, pp. 99-118.

Coppé, J.P., Patil, C., Rodier, F., Sun, Y., Muñoz, D., Goldstein, J., Nelson, P., Desprez, P.Y. and Campisi, J. (2008) 'Senescence-Associated Secretory Phenotypes Reveal Cell-Nonautonomous Functions of Oncogenic RAS and the p53 Tumor Suppressor', *PLoS Biology*, vol. 6, pp. 2853-2868.

Crossley, M., Bocek, M. and Cimprich, K. (2019) 'R-Loops as Cellular Regulators and Genomic Threats', *Molecular Cell*, vol. 73, pp. 398-411.

Dai, M.S. and Lu, H. (2004) 'Inhibition of MDM2-mediated p53 Ubiquitination and Degradation by Ribosomal Protein L5', *The Journal of Biological Chemistry*, vol. 279, pp. 44475-44482.

Dai, M.S., Zeng, S., Jin, Y., Sun, X.X., David, L. and Lu, H. (2004) 'Ribosomal Protein L23 Activates p53 by Inhibiting MDM2 Function in Response to Ribosomal Perturbation but Not to Translation Inhibition', *Molecular and Cellular Biology*, vol. 24, pp. 7654-7668.

De Silva, I., McHugh, P., Clingen, P. and Hartley, J. (2000) 'Defining the Roles of Nucleotide Excision Repair and Recombination in the Repair of DNA Interstrand Cross-Links in Mammalian Cells', *Molecular and Cellular Biology*, vol. 20, pp. 7980-7990.

Deans, A. and West, S. (2011) 'DNA interstrand crosslink repair and cancer', *Nature Reviews Cancer*, vol. 11, pp. 467-480.

Demaria, M., Ohtani, N., Youssef, S., Rodier, F., Toussaint, W., Mitchell, J., Laberge R-M, J., Van Steeg, H., Dollé, M., Hoeijmakers, J., Bruin, A., Hara, E. and Campisi, J. (2014) 'An Essential Role for Senescent Cells in Optimal Wound Healing through Secretion of PDGF-AA', *Developmental Cell*, vol. 31, pp. 1-12.

Demidenko, Z. and Blagosklonny, M. (2008) 'Growth stimulation leads to cellular senescence when the cell cycle is blocked', *Cell Cycle*, vol. 7, pp. 3355-3361.

Denchi, E. and Lange, T. (2007) 'Protection of telomeres through independent control of ATM and ATR by TRF2 and POT1', *Nature*, vol. 448, pp. 1068-1071.

Deng, C., Zhang, P., Harper, J., Elledge, S. and Leder, P. (1995) 'Mice Lacking p21 CIP1/WAF1 Undergo Normal Development, but Are Defective in G1 Checkpoint Control ', *Cell*, vol. 82, pp. 675-684.

Derenzini, M., Trerè, D., Pession, A., Govoni, M., Sirri, V. and Chieco, P. (2000) 'Nucleolar size indicates the rapidity of cell proliferation in cancer tissues', *Journal of Pathology*, vol. 191, pp. 181-186.

Di Micco, R., Fumagalli, M., Cicalese, A., Piccinin, S., Gasparini, P., Luise, C., Schurra, C., Garré, M., Nuciforo, P., Bensimon, A., Maestro, R., Pelicci, P. and Fagagna, F. (2006) 'Oncogene-induced senescence is a DNA damage response triggered by DNA hyper-replication', *Nature*, vol. 444, pp. 638-642.

Di Pietro, C., Rapisarda, A., Amico, V., Bonaiuto, C., Viola, A., Scalia, M., Motta, S., Amato, A., Engel, H., Messina, A., Sichel, G., Grzeschik, K.H. and Purrello, M. (2000) 'Genomic localization of the human genes TAF1A, TAF1B and TAF1C, encoding TAFI48, TAFI63 and TAFI110 subunits of class I general transcription initiation factor SL1', *Cytogenetics and Cell Genetics*, vol. 89, pp. 133-136.

Dimri, G., Lee, X., Basile, G., Acosta, M., Scott, G., Roskelley, C., Medrano, E., Linskens, M., Rubelj, I., Pereira-Smith, O., Peacocke, M. and Campisi, J. (1995) 'A biomarker that identifies senescent human cells in culture and in aging skin in vivo', *Proceedings of the National Academy of Sciences*, vol. 92, pp. 9363-9367.

Dobbelstein, M. and Sørensen, C. (2015) 'Exploiting replicative stress to treat cancer', *Nature Reviews Drug Discovery*, vol. 14, pp. 405-423.

Drolet, M., Phoenix, P., Menzel, R., Massé, E., Liu, L. and Crouch, R. (1995) 'Overexpression of RNase H partially complements the growth defect of an Escherichia coli delta topA mutant: R-loop formation is a major problem in the absence of DNA topoisomerase I', *Proceedings of the National Academy of Sciences*, vol. 92, pp. 3526-3530.

Drygin, D., Lin, A., Bliesath, J., Ho, C., O'Brien, S., Proffitt, C., Omori, M., Haddach, M., Schwaebe, M., Siddiqui-Jain, A., Streiner, N., Quin, J., Sanij, E., Bywater, M., Hannan, R., Ryckman, D., Anderes, K. and Rice, W. (2011) 'Targeting RNA Polymerase I with an Oral Small Molecule CX-5461 Inhibits Ribosomal RNA Synthesis and Solid Tumor Growth', *Cancer Research*, vol. 71, pp. 1418-1430.

Dulić, V., Stein, G., Far, D. and Reed, S. (1998) 'Nuclear Accumulation of p21Cip1 at the Onset of Mitosis: a Role at the G2/M-Phase Transition', *Molecular and Cellular Biology*, vol. 18, pp. 546-557.

Dundr, M., Hoffmann-Rohrer, U., Hu, Q., Grummt, I., Rothblum, L., Phair, R. and Misteli, T. (2002) 'A Kinetic Framework for a Mammalian RNA Polymerase in Vivo', *Science*, vol. 298, pp. 1623-1626.

Dutertre, S., Cazales, M., Quaranta, M., Froment, C., Trabut, V., Dozier, C., Mirey, G., Bouché, J.P., Theis-Febvre, N., Schmitt, E., Monsarrat, B., Prigent, C. and Ducommun, B. (2004) 'Phosphorylation of CDC25B by Aurora-A at the centrosome contributes to the G2–M transition', *Journal of Cell Science*, vol. 117, pp. 2523-2531.

Eastman, A. (1987) 'The formation, isolation and characterization of DNA adducts produced by anticancer platinum complexes', *Pharmacology & Therapeutics*, vol. 34, pp. 155-166.

Eggert, T., Wolter, K., Ji, J., Ma, C., Yevsa, T., Klotz, S., Medina-Echeverz, J., Longerich, T., Forgues, M., Reisinger, F., Heikenwalder, M., Wang, X.W., Zender, L. and Greten, T. (2016) 'Distinct Functions of Senescence-Associated Immune Responses in Liver Tumor Surveillance and Tumor Progression', *Cancer Cell*, vol. 30, pp. 533-547.

El Hage, A., French, S., Beyer, A. and Tollervey, D. (2010) 'Loss of Topoisomerase I leads to R-loop-mediated transcriptional blocks during ribosomal RNA synthesis', *Genes & Development*, vol. 24, pp. 1546-1558.

El-Deiry, W., Tokino, T., Velculescu, V., Levy, D., Parsons, R., Trent, J., Lin, D., Mercer, W., Kinzler, K. and Vogelstein, B. (1993) 'WAF1, a Potential Mediator of p53 Tumor Suppression', *Cell*, vol. 75, pp. 817-825.

Engel, C., Sainsbury, S., Cheung, A., Kostrewa, D. and Cramer, P. (2013) 'RNA polymerase I structure and transcription regulation', *Nature*, vol. 502, pp. 650-655.

Escribano-Díaz, C., Orthwein, A., Fradet-Turcotte, A., Xing, M., Young, J., Tkác, J., Cook, M., Rosebrock, A., Munro, M., Canny, M., Xu, D. and Durocher, D. (2013) 'A Cell Cycle-Dependent Regulatory Circuit Composed of 53BP1-RIF1 and BRCA1-CtIP Controls DNA Repair Pathway Choice', *Molecular Cell*, vol. 49, pp. 872-883.

Ewald, J., Desotelle, A., Wilding, G. and Jarrard, D. (2010) 'Therapy-Induced Senescence in Cancer', *Journal of the National Cancer Institute*, vol. 102, pp. 1536-1546.

Fagagna, F. (2008) 'Living on a break: cellular senescence as a DNA-damage response', *Nature*, vol. 8, pp. 512-522.

Fagagna, F., Reaper, P., Clay-Farrace, L., Fiegler, H., Carr, P., Zglinicki, T., Saretzki, G., Carter, N. and Jackson, S. (2003) 'A DNA damage checkpoint response in telomere-initiated senescence', *Nature*, vol. 426, pp. 194-198.

Fang, L., Igarashi, M., Leung, J., Sugrue, M., Lee, S. and Aaronson, S. (1999) 'p21Waf1/Cip1/Sdi1 induces permanent growth arrest with markers of replicative senescence in human tumor cells lacking functional p53', *Oncogene*, vol. 18, pp. 2789-2797.

Farmer, H., McCabe, N., Lord, C., Tutt, A., Johnson, D., Richardson, T., Santarosa, M., Dillon, K., Hickson, I., Knights, C., Martin, N., Jackson, S., Smith, G. and Ashworth, A. (2005) 'Targeting the DNA repair defect in BRCA mutant cells as a therapeutic strategy', *Nature*, vol. 434, pp. 917-921.

Feraudy, S., Revet, I., Bezrookove, V., Feeney, L. and Cleaver, J. (2010) 'A minority of foci or pan-nuclear apoptotic staining of gamma-H2AX in the S phase after UV damage contain DNA double-strand breaks', *Proceedings of the National Academy of Sciences*, vol. 107, pp. 6870-6875.

Fernández-Tornero, C., Moreno-Morcillo, M., Rashid, U., Taylor, N., Ruiz, F., Gruene, T., Legrand, P., Steuerwald, U. and Müller, C. (2013) 'Crystal structure of the 14-subunit RNA polymerase I', *Nature*, vol. 502, pp. 644-649.

Fetherston, J., Werner, E. and Patterson, R. (1984) 'Processing of the external transcribed spacer of murine rRNA and site of action of actinomycin D', *Nucleic Acids Research*, vol. 12, pp. 7187-7198.

Finlay, C., Hinds, P. and Levine, A. (1989) 'The p53 Proto-Oncogene Can Act as a Suppressor of Transformation ', *Cell*, vol. 57, pp. 1083-1093.

Fishel, R., Lescoe, M., Rao, M., Copeland, N., Jenkins, N., Garber, J., Kane, M. and Kolodner, R. (1993) 'The Human Mutator Gene Homolog MSH2 and Its Association with Hereditary Nonpolyposis Colon Cancer ', *Cell*, vol. 75, pp. 1027-1038.

Freund, A., Laberge, R.M., Demaria, M. and Campisi, J. (2012) 'Lamin B1 loss is a senescence-associated biomarker', *Molecular Biology of the Cell*, vol. 23, pp. 2066-2075.

Fukami, J., Anno, K., Ueda, K., Takahashi, T. and Ide, T. (1995) 'Enhanced expression of cyclin D1 in senescent human fibroblasts', *Mechanisms of Ageing and Development*, vol. 81, pp. 139-157.

Fulda, S., Gorman, A., Hori, O. and Samali, A. (2009) 'Cellular Stress Responses: Cell Survival and Cell Death', *International Journal of Cell Biology*, vol. 2010, pp. 1-23.

Gan, W., Guan, Z., Liu, J., Gui, T., Shen, K., Manley, J. and Li, X. (2011) 'R-loop-mediated genomic instability is caused by impairment of replication fork progression', *Genes & Development*, vol. 25, pp. 2041-2056.

Garcia-Higuera, I., Taniguchi, T., Ganesan, S., Meyn, M., Timmers, C., Hejna, J., Grompe, M. and D'Andrea, A. (2001) 'Interaction of the Fanconi Anemia Proteins and BRCA1 in a Common Pathway', *Molecular Cell*, vol. 7, pp. 249-262.

García-Muse, T. and Aguilera, A. (2016) 'Transcription-replication conflicts: how they occur and how they are resolved', *Nature Reviews Molecular Cell Biology*, vol. 17, pp. 553-563.

García-Rubio, M., Pérez-Calero, C., Barroso, S., Tumini, E., Herrera-Moyano, E., Rosado, I. and Aguilera, A. (2015) 'The Fanconi Anemia Pathway Protects Genome Integrity from R-loops', *PLoS Genetics*, vol. 11:e1005674, pp. 1-17.

Gates, K. (2009) 'An Overview of Chemical Processes That Damage Cellular DNA: Spontaneous Hydrolysis, Alkylation, and Reactions with Radicals', *Chemical Research in Toxicology*, vol. 22, pp. 1747-1760.

Georgakopoulou, E., Tsimaratou, K., Evangelou, K., Fernandez Marcos, P., Zoumpourlis, V., Trougakos, I., Kletsas, D., Bartek, J., Serrano, M. and Gorgoulis, V. (2013) 'Specific lipofuscin staining as a novel biomarker to detect replicative and stress-induced senescence. A method applicable in cryo-preserved and archival tissues', *Aging*, vol. 5, pp. 37-50.

Gerdes, J., Schwab, U., Lemke, H. and Stein, H. (1983) 'Production of a mouse monoclonal antibody reactive with a human nuclear antigen associated with cell proliferation', *International Journal of Cancer*, vol. 31, pp. 13-20.

Ginno, P., Lott, P., Christensen, H., Korf, I. and Chédin, F. (2012) 'R-Loop Formation Is a Distinctive Characteristic of Unmethylated Human CpG Island Promoters', *Molecular Cell*, vol. 45, pp. 814-825.

Glotzer, M., Murray, A. and Kirschner, M. (1991) 'Cyclin is degraded by the ubiquitin pathway', *Nature*, vol. 349, pp. 132-138.

Glover, D., Leibowitz, M., McLean, D. and Parry, H. (1995) 'Mutations in aurora Prevent Centrosome Separation Leading to the Formation of Monopolar Spindles', *Cell*, vol. 81, pp. 95-105.

Goodarzi, A. and Jeggo, P. (2011) 'KAP-1 phosphorylation regulates CHD3 nucleosome remodeling during the DNA double-strand break response', *Nature Structural & Molecular Biology*, vol. 18, pp. 831-839.

Goodarzi, A., Yu, Y., Riballo, E., Douglas, P., Walker, S., Ye, R., Härer, C., Marchetti, C., Morrice, N., Jeggo, P. and Lees-Miller, S. (2006) 'DNA-PK autophosphorylation facilitates Artemis endonuclease activity', *The EMBO Journal*, vol. 25, pp. 3880-3889.

Gordon, D., Resio, B. and Pellman, D. (2012) 'Causes and consequences of aneuploidy in cancer', *Nature Reviews Genetics*, vol. 13, pp. 189-203.

Goto, H., Yasui, Y., Nigg, E. and Inagaki, M. (2002) 'Aurora-B phosphorylates Histone H3 at serine28 with regard to the mitotic chromosome condensation', *Genes to Cells*, vol. 7, pp. 11-17.

Goto, H., Yasui, Y., Nigg, E. and Inagaki, M. (2002) 'Aurora-B phosphorylates Histone H3 at serine28 with regard to the mitotic chromosome condensation', *Genes to Cells*, vol. 7, pp. 11-17.

Gottlieb, T. and Jackson, S. (1993) 'The DNA-dependent protein kinase: Requirement for DNA ends and association with Ku antigen', *Cell* , vol. 72, pp. 131-142.

Grawunder, U., Wilm, M., Wu, X., Kulesza, P., Wilson, T., Mann, M. and Lieber, M. (1997) 'Activity of DNA ligase IV stimulated by complex formation with XRCC4 protein in mammalian cells', *Nature*, vol. 388, pp. 492-495.

Griffith, J., Comeau, L., Rosenfield, S., Stansel, R., Biachi, A., Moss, H. and Lange, T. (1999) 'Mammalian telomeres end in a large duplex loop', *Cell*, vol. 97, pp. 503-514.

Guerrero, A., Herranz, N., Sun, B., Wagner, V., Gallage, S., Guiho, R., Wolter, K., Pombo, J., Irvine, E., Innes, A., Birch, J., Glegola, J., Manshaei, S., Heide, D., Dharmalingam, G., Harbig, J., Olona, A., Behmoaras, J., Dauch, D., Uren, A., Zender, L., Vernia, S., Martínez-Barbera, J., Heikenwalder, M., Withers, D. and Gil, J. (2019) 'Cardiac glycosides are broad-spectrum senolytics', *Nature Metabolism*, vol. 1, pp. 1074-1088.

Haddach, M., Schwaebe, M., Michaux, J., Nagasawa, J., O'Brien, S., Whitten, J., Pierre, F., Kerdoncuff, P., Darjania, L., Stansfield, R., Drygin, D., Anderes, K., Proffitt, C., Bliesath, J., Siddiqui-Jain, A., Omori, M., Huser, N., Rice, W. and Ryckman, D. (2012) 'Discovery of CX-5461, the First Direct and Selective Inhibitor of RNA Polymerase I, for Cancer Therapeutics', *ACS Medicinal Chemistry Letters*, vol. 3, pp. 602-606.

Haferkamp, S., Scurr, L., Becker, T., Frausto, M., Kefford, R. and Rizos, H. (2009) 'Oncogene-Induced Senescence Does Not Require the p16INK4a or p14ARF Melanoma Tumor Suppressors', *Journal of Investigative Dermatology*, vol. 129, pp. 1983-1991.

Hafner, A., Bulyk, M., Jambhekar, A. and Lahav, G. (2019) 'The multiple mechanisms that regulate p53 activity and cell fate', *Nature Reviews Molecular Cell Biology*, vol. 20, pp. 199-210.

Hanahan, D. and Weinberg, R. (2011) 'Hallmarks of Cancer: The Next Generation', *Cell*, vol. 144, pp. 646-674.

Harley, C., Futcher, A. and Greider, C. (1990) 'Telomeres shorten during ageing of human fibroblasts.', *Nature*, vol. 345, pp. 458-460.

Harper, J., Adami, G., Wei, N., Keyomarsi, K. and Elledge, S. (1993) 'The p21 Cdk-Interacting Protein Cipl Is a Potent Inhibitor of G1 Cyclin-Dependent Kinases', *Cell*, vol. 75, pp. 805-816.

Harper, J., Elledge, S., Keyomarsi, K., Dynlacht, B., Tsai, L.H., Zhang, P., Dobrowolski, S., Bai, C., Connell-Crowley, L., Swindell, E., Fox, M. and Wei, N. (1995) 'Inhibition of cyclin-dependent kinases by p21', *Molecular Biology of the Cell*, vol. 6, pp. 387-400.

Hartwell, L. and Weinert, T. (1989) 'Checkpoints: controls that ensure the order of cell cycle events', *Science*, vol. 246, pp. 629-634.

Hatchi, E., Skourti-Stathaki, K., Ventz, S., Pinello, L., Yen, A., Kamieniarz-Gdula, K., Dimitrov, S., Pathania, S., McKinney, K., Eaton, M., Kellis, M., Hill, S., Parmigiani, G., Proudfoot, N. and Livingston, D. (2015) 'BRCA1 Recruitment to Transcriptional Pause Sites Is Required for R-Loop-Driven DNA Damage Repair', *Molecular Cell*, vol. 57, pp. 636-647.

Hauf, S., Cole, R., LaTerra, S., Zimmer, C., Schnapp, G., Walter, R., Heckel, A., Meel, J., Rieder, C. and Peters, J.M. (2003) 'The small molecule Hesperadin reveals a role for Aurora B in correcting kinetochore-microtubule attachment and in maintaining the spindle assembly checkpoint', *The Journal of Cell Biology*, vol. 161, pp. 281-294.

Haupt, Y., Maya, R., Kazaz, A. and Oren, M. (1997) 'Mdm2 promotes the rapid degradation of p53', *Nature*, vol. 387, pp. 296-299.

Hayflick, L. and Moorhead, P. (1961) 'The serial cultivation of human diploid cell strains', *Experimental Cell Research*, vol. 25, pp. 585-621.

Herbig, U., Jobling, W., Chen, B., Chen, D. and Sedivy, J. (2004) 'Telomere Shortening Triggers Senescence of Human Cells through a Pathway Involving ATM, p53, and p21CIP1, but Not p16INK4a', *Molecular Cell*, vol. 14, pp. 501-513.

Herbig, U., Wei, W., Dutriaux, A., Jobling, W. and Sedivy, J. (2008) 'Real-time imaging of transcriptional activation in live cells reveals rapid up-regulation of the cyclin-dependent kinase inhibitor gene CDKN1A in replicative cellular senescence', *Aging Cell*, vol. 2, pp. 295-304.

Hernandez-Segura, A., Nehme, J. and Demaria, M. (2018) 'Hallmarks of cellular senescence', *Trends in Cell Biology*, vol. 28, pp. 436-453.

Hirota, T., Kunitoku, N., Sasayama, T., Marumoto, T., Zhang, D., Nitta, M., Hatakeyama, K. and Saya, H. (2003) 'Aurora-A and an Interacting Activator, the LIM Protein Ajuba, Are Required for Mitotic Commitment in Human Cells', *Cell*, vol. 114.

Hochegger, H., Takeda, S. and Hunt, T. (2008) 'Cyclin-dependent kinases and cell-cycle transitions: does one fit all?', *Nature Reviews Molecular Cell Biology*, vol. 9, pp. 910-916.

Hoffmann, I., Draetta, G. and Karsenti, E. (1994) 'Activation of the phosphatase activity of human cdc25A by a cdk2-cyclin E dependent phosphorylation at the G1/S transition', *The EMBO Journal*, vol. 13, pp. 4302-4310.

Howe, B., Umrigar, A. and Tsien, F. (2014) 'Chromosome Preparation From Cultured Cells', *Journal of Visualized Experiments*, vol. 83, e50203, pp. 1-5.

Hsu, J.Y., Sun, Z.W., Li, X., Reuben, M., Tatchell, K., Bishop, D., Grushcow, J., Brame, C., Caldwell, J., Hunt, D., Lin, R., Smith, M. and Allis, C. (2000) 'Mitotic Phosphorylation of Histone H3 Is Governed by Ipl1/aurora Kinase and Glc7/PP1 Phosphatase in Budding Yeast and Nematodes', *Cell*, vol. 102, pp. 279-291.

Jackson, S. and Bartek, J. (2009) 'The DNA-damage response in human biology and disease', *Nature*, vol. 461, pp. 1071-1078.

Jackson, J., Pant, V., Li, Q., Chang, L., Quintás-Cardama, A., Garza, D., Tavana, O., Yang, P., Manshouri, T., Li, Y., El-Naggar, A. and Lozano, G. (2012) 'p53-Mediated Senescence Impairs the Apoptotic Response to Chemotherapy and Clinical Outcome in Breast Cancer', *Cancer Cell*, vol. 21, pp. 793-806.

Jazayeri, A., Balestrini, A., Garner, E., Haber, J. and Costanzo, V. (2008) 'Mre11–Rad50–Nbs1-dependent processing of DNA breaks generates oligonucleotides that stimulate ATM activity', *The EMBO Journal*, vol. 27, pp. 1953-1962.

Jensen, R., Carreira, A. and Kowalczykowski, S. (2010) 'Purified human BRCA2 stimulates RAD51-mediated recombination', *Nature*, vol. 467, pp. 678-683.

Jeyapalan, J., Ferreira, M., Sedivy, J. and Herbig, U. (2007) 'Accumulation of senescent cells in mitotic tissue of aging primates', *Mechanisms of Ageing and Development* , vol. 128, pp. 36-44.

Jiricny, J. (2006) 'The multifaceted mismatch-repair system', *Nature Reviews Molecular Cell Biology*, vol. 7, pp. 335-346.

Jun, J. and Lau, L. (2010) 'The matricellular protein CCN1 induces fibroblast senescence and restricts fibrosis in cutaneous wound healing', *Nature Cell Biology*, vol. 12, pp. 676-685.

Kang, T.W., Yevsa, T., Woller, N., Hoenicke, L., Wuestefeld, T., Dauch, D., Hohmeyer, A., Gereke, M., Rudalska, R., Potapova, A., Iken, M., Vucur, M., Weiss, S., Heikenwalder, M., Khan, S., Gil, J., Bruder, D., Manns, M., Schirmacher, P., Tacke, F., Ott, M., Luedde, T., Longerich, T., Kubicka, S. and Zender, L. (2011) 'Senescence surveillance of pre-malignant hepatocytes limits liver cancer development', *Nature*, vol. 479, pp. 547-551.

Karlseder, J., Hoke, K., Mirzoeva, O., Bakkenist, C., Kastan, M., Petrini, J. and Lange, T. (2004) 'The Telomeric Protein TRF2 Binds the ATM Kinase and Can Inhibit the ATM-Dependent DNA Damage Response', *PLoS biology*, vol. 2, pp. 1150-1156.

Killander, D. and Zetterberg, A. (1965) 'A quantitative cytochemical investigation of the relationship between cell mass and initiation of DNA synthesis in mouse fibroblasts in vitro.', *Experimental Cell Research*, vol. 40, pp. 12-20.

Knezevic, C., Wright, G., Rix, L., Kim, W., Kuenzi, B., Luo, Y., Watters, J., Koomen, J., Haura, E., Monteiro, A., Radu, C., Lawrence, H. and Rix, U. (2016) 'Proteome-wide Profiling of Clinical PARP Inhibitors Reveals Compound-Specific Secondary Targets', *Cell Chemical Biology*, vol. 23, pp. 1-14.

Kobayashi, J., Tauchi, H., Sakamoto, S., Nakamura, A., Morishima, K., Matsuura, S., Kobayashi, T., Tamai, K., Tanimoto, K. and Komatsu, K. (2002) 'NBS1 localizes to gamma-H2AX foci through interaction with the FHA/BRCT domain', *Current Biology*, vol. 12, pp. 1846-1851.

Krishnamurthy, J., Torrice, C., Ramsey, M., Kovalev, G., Al-Regaiey, K., Su, L. and Sharpless, N. (2004) 'Ink4a/Arf expression is a biomarker of aging', *The Journal of Clinical Investigation*, vol. 114, pp. 1299-1307.

Krizhanovsky, V., Yon, M., Dickins, R., Hearn, S., Simon, J., Miething, C., Yee, H., Zender, L. and Lowe, S. (2008) 'Senescence of Activated Stellate Cells Limits Liver Fibrosis', *Cell*, vol. 134, pp. 657-667.

Krokan, H. and Bjørås, M. (2013) 'Base Excision Repair', *Cold Spring Harbor Perspectives in Biology*, vol. 5, pp. 1-22.

Krtolica, A., Parrinello, S., Lockett, S., Desprez, P.Y. and Campisi, J. (2001) 'Senescent fibroblasts promote epithelial cell growth and tumorigenesis: a link between cancer and aging', *Proceedings of the National Academy of Sciences*, vol. 98, pp. 12072-12077.

Kubbutat, M., Jones, S. and Vousden, K. (1997) 'Regulation of p53 stability by Mdm2', *Nature*, vol. 387, pp. 299-303.

Kuilman, T. and Peeper, D. (2009) 'Senescence-messaging secretome: SMS-ing cellular stress', *Nature Reviews*, vol. 9, pp. 81-94.

Lagger, G., O'Carroll, D., Rembold, M., Khier, H., Tischler, J., Weitzer, G., Schuettengruber, B., Hauser, C., Brunmeir, R., Jenuwein, T. and Seiser, C. (2002) 'Essential function of histone deacetylase 1 in proliferation control and CDK inhibitor repression', *The EMBO Journal*, vol. 21, pp. 2672-2681.

Lavin, M. (2007) 'ATM and the Mre11 complex combine to recognize and signal DNA double-strand breaks', *Oncogene*, vol. 26, pp. 7749-7758.

Learned, R., Cordes, S. and Tjian, R. (1985) 'Purification and Characterization of a Transcription Factor That Confers Promoter Specificity to Human RNA Polymerase I', *Molecular and Cellular Biology*, vol. 5, pp. 1358-1369.

Lee, J.H., Cheong, H.M., Kang, M.Y., Kim, S.Y. and Kang, Y. (2009) 'Ser1778 of 53BP1 Plays a Role in DNA Double-strand Break Repairs', *The Korean Journal of Physiology and Pharmacology*, vol. 13, pp. 343-348.

Lee, B., Han, J., Im, J., Morrone, A., Johung, K., Goodwin, E., Kleijer, W., DiMaio, D. and Hwang, E. (2006) 'Senescence-associated beta-galactosidase is lysosomal beta-galactosidase', *Aging Cell*, vol. 5, pp. 187-195.

Lee, J.H. and Paull, T. (2004) 'Direct activation of the ATM protein kinase by the Mre11/Rad50/Nbs1 complex', *Science*, vol. 304, pp. 93-96.

Lee, J.H. and Paull, T. (2005) 'ATM Activation by DNA Double-Strand Breaks Through the Mre11-Rad50-Nbs1 Complex', *Science*, vol. 308, pp. 551-554.

Lewis, C. and Golsteyn, R. (2016) 'Cancer cells that survive checkpoint adaptation contain micronuclei that harbor damaged DNA', *Cell Cycle*, vol. 15, pp. 3131-3145.

Liang, C.C., Li, Z., Lopez-Martinez, D., Nicholson, W., Vénien-Bryan, C. and Cohn, M. (2016) 'The FANCD2–FANCI complex is recruited to DNA interstrand crosslinks before monoubiquitination of FANCD2', *Nature Communications*, vol. 7, pp. 1-11.

Li, L., Li, Y., Zhao, J., Fan, S., Wang, L. and Li, X. (2016) 'CX-5461 induces autophagy and inhibits tumor growth via mammalian target of rapamycin-related signaling pathways in osteosarcoma', *Onco Targets and Therapy*, vol. 9, pp. 5985-5997.

Lindahl, T. and Barnes, D. (2000) 'Repair of Endogenous DNA Damage', *Cold Spring Harbor Symposia on Quantitative Biology*, vol. 65, pp. 127-1333.

Lindström, M., Jurada, D., Bursac, S., Orsolic, I., Bartek, J. and Volarevic, S. (2018) 'Nucleolus as an emerging hub in maintenance of genome stability and cancer pathogenesis', *Oncogene*, vol. 37, pp. 2351-2366.

Liu, T., Ghosal, G., Yuan, J., Chen, J. and Huang, J. (2010) 'FAN1 Acts with FANCI-FANCD2 to Promote DNA Interstrand Cross-Link Repair', *Science*, vol. 329, pp. 693-696.

Liu, Q., Guntuku, S., Cui, X.S., Matsuoka, S., Cortez, D., Tamai, K., Luo, G., Carattini-Rivera, S., DeMayo, F., Bradley, A., Donehower, L. and Elledge, S. (2000) 'Chk1 is an essential kinase that is regulated by Atr and required for the G2/M DNA damage checkpoint', *Genes & Development*, vol. 14, pp. 1448-1459.

Liu, S., Shiotani, B., Lahiri, M., Maréchal, A., Tse, A., Leung, C., Glover, J., Yang, X. and Zou, L. (2011) 'ATR Autophosphorylation as a Molecular Switch for Checkpoint Activation', *Molecular Cell*, vol. 43, pp. 192-202.

Lohrum, M., Ludwig, R., Kubbutat, M., Hanlon, M. and Vousden, K. (2003) 'Regulation of HDM2 activity by the ribosomal protein L11', *Cancer Cell*, vol. 3, pp. 577-587.

Longhese, M., Neecke, H., Paciotti, V., Lucchini, G. and Plevani, P. (1996) 'The 70 kDa subunit of replication protein A is required for the G1/S and intra-S DNA damage checkpoints in budding yeast', *Nucleic Acids Research*, vol. 24, pp. 3533-3537.

Luijsterburg, M. and Attikum, H. (2011) 'Chromatin and the DNA damage response: The cancer connection', *Molecular Oncology*, vol. 5, pp. 349-367.

MacPhail, S., Banáth, J., Yu, Y., Chu, E. and Olive, P. (2003) 'Cell Cycle-Dependent Expression of Phosphorylated Histone H2AX: Reduced Expression in Unirradiated but not X-Irradiated G1-Phase Cells', *Radiation Research*, vol. 159, pp. 759-767.

Maggi, L. and Weber, J. (2005) 'Nucleolar Adaptation in Human Cancer', *Cancer Investigation*, vol. 23, pp. 599-608.

Mahajan, K., McElhinny, S., Mitchell, B. and Ramsden, D. (2002) 'Association of DNA Polymerase mu with Ku and Ligase IV: Role for pol mu in End-Joining Double-Strand Break Repair', *Molecular and Cellular Biology*, vol. 22, pp. 5194-5202.

Malumbres, M. and Barbacid, M. (2001) 'To cycle or not to cycle: a critical decision in cancer', *Nature Reviews Cancer*, vol. 1, pp. 222-231.

Malumbres, M. and Barbacid, M. (2009) 'Cell cycle, CDKs and cancer: a changing paradigm', *Nature Reviews Cancer*, vol. 9, pp. 153-166.

Mao, Z., Ke, Z., Gorbunova, V. and Seluanov, A. (2013) 'Replicatively senescent cells are arrested in G1 and G2 phases', *Aging*, vol. 4, pp. 431-435.

Marcotte, R., Lacelle, C. and Wang, E. (2004) 'Senescent fibroblasts resist apoptosis by downregulating caspase-3', *Mechanisms of Ageing and Development*, vol. 125, pp. 777-783.

Maréchal, A. and Zou, L. (2013) 'DNA Damage Sensing by the ATM and ATR Kinases', *Cold Spring Harbor Perspectives in Biology*, vol. 5, pp. 1-17.

Marteijn, J., Lans, H., Vermeulen, W. and Hoeijmakers, J. (2014) 'Understanding nucleotide excision repair and its roles in cancer and ageing', *Nature Reviews Molecular Cell Biology*, vol. 15, pp. 465-481.

Marumoto, T., Hirota, T., Morisaki, T., Kunitoku, N., Zhang, D., Ichikawa, Y., Sasayama, T., Kuninaka, S., Mimori, T., Tamaki, N., Kimura, M., Okano, Y. and Saya, H. (2002) 'Roles of aurora-A kinase in mitotic entry and G2 checkpoint in mammalian cells', *Genes to Cells*, vol. 7, pp. 1173-1182.

Massagué, J. (2004) 'G1 cell-cycle control and cancer', *Nature*, vol. 432, pp. 298-306.

Matsuoka, S., Huang, M. and Elledge, S. (1998) 'Linkage of ATM to Cell Cycle Regulation by the Chk2 Protein Kinase', *Science*, vol. 282, pp. 1893-1897.

McConnell, B., Gregory, F., Stott, F., Hara, E. and Peters, G. (1981) 'Induced Expression of p16INK4a Inhibits Both CDK4- and CDK2-Associated Kinase Activity by Reassortment of Cyclin-CDK-Inhibitor Complexes', *Molecular and Cellular Biology*, vol. 19, pp. 1981-1989.

McHugh, D. and Gil, J. (2018) 'Senescence and aging: Causes, consequences, and therapeutic avenues', *Journal of Cell Biology*, vol. 217, pp. 65-77.

McIlwraith, M., Vaisman, A., Liu, Y., Fanning, E., Woodgate, R. and West, S. (2005) 'Human DNA Polymerase eta Promotes DNA Synthesis from Strand Invasion Intermediates of Homologous Recombination', *Molecular Cell*, vol. 20, pp. 783-792.

Meetei, A., Winter, J., Medhurst, A., Wallisch, M., Waisfisz, Q., Vrugt, H., Oostra, A., Yan, Z., Ling, C., Bishop, C., Hoatlin, M., Joenje, H. and Wang, W. (2003) 'A novel ubiquitin ligase is deficient in Fanconi anemia', *Nature Genetics*, vol. 35, pp. 165-170.

Meetei, A., Yan, Z. and Wang, W. (2004) 'FANCL replaces BRCA1 as the likely ubiquitin ligase responsible for FANCD2 monoubiquitination.', *Cell Cycle*, vol. 3, pp. 179-181.

Miller, I., Min, M., Yang, C., Tian, C., Gookin, S., Carter, D. and Spencer, S. (2018) 'Ki67 is a Graded Rather than a Binary Marker of Proliferation versus Quiescence', *Cell Reports*, vol. 24, pp. 1105-1112.

Mimitou, E. and Symington, L. (2010) 'Ku prevents Exo1 and Sgs1-dependent resection of DNA ends in the absence of a functional MRX complex or Sae2', *The EMBO Journal*, vol. 29, pp. 3358-3369.

Mimori, T. and Hardin, J. (1986) 'Mechanism of Interaction between Ku Protein and DNA', *The Journal of Biological Chemistry*, vol. 261, pp. 10375-10379.

Moreira, M.C., Barbot, C., Tachi, N., Kozuka, N., Uchida, E., Gibson, T., Mendonça, P., Costa, M., Barros, J., Yanagisawa, T., Watanabe, M., Ikeda, Y., Aoki, M., Nagata, T., Coutinho, P., Sequeiros, J. and Koenig, M. (2001) 'The gene mutated in ataxia-ocular apraxia 1 encodes the new HIT/Zn-finger protein aprataxin', *Nature Genetics*, vol. 29, pp. 189-193.

Moss, T. and Stefanovsky, V. (2002) 'At the Center of Eukaryotic Life', *Cell*, vol. 109, pp. 545-548.

Moynahan, M., Chiu, J., Koller, B. and Jasin, M. (1999) 'Brca1 Controls Homology-Directed DNA Repair', *Molecular Cell*, vol. 4, pp. 511-518.

Muñoz-Espín, D., Cañamero, M., Maraver, A., Gómez-López, G., Contreras, J., Murillo-Cuesta, S., Rodríguez-Baeza, A., Varela-Nieto, I., Ruberte, J., Collado, M. and Serrano, M. (2013) 'Programmed cell senescence during mammalian embryonic development.', *Cell*, vol. 155, pp. 1104-1118.

Nadel, J., Athanasiadou, R., Lemetre, C., Wijetunga, N., Broin, P., Sato, H., Zhang, Z., Jeddeloh, J., Montagna, C., Golden, A., Seoighe, C. and Greally, J. (2015) 'RNA:DNA hybrids in the human genome have distinctive nucleotide characteristics, chromatin composition, and transcriptional relationships', *Epigenetics & Chromatin*, vol. 8:e46, pp. 1-19.

Nakamura, K., Sakai, W., Kawamoto, T., Bree, R., Lowndes, N., Takeda, S. and Taniguchi, Y. (2006) 'Genetic dissection of vertebrate 53BP1: A major role in non-homologous end joining of DNA double strand breaks', *DNA Repair*, vol. 5, pp. 741-749.

Nam, E., Zhao, R., Glick, G., Bansbach, C., Friedman, D. and Cortez, D. (2011) 'Thr-1989 Phosphorylation Is a Marker of Active Ataxia Telangiectasia-mutated and Rad3-related (ATR) Kinase', *Journal of Biological Chemistry*, vol. 286, pp. 28707-28714.

Narita, M., Narita, M., Krizhanovsky, V., Nuñez, S., Chicas, A., Hearn, S., Myers, M. and Lowe, S. (2006) 'A Novel Role for High-Mobility Group A Proteins in Cellular Senescence and Heterochromatin Formation', *Cell*, vol. 126, pp. 503-514.

Narita, M., Nuñez, S., Narita, M., Lin, A., Hearn, S., Hannon, G., Spector, D. and Lowe, S. (2003) 'Rb-Mediated Heterochromatin Formation and Silencing of E2F Target Genes during Cellular Senescence', *Cell*, vol. 113, pp. 703–716.

Nassif, N., Penney, J., Pal, S., Engels, W. and Gloor, G. (1994) 'Efficient Copying of Nonhomologous Sequences from Ectopic Sites via P-Element-Induced Gap Repair', *Molecular and Cellular Biology*, vol. 14, pp. 1613-1625.

Negi, S. and Brown, P. (2015) 'rRNA synthesis inhibitor, CX-5461, activates ATM/ATR pathway in acute lymphoblastic leukemia, arrests cells in G2 phase and induces apoptosis', *Oncotarget*, vol. 6, pp. 18094-18104.

Nguyen, H., Yadav, T., Giri, S., Saez, B., Graubert, T. and Zou, L. (2017) 'Functions of Replication Protein A as a Sensor of R Loops and a Regulator of RNaseH1', *Molecular Cell*, vol. 65, pp. 832-847.

Niccoli, T. and Partridge, L. (2012) 'Ageing as a Risk Factor for Disease', *Current Biology*, vol. 22, pp. 741-752.

Niehrs, C. and Luke, B. (2020) 'Regulatory R-loops as facilitators of gene expression and genome stability', *Nature Reviews Molecular Cell Biology*, vol. 21, pp. 167-178.

Nieminuszczy, J., Schwab, R. and Niedzwiedz, W. (2016) 'The DNA fibre technique – tracking helicases at work'.

Nishio, K., Inoue, A., Qiao, S., Kondo, H. and Mimura, A. (2001) 'Senescence and cytoskeleton: overproduction of vimentin induces senescent-like morphology in human fibroblasts', *Histochemistry and Cell Biology*, vol. 116, pp. 321-327.

O'Connell, M., Raleigh, J., Verkade, H. and Nurse, P. (1997) 'Chk1 is a wee1 kinase in the G2 DNA damage checkpoint inhibiting cdc2 by Y15 phosphorylation', *16*, vol. 3, pp. 545-554.

O'Farrell, P. (2001) 'Triggering the all-or-nothing switch into mitosis', *Trends in Cell Biology*, vol. 11, pp. 512-519.

Orth, J., Loewer, A., Lahav, G. and Mitchison, T. (2011) 'Prolonged mitotic arrest triggers partial activation of apoptosis, resulting in DNA damage and p53 induction', *Molecular Biology of the Cell*, vol. 23, pp. 567-576.

Pagano, M., Pepperkok, R., Verde, F., Ansorge, W. and Draetta, G. (1992) 'Cyclin A is required at two points in the human cell cycle', *The EMBO Journal*, vol. 11, pp. 961-971.

Parker, L. and Piwnica-Worms, H. (1992) 'Inactivation of the p34cdc2-cyclin B complex by the human WEE1 tyrosine kinase', *Science*, vol. 257, pp. 1955-1957.

Passos, J., Saretzki, G., Ahmed, S., Nelson, G., Richter, T., Peters, H., Wappler, I., Birket, M., Harold, G., Schaeuble, K., Birch-Machin, M., Kirkwood, T. and Zglinicki, T. (2007) 'Mitochondrial Dysfunction Accounts for the Stochastic Heterogeneity in Telomere-Dependent Senescence', *PLoS biology*, vol. 5, pp. 1138-1151.

Paull, T., Rogakou, E., Yamazaki, V., Kirchgessner, C., Gellert, M. and Bonner, W. (2000) 'A critical role for histone H2AX in recruitment of repair factors to nuclear foci after DNA damage', *Cell*, vol. 10, pp. 886-895.

Pelengaris, S., Khan, M. and Evan, G. (2002) 'c-MYC: more than just a matter of life and death', *Nature*, vol. 2, pp. 764-776.

Peng, C.Y., Graves, P., Thoma, R., Wu, Z., Shaw, A. and Piwnica-Worms, H. (1997) 'Mitotic and G2 checkpoint control: regulation of 14-3-3 protein binding by phosphorylation of Cdc25C on serine-216', *Science*, vol. 277, pp. 1501-1505.

Pizzolato, J., Mukherjee, S., Schärer, O. and Jiricny, J. (2015) 'FANCD2-associated Nuclease 1, but Not Exonuclease 1 or Flap Endonuclease 1, Is Able to Unhook DNA Interstrand Cross-links in Vitro', *The Journal of Biological Chemistry*, vol. 290, pp. 22602-22611.

Poele, R., Okorokov, A., Jardine, L., Cummings, J. and Joel, S. (2002) 'DNA Damage Is Able to Induce Senescence in Tumor Cells in Vitro and in Vivo', *Cancer Research*, vol. 62, pp. 1876-1883.

Quin, J., Chan, K., Devlin, J., Cameron, D., Diesch, J., Cullinane, C., Ahern, J., Khot, A., Hein, N., George, A., Hannan, K., Poortinga, G., Sheppard, K., Khanna, K., Johnstone, R., Drygin, D., McArthur, G., Pearson, R., Sanij, E. and Hannan, R. (2016) 'Inhibition of RNA polymerase I transcription initiation by CX-5461 activates non-canonical ATM/ATR signaling', *Oncotarget*, vol. 7, pp. 49800-49818.

Raderschall, E., Golub, E. and Haaf, T. (1999) 'Nuclear foci of mammalian recombination proteins are located at single-stranded DNA regions formed after DNA damage', *Proceedings of the National Academy of Sciences*, vol. 96, pp. 1921-1926.

Rajagopalan, S. and Long, E. (2012) 'Cellular senescence induced by CD158d reprograms natural killer cells to promote vascular remodeling', *Proceedings of the National Academy of Sciences*, vol. 109, pp. 20596-20601.

Rasmussen, R. and Painter, R. (1964) 'Evidence for Repair of Ultra-Violet Damaged Deoxyribonucleic Acid in Cultured Mammalian Cells', *Nature*, vol. 203, pp. 1360-1362.

Resnick, M. (1976) 'The repair of double-strand breaks in DNA: A model involving recombination', *Journal of Theoretical Biology*, vol. 59, pp. 97-106.

Ritschka, B., Storer, M., Mas, A., Heinzmann, F., Ortells, M., Morton, J., Sansom, O., Zender, L. and Keyes, W. (2017) 'The senescence-associated secretory phenotype induces cellular plasticity and tissue regeneration.', *Genes & Development*, vol. 31, pp. 172-183.

Robles, S. and Adami, G. (1998) 'Agents that cause DNA double strand breaks lead to p16INK4a enrichment and the premature senescence of normal fibroblasts', *Oncogene*, vol. 16, pp. 1113-1123.

Rodríguez, A. and D'Andrea, A. (2017) 'Fanconi anemia pathway', *Current Biology*, vol. 27, pp. 986-988.

Roeder, R. and Rutter, W. (1969) 'Multiple Forms of DNA-dependent RNA Polymerase in Eukaryotic Organisms', *Nature*, vol. 224, pp. 234-237.

Rogakou, E., Pilch, D., Orr, A., Ivanova, V. and Bonner, W. (1998) 'DNA Double-stranded Breaks Induce Histone H2AX Phosphorylation on Serine 139', *The Journal of Biological Chemistry*, vol. 273, pp. 5858-5868.

Roy, D. and Lieber, M. (2009) 'G Clustering Is Important for the Initiation of Transcription-Induced R-Loops In Vitro, whereas High G Density without Clustering Is Sufficient Thereafter', *Molecular and Cellular Biology*, vol. 29, pp. 3124-3133.

Rubbi, C. and Milner, J. (2003) 'Disruption of the nucleolus mediates stabilization of p53 in response to DNA damage and other stresses', *The EMBO Journal*, vol. 22, pp. 6068-6077.

Russell, J. and Zomerdijk, J. (2006) 'The RNA polymerase I transcription machinery', *Biochemical Society Symposia*, vol. 73, pp. 203-216.

Ryu, S., Oh, Y. and Park, S. (2007) 'Failure of stress-induced downregulation of Bcl-2 contributes to apoptosis resistance in senescent human diploid fibroblasts', *Cell Death and Differentiation*, vol. 14, pp. 1020-1028.

Saada, A., Teixeira-Silva, A., Iraqui, I., Costes, A., Hardy, J., Paoletti, G., Fréon, K. and Lambert, S. (2017) 'Unprotected Replication Forks Are Converted into Mitotic Sister Chromatid Bridges', *Molecular Cell*, vol. 66, pp. 398-410.

Sakaguchi, K., Saito, S., Higashimoto, Y., Roy, S., Anderson, C. and Appella, E. (2000) 'Damage-mediated Phosphorylation of Human p53 Threonine 18 through a Cascade Mediated by a Casein 1-like Kinase', *The Journal of Biological Chemistry*, vol. 275, pp. 9278-9283.

Sanchez, Y., Wong, C., Thoma, R., Richman, R., Wu, Z., Piwnica-Worms, H. and Elledge, S. (1997) 'Conservation of the Chk1 Checkpoint Pathway in Mammals: Linkage of DNA Damage to Cdk Regulation Through Cdc25', *Science*, vol. 277, pp. 1497-1501.

Sanders, Y., Liu, H., Zhang, X., Hecker, L., Bernard, K., Desai, L., Liu, G. and Thannickal, V. (2013) 'Histone Modifications in Senescence-Associated Resistance to Apoptosis by Oxidative Stress', *Redox Biology*, vol. 1, pp. 8-16.

Savitsky, K., Bar-Shira, A., Gilad, S., Rotman, G., Ziv, Y., Vanagaite, L., Tagle, D., Smith, S., Uziel, T., Sfez, S., Ashkenazi, M., Pecker, I., Frydman, M., Harnik, R., Patanjali, S., Simmons, A., Clines, G., Sartiel, A., Gatti, R., Chessa, L., Sanal, O., Lavin, M., Jaspers, N., Taylor, A., Arlett, C., Miki, T., Weissman, S., Lovett, M., Collins, F. and Shiloh, Y. (1995) 'A Single Ataxia Telangiectasia Gene with a Product Similar to P1-3 Kinase', *Science*, vol. 268, pp. 1749-1753.

Schwab, R., Nieminuszczy, J., Shah, F., Langton, J., Martinez, D., Liang, C.C., Cohn, M., Gibbons, R., Deans, A. and Niedzwiedz, W. (2015) 'The Fanconi

Anemia Pathway Maintains Genome Stability by Coordinating Replication and Transcription', *Molecular Cell*, vol. 60, pp. 351-361.

Scully, R., Panday, A., Elango, R. and Willis, N. (2019) 'DNA double- strand break repair- pathway choice in somatic mammalian cells', *Nature Reviews Molecular Cell Biology*, vol. 20, pp. 698-714.

Serrano, M., Lin, A., McCurrach, M., Beach, D. and Lowe, S. (1997) 'Oncogenic ras Provokes Premature Cell Senescence Associated with Accumulation of p53 and p16INK4a', *Cell*, vol. 88, pp. 593-602.

Shakeel, S., Rajendra, E., Alcón, P., O'Reilly, F., Chorev, D., Maslen, S., Degliesposti, G., Russo, C., He, S., Hill, C., Skehel, J., Scheres, S., Patel, K., Rappsilber, J., Robinson, C. and Passmore, L. (2019) 'Structure of the Fanconi anaemia monoubiquitin ligase complex', *Nature*, vol. 575, pp. 234-237.

Shaltiel, I., Krenning, L., Bruinsma, W. and Medema, R. (2015) 'The same, only different – DNA damage checkpoints and their reversal throughout the cell cycle', *Journal of Cell Science*, vol. 128, pp. 607–620.

Sharma, S., Javadekar, S., Pandey, M., Srivastava, M., Kumari, R. and Raghavan, S. (2015) 'Homology and enzymatic requirements of microhomology-dependent alternative end joining', *Cell Death and Disease*, vol. 6, pp. 1-12.

Sherr, C. and McCormick, F. (2002) 'The RB and p53 pathways in cancer', *Cancer Cell*, vol. 2, pp. 103-112.

Shinohara, A., Ogawa, H. and Ogawa, T. (1992) 'Rad51 Protein Involved in Repair and Recombination in S. cerevisiae Is a RecA-like Protein', *Cell*, vol. 69, pp. 457-470.

Shinohara, A., Shinohara, M., Ohta, T., Matsuda, S. and Ogawa, T. (1998) 'Rad52 forms ring structures and co-operates with RPA in single-strand DNA annealing', *Genes to Cells*, vol. 3, pp. 145-156.

Shiotani, B. and Zou, L. (2009) 'Single-Stranded DNA Orchestrates an ATM-to-ATR Switch at DNA Breaks', *Molecular Cell*, vol. 33, pp. 547-558.

Shivji, M., Renaudin, X., Williams, C. and Venkitaraman, A. (2018) 'BRCA2 Regulates Transcription Elongation by RNA Polymerase II to Prevent R-Loop Accumulation', *Cell Reports*, vol. 22, pp. 1031-1039.

Sidi, R., Pasello, G., Opitz, I., Soltermann, A., Tutic, M., Rehrauer, H., Weder, W., Stahel, R. and Felley-Bosco, E. (2011) 'Induction of senescence markers after neo-adjuvant chemotherapy of malignant pleural mesothelioma and association with clinical outcome: An exploratory analysis', *European Journal of Cancer*, vol. 47, pp. 326-332.

Smogorzewska, A., Matsuoka, S., Vinciguerra, P., McDonald, E., Hurov, K., Luo, J., Ballif, B., Gygi, S., Hofmann, K., D'Andrea, A. and Elledge, S. (2007)

'Identification of the FANCI Protein, a Monoubiquitinated FANCD2 Paralog Required for DNA Repair', *Cell*, vol. 129, pp. 289-301.

Sollier, J. and Cimprich, K. (2015) 'Breaking bad: R-loops and genome integrity', *Trends in Cell Biology*, vol. 25, pp. 514-522.

Sollier, J., Stork, C., García-Rubio, M., Paulsen, R., Aguilera, A. and Cimprich, K. (2014) 'Transcription-Coupled Nucleotide Excision Repair Factors Promote R-Loop-Induced Genome Instability', *Molecular Cell*, vol. 56, pp. 777-785.

Srinivas, U., Tan, B., Vellayappan, B. and Jeyasekharan, A. (2019) 'ROS and the DNA damage response in cancer', *Redox Biology*, vol. 25, pp. 1-9.

St. Clair, S., Giono, L., Varmeh-Ziaie, S., Resnick-Silverman, L., Liu, W.J., Padi, A., Dastidar, J., DaCosta, A., Mattia, M. and Manfredi, J. (2004) 'DNA Damage-Induced Downregulation of Cdc25C Is Mediated by p53 via Two Independent Mechanisms: One Involves Direct Binding to the cdc25C Promoter', *Molecular Cell*, vol. 16, pp. 725-736.

Storer, M., Mas, A., Robert-Moreno, A., Pecoraro, M., Ortells, M., Di Giacomo, V., Yosef, R., Pilpel, N., Krizhanovsky, V., Sharpe, J. and Keyes, W. (2013) 'Senescence Is a Developmental Mechanism that Contributes to Embryonic Growth and Patterning', *Cell*, vol. 155, pp. 1119-1130.

Strausfeld, U., Labbé, J., Fesquet, D., Cavadore, J., Picard, A., Sadhu, K., Russell, P. and Dorée, M. (1991) 'Dephosphorylation and activation of a p34cdc2/cyclin B complex in vitro by human CDC25 protein', *Nature*, vol. 351, pp. 242-245.

Sundar, I., Rashid, K., Gerloff, J., Li, D. and Rahman, I. (2018) 'Genetic ablation of p16(Ink4a) does not protect against cellular senescence in mouse models of COPD/emphysema', *American Journal of Respiratory Cell and Molecular Biology*, vol. 59, pp. 189-199.

Sung, P. (1994) 'Catalysis of ATP-dependent homologous DNA pairing and strand exchange by yeast RAD51 protein', *Science*, vol. 265, pp. 1241-1243.

Tanaka, M., Ueda, A., Kanamori, H., Ideguchi, H., Yang, J., Kitajima, S. and Ishigatsubo, Y. (2002) 'Cell-cycle-dependent Regulation of Human aurora A Transcription Is Mediated by Periodic Repression of E4TF1', *The Journal of Biological Chemistry*, vol. 277, pp. 10719-10726.

Tan, S., Chadha, S., Liu, Y., Gabasova, E., Perera, D., Ahmed, K., Constantinou, S., Renaudin, X., Lee, M.Y., Aebersold, R. and Venkitaraman, A. (2017) 'A Class of Environmental and Endogenous Toxins Induces BRCA2 Haploinsufficiency and Genome Instability', *Cell*, vol. 169, pp. 1105-1118.

Tapia, C., Kutzner, H., Mentzel, T., Savic, S., Baumhoer, D. and Glatz, K. (2006) 'Two Mitosis-Specific Antibodies, MPM-2 and Phospho-Histone H3 (Ser28), Allow Rapid and Precise Determination of Mitotic Activity', *The American Journal of Surgical Pathology*, vol. 30, pp. 83-89.

Thomas, M., White, R. and Davis, R. (1976) 'Hybridization of RNA to double-stranded DNA: Formation of R-loops', *Proceedings of the National Academy of Sciences*, vol. 73, pp. 2294-2298.

Toledo, L., Murga, M., Gutierrez-Martinez, P., Soria, R. and Fernandez-Capetillo, O. (2008) 'ATR signaling can drive cells into senescence in the absence of DNA breaks', *Genes & Development*, vol. 22, pp. 297-302.

Toso, A., Revandkar, A., Di Mitri, D., Guccini, I., Proietti, M., Sarti, M., Pinton, S., Zhang, J., Kalathur, M., Civenni, G., Jarrossay, D., Montani, E., Marini, C., Garcia-Escudero, R., Scanziani, E., Grassi, F., Pandolfi, P., Catapano, C. and Alimonti, A. (2014) 'Enhancing Chemotherapy Efficacy in Pten-Deficient Prostate Tumors by Activating the Senescence-Associated Antitumor Immunity', *Cell Reports*, vol. 9, pp. 75-89.

Triana-Martínez, F., Picallos-Rabina, P., Da Silva-Álvarez, S., Pietrocola, F., Llanos, S., Rodilla, V., Soprano, E., Pedrosa, P., Ferreirós, A., Barradas, M., Hernández-González, F., Lalinde, M., Prats, N., Bernadó, C., González, P., Gómez, M., Ikonomopoulou, M., Fernández-Marcos, P., García-Caballero, T., Pino, P., Arribas, J., Vidal, A., González-Barcia, M., Serrano, M., Loza, M., Domínguez, E. and Collado, M. (2019) 'Identification and characterization of Cardiac Glycosides as senolytic compounds', *Nature Communications*, vol. 10:4731, pp. 1-12.

Tubbs, A. and Nussenzweig, A. (2017) 'Endogenous DNA Damage as a Source of Genomic Instability in Cancer', *Cell*, vol. 168, pp. 644-656.

Vinciguerra, P., Godinho, S., Parmar, K., Pellman, D. and D’Andrea, A. (2010) 'Cytokinesis failure occurs in Fanconi anemia pathway–deficient murine and human bone marrow hematopoietic cells', *The Journal of Clinical Investigation*, vol. 120, pp. 3834-3842.

Wahba, L., Gore, S. and Koshland, D. (2013) 'The homologous recombination machinery modulates the formation of RNA–DNA hybrids and associated chromosome instability', *eLife*, vol. 2:e00505, pp. 1-20.

Wang, C., Jurk, D., Maddick, M., Nelson, G., Martin-Ruiz, C. and Zglinicki, T. (2009) 'DNA damage response and cellular senescence in tissues of aging mice', *Aging Cell*, vol. 8, pp. 311-323.

Wang, L., Stone, S., Hoatlin, M. and Gautier, J. (2008) 'Fanconi anemia proteins stabilize replication forks', *DNA Repair*, vol. 7, pp. 1973-1981.

Ward, I. and Chen, J. (2001) 'Histone H2AX Is Phosphorylated in an ATR-dependent Manner in Response to Replicational Stress', *The Journal of Biological Chemistry*, vol. 276, pp. 47759-47762.

Ward, I., Minn, K., Jorda, K. and Chen, J. (2003) 'Accumulation of Checkpoint Protein 53BP1 at DNA Breaks Involves Its Binding to Phosphorylated Histone H2AX', *The Journal of Biological Chemistry*, vol. 278, pp. 19579-19582.

White, R. (2005) 'RNA polymerases I and III, growth control and cancer', *Nature Reviews Molecular Cell Biology*, vol. 6, pp. 69-78.

White, E. and Lowe, S. (2009) 'Eating to exit: autophagy-enabled senescence revealed', *Genes & Development*, vol. 23, pp. 784-787.

Wiley, C., Velarde, M., Lecot, P., Gerencser, A., Verdin, E. and Campisi, J. (2016) 'Mitochondrial Dysfunction Induces Senescence with a Distinct Secretory Phenotype', *Cell Metabolism*, vol. 23, pp. 303-314.

Williamson, D., Lu, Y.J., Fang, C., Pritchard-Jones, K. and Shipley, J. (2006) 'Nascent Pre-rRNA Overexpression Correlates with an Adverse Prognosis in Alveolar Rhabdomyosarcoma', *Genes, Chromosomes and Cancer*, vol. 45, pp. 839-845.

Wold, M. and Kelly, T. (1988) 'Purification and characterization of replication protein A, a cellular protein required for in vitro replication of simian virus 40 DNA', *Proceedings of the National Academy of Sciences*, vol. 85, pp. 2523-2527.

Wu, C.-H., Riggelen, J., Yetil, A., Fan, A., Bachireddy, P. and Felsher, D. (2007) 'Cellular senescence is an important mechanism of tumor regression upon c-Myc inactivation', *Proceedings of the National Academy of Sciences*, vol. 104, pp. 13028-13033.

Xiong, Y., Hannon, G., Zhang, H., Casso, D., Kobayashi, R. and Beach, D. (1993) 'p21 is a universal inhibitor of cyclin kinases', *Nature*, vol. 366, pp. 701-704.

Xu, H., Di Antonio, M., McKinney, S., Mathew, V., Ho, B., O'Neil, N., Dos Santos, N., Silvester, J., Wei, V., Garcia, J., Kabeer, F., Lai, D., Soriano, P., Banáth, J., Chiu, D., Yap, D., Le, D., Ye, F., Zhang, A., Thu, K., Soong, J., Lin, S.C., Tsai, A., Osako, T., Algara, T., Saunders, D., Wong, J., Xian, J., Bally, M., Brenton, J., Brown, G., Shah, S., Cescon, D., Mak, T., Caldas, C., Stirling, P., Hieter, P., Balasubramanian, S. and Aparicio, S. (2017) 'CX-5461 is a DNA G-quadruplex stabilizer with selective lethality in BRCA1/2 deficient tumours', *Nature*, vol. 8, pp. 1-18.

Yan, S., Frank, D., Son, J., Hannan, K., Hannan, K., Chan, K., Pearson, R. and Sanij, E. (2016) 'The Potential of Targeting Ribosome Biogenesis in High-Grade Serous Ovarian Cancer', *International Journal of Molecular Sciences*, vol. 18, pp. 1-17.

Yeo, C., Alexander, I., Lin, Z., Lim, S., Aning, O., Kumar, R., Sangthongpitag, K., Pendharkar, V., Ho, V. and Cheok, C. (2016) 'p53 Maintains Genomic Stability by Preventing Interference between Transcription and Replication', *Cell Reports*, vol. 15, pp. 132-146.

Ye, C., Zhang, X., Wan, J., Chang, L., Hu W, Bing, Z., Zhang, S., Li, J., He, J., Wang, J. and Zhou, G. (2013) 'Radiation-induced cellular senescence results from a slippage of long-term G2 arrested cells into G1 phase', *Cell Cycle*, vol. 12, pp. 1424-1432.

Yosef, R., Pilpel, N., Papismadov, N., Gal, H., Ovadya, Y., Vadai, E., Miller, S., Porat, Z., Ben-Dor, S. and Krizhanovsky, V. (2017) 'p21 maintains senescent cell viability under persistent DNA damage response by restraining JNK and caspase signaling', *The EMBO Journal*, vol. 36, pp. 2280-2295.

Young, A., Narita, M., Ferreira, M., Kirschner, K., Sadaie, M., Darot, F., Tavaré, S., Arakawa, S., Shimizu, S., Watt, F. and Narita, M. (2009) 'Autophagy mediates the mitotic senescence transition', *Genes & Development*, vol. 23, pp. 798-803.

Young, J. and Smith, J. (2001) 'DNA Methyltransferase Inhibition in Normal Human Fibroblasts Induces a p21-dependent Cell Cycle Withdrawal', *The Journal of Biological Chemistry*, vol. 276, pp. 19610-19616.

Zhang, X., Chiang, H.C., Wang, Y., Zhang, C., Smith, S., Zhao, X., Nair, S., Michalek, J., Jatoi, I., Lautner, M., Oliver, B., Wang, H., Petit, A., Soler, T., Brunet, J., Mateo, F., Pujana, M., Poggi, E., Chaldekas, K., Isaacs, C., Peshkin, B., Ochoa, O., Chedin, F., Theoharis, C., Sun, L.Z., Curiel, T., Elledge, R., Jin, V., Hu, Y. and Li, R. (2017) 'Attenuation of RNA polymerase II pausing mitigates BRCA1-associated R-loop accumulation and tumorigenesis', *Nature Communications*, vol. 8, pp. 1-11.

Zhu, Y., Tchkonia, T., Fuhrmann-Stroissnigg, H., Dai, H., Ling, Y., Stout, M., Pirtskhalava, T., Giorgadze, N., Johnson, K., Giles, C., Wren, J., Niedernhofer, L., Robbins, P. and Kirkland, J. (2016) 'Identification of a novel senolytic agent, navitoclax, targeting the Bcl-2 family of anti-apoptotic factors', *Aging Cell*, vol. 15, pp. 428-435.

Zhu, Y., Tchkonia, T., Pirtskhalava, T., Gower, A., Ding, H., Giorgadze, N., Palmer, A., Ikeno, Y., Hubbard, G., Lenburg, M., O'Hara, S., LaRusso, N., Miller, J., Roos, C., Verzosa, G., LeBrasseur, N., Wren, J., Farr, J., Khosla, S., Stout, M., McGowan, S., Fuhrmann-Stroissnigg, H., Gurkar, A., Zhao, J., Colangelo, D., Dorronsoro, A., Ling, Y., Barghouthy, A., Navarro, D., Sano, T., Robbins, P., Niedernhofer, L. and Kirkland, J. (2015) 'The Achilles' heel of senescent cells: from transcriptome to senolytic drugs', *Aging Cell*, vol. 14, pp. 644-658.

Zielke, N., Edgar, B. and DePamphilis, M. (2013) 'Endoreplication', *Cold Spring Harbor Perspectives in Biology*, vol. 5:a012948, pp. 1-16.

Zindy, F., Quelle, D., Roussel, M. and Sherr, C. (1997) 'Expression of the p16INK4a tumor suppressor versus other INK4 family members during mouse development and aging', *Oncogene*, vol. 15, pp. 203-211.

Ziv, Y., Bielopolski, D., Galanty, Y., Lukas, C., Taya, Y., Schultz, D., Lukas, J., Bekker-Jensen, S., Bartek, J. and Shiloh, Y. (2006) 'Chromatin relaxation in response to DNA double-strand breaks is modulated by a novel ATM and KAP-1 dependent pathway', *Nature Cell Biology*, vol. 8, pp. 870-876.

Zou, L. and Elledge, S. (2003) 'Sensing DNA Damage Through ATRIP Recognition of RPA-ssDNA Complexes', *Science*, vol. 300, pp. 1542-1548.

Zou, Y., Sfeir, A., Gryaznov, S., Shay, J. and Wright, W. (2004) 'Does a Sentinel or a Subset of Short Telomeres Determine Replicative Senescence?', *Molecular Biology of the Cell*, vol. 15, pp. 3709-3718.

Declaration of personal contribution

Die Arbeit wurde in der Medizinischen Universitätsklinik Tübingen in der Abteilung Innere Medizin VIII (Medizinische Onkologie und Pneumologie) unter Betreuung von Professor Dr. med. Lars Zender durchgeführt.

Die Konzeption der Experimente erfolgte durch mich in Zusammenarbeit mit Stefan Zwirner, Athina Moschopoulou und Katharina Wolter. Sämtliche Versuche wurden, nach Einarbeitung durch oben genannte Labormitglieder, von mir eigenständig durchgeführt. Die Datenanalyse und die Erstellung der Abbildungen erfolgten eigenständig durch mich.

Ich versichere, das Manuskript selbständig verfasst und keine weiteren als die von mir angegebenen Quellen verwendet zu haben.

Tübingen, den 07.01.2023

Acknowledgements

Ich bedanke mich bei Prof. Dr. med. Lars Zender für die Möglichkeit, meine Doktorarbeit in seinem Labor durchzuführen und für die Förderung meiner wissenschaftlichen Ausbildung. Mein besonderer Dank gilt Stefan Zwirner, Katharina Wolter und Athina Moschopoulou für die Einarbeitung und Zusammenarbeit im Labor, fortlaufende Diskussion meiner Ergebnisse und Korrektur dieser Dissertationsschrift. Zudem danke ich allen weiteren Mitgliedern des Labors und allen Kollaborationspartnern für gute Zusammenarbeit. Des Weiteren danke ich den Veranstaltern des 20th International AEK Cancer Congress für die Möglichkeit, diese Arbeit im Rahmen einer Posterpräsentation vorzustellen.